



HAL
open science

A review on fused deposition modeling materials with analysis of key process parameters influence on mechanical properties

Silvain William Tieuna Tientcheu, Joseph Marae Djouda, Mohamed Ali Bouaziz, Elisabeth Lacazedieu

► To cite this version:

Silvain William Tieuna Tientcheu, Joseph Marae Djouda, Mohamed Ali Bouaziz, Elisabeth Lacazedieu. A review on fused deposition modeling materials with analysis of key process parameters influence on mechanical properties. *International Journal of Advanced Manufacturing Technology*, 2023, 130 (5-6), pp.2119-2158. 10.1007/s00170-023-12823-x . hal-04662462

HAL Id: hal-04662462

<https://hal.science/hal-04662462>

Submitted on 26 Jul 2024

HAL is a multi-disciplinary open access archive for the deposit and dissemination of scientific research documents, whether they are published or not. The documents may come from teaching and research institutions in France or abroad, or from public or private research centers.

L'archive ouverte pluridisciplinaire **HAL**, est destinée au dépôt et à la diffusion de documents scientifiques de niveau recherche, publiés ou non, émanant des établissements d'enseignement et de recherche français ou étrangers, des laboratoires publics ou privés.



A review on fused deposition modeling materials with analysis of key process parameters influence on mechanical properties

Silvain William Tieuna Tientcheu¹ · Joseph Marae Djouda^{2,3} · Mohamed Ali Bouaziz⁴ · Elisabeth Lacazedieu⁵

Received: 13 July 2023 / Accepted: 28 November 2023

© The Author(s), under exclusive licence to Springer-Verlag London Ltd., part of Springer Nature 2023

Abstract

Fused deposition modeling (FDM) also called fused filament fabrication (FFF) is the most used additive manufacturing (AM) technology. The growing impact of AM is due to its various advantages and its applicability to many domains. Many research works have focused on the improvements of FDM technique and optimization of the mechanical properties in order to fabricate parts that can be used in realm industrial applications. In the present work, a review of materials used in the FDM process is proposed together with an analysis of the key parameters affecting their mechanical behaviors. In this framework, FDM materials have been classified into three groups: standard, composite, and smart materials. Previous works have clearly shown that the process parameters have a greater influence on parts made with standard materials than on those made with composites. The effect of the process parameters such as air gap, layer thickness, build orientation, raster orientation, and contour number is discussed in regard to the mechanical solicitations: tensile and compression, three- or four-point bending tests and fatigue. The impact of these process parameters on different material categories is also analyzed. This reveals the specificities related to each materials group. This work can be considered like a global insight for the comprehension of the process—structure—mechanical property relations of common FDM materials. Synthetic remarks and recommendations are proposed for future investigations.

Keywords Fused deposition modeling · Thermoplastics · Composites · Smart materials · Process parameters · Mechanical properties

1 Introduction

Additive manufacturing (AM) is known as a technology consisting in producing parts layer by layer. At the beginning, AM was mostly limited to rapid prototyping but progressively many functional parts have been manufactured by AM

in many industrial sectors. AM finds many applications in most industrial fields like automotive, aeronautics, energy, and medicine [1–4] as well as fashion and food. The growing interest for AM and especially for fused deposition modeling (FDM) is due to its advantages such as saving time through flexibility with possibility of manufacturing complex shapes, and weight reduction while maintaining performance and avoiding assemblies. In addition, superimposing materials of different natures and properties is made easier and more precisely thanks to the combination of two or more extruders in a given AM machine. It can be done in a specific way such that it is possible to add new functionalities to a given component. For all these reasons, AM is a technology in line with the latest industrial revolution the so-called Industry 4.0 [5].

When it comes to AM, there are various techniques commonly employed for part fabrication, including binder jetting, directed energy deposition, material extrusion, material jetting, powder bed fusion, sheet lamination, and vat photopolymerization [6]. All of these techniques have a common principle: the layer-by-layer deposition of material to create

✉ Joseph Marae Djouda
joseph.marae_djouda@ens-paris-saclay.fr

¹ Ecole Nationale Supérieure Polytechnique, Université de Yaoundé I, BP 8390, Yaoundé, Cameroon

² EPF School of Engineering, 55 Avenue du Président Wilson, 94 230, Cachan, France

³ CentraleSupélec, ENS Paris-Saclay, CNRS, LMPS – Laboratoire de Mécanique Paris-Saclay, Université Paris – Saclay, 91190 Gif-Sur-Yvette, France

⁴ CEA, Service d'Étude Des Matériaux Irradiés, Université Paris-Saclay, 91191 Gif-Sur-Yvette, France

⁵ INSA Hauts-de-France, LAMIH UMR CNRS 8201, Valenciennes, France

a complete part. Among these methods, FDM also known as fused filament fabrication (FFF) or material extrusion (ME) stands out as one of the most widely used. This popularity is the result of its simplicity and numerous advantages over other AM techniques: *cost-efficiency* making it accessible to a wide range of users; *material variety* offering versatility in material selection for specific applications; *ease of use* making them suitable for both beginners and experienced users; *speed* (particularly when compared to some powder-based techniques); *layer adhesion* ensuring the structural integrity of printed parts; *environmental friendliness* (generates less waste material compared to other techniques like powder bed fusion); *education and prototyping*: FDM is often the preferred choice for educational institutions, rapid prototyping, and quick design iterations [7]. These advantages collectively contribute to FDM's prominence in the world of AM.

FDM was created by Scott Crump in 1980 [8] and trademarked by Stratasys Inc. [9]. The process is based on the extrusion of a filament or pellets. It consists in using a computer-aided design (CAD) system, with selection of material(s), automation using computer numerical control, and extrusion process to manufacture 3D parts (Fig. 1) [10].

The first step of the FDM process is to design the part using a CAD software. A solid model is created and converted into a stereolithography format by tessellating the model to make a faceted approximation of the model. After the CAD modeling step, the pre-processing of the FDM software is used. It involves estimation of the part orientation, slicing into the thin layers, selecting FDM parameters, and choosing the supports, which have to be generated. The further pre-processed file is then fed into the FDM. As shown in Fig. 2, on the FDM machine material, in most cases in the form of coil reel or spool, is heated into the molten state in a liquefier head, and further extruded out to deposit a thin layer onto the platform [11]. This layer-by-layer process is repeated until the required thickness is obtained. Completed parts are removed from FDM machines and support structures are directly cut out from the model.

Many parameters have to be chosen during this process and the choice of these parameters has a major impact on the quality of the obtained parts. The effect of parameters on the mechanical properties of the material has been widely investigated. For example, Popescu et al. [12] made a literature review and classified those process parameters in three categories: slicing parameters, building orientation, and temperature conditions. It emerges from the literature that the key parameters influencing mechanical properties are as follows: layer thickness, raster orientation, air gap, and build orientation [12]. It was shown that the effect of

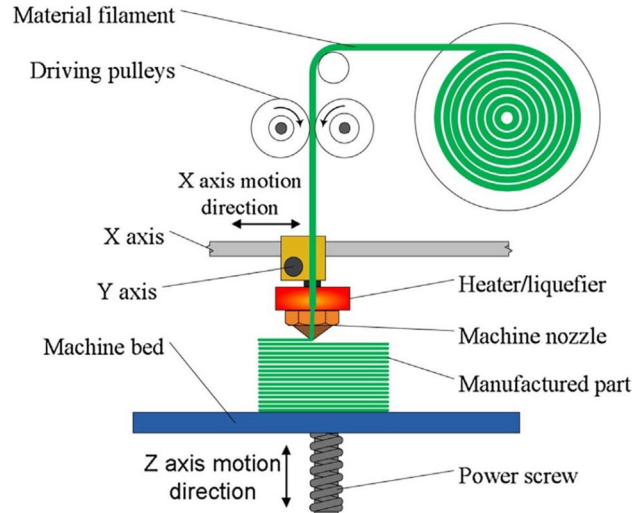


Fig. 2 Principle of FDM process [11]

each parameter on mechanical properties depends on the type of used material.

In the present work, an overview is proposed, on the various types of materials used in 3D printing. Then FDM process parameters' effects on mechanical properties are investigated by considering the correlation between printing parameters and types of materials. The review focuses on thermoplastic polymers, composite materials, and smart materials. The case of the metallic alloys fabricated by material extrusion is not treated in this work. A survey of the main developments made in process–structure–mechanical properties relations of common materials used in FDM technique is detailed.

2 Materials used in fused deposition modeling

In the FDM process, a spool of filament is loaded into the 3D printer and fed through the print head, which is equipped with a heated nozzle. Once the nozzle reaches the desired temperature, a motor drives the filament through it, causing it to melt. The printer moves the print head, depositing the molten material in specific locations where it cools and solidifies. When a layer is complete, the build platform moves down and the process is repeated, layer by layer.

A wide range of thermoplastics are used as feedstock materials in FDM process; among them, the most popular are as follows: acrylonitrile butadiene styrene (ABS),

Fig. 1 Different steps of FDM process [10]



polylactic acid (PLA), polycarbonate (PC), polyamide (PA), polystyrene (PS), polypropylene (PP), polyether ether ketone (PEEK), polymethyl methacrylate (PMMA)... In addition to these, other materials are of great interest and their list may be not exhaustive due to the widespread adoption of this manufacturing process across various industrial sectors. The material choice in 3D printing depends on the application sector, structural requirements, mechanical properties [13], and environmental and other limitations or conditions [14]. In addition to this large range of materials available for part fabrication by FDM, the process parameters can be optimized in order to fill the engineering requirements. Recent works aim to take advantage of the huge advantages of FDM for the fabrication of parts with metal alloys or ceramics. This leads to new approaches based on FDM principle which are in development [15–18]. These methods are beyond the scope of the present article. In the following sections, materials used in FDM process are classified into three categories: standard, composite, and smart materials.

2.1 Standard materials

Standard materials class includes materials which are widespread and commonly used in FDM; they are mostly constituted of thermoplastic polymers. In the present section, we will focus on each of these materials in terms of mechanical properties, advantages, and applications.

2.1.1 Acrylonitrile butadiene styrene

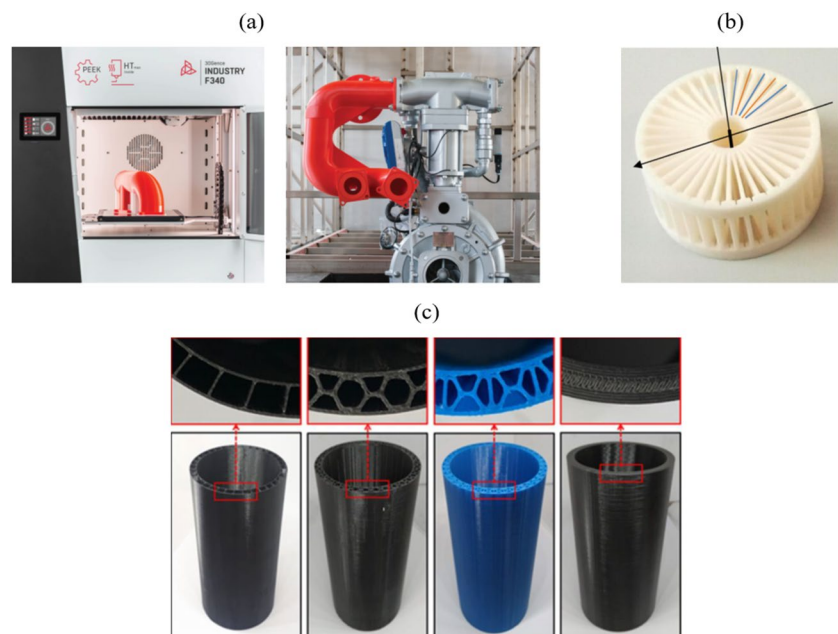
ABS is one of the most used thermoplastic polymers in FDM. It results from the polymerization of styrene and

acrylonitrile in the presence of polybutadiene. This polymer combines many advantages in terms of mechanical and chemical properties [19]. Because of its good properties in terms of resistance of impact, heat, chemical and abrasion resistance, dimensional stability, tensile strength, surface hardness, rigidity, and electrical characteristics, ABS is commonly encountered in mechanical engineering in addition of its function of prototype design [20–22]. Figure 3 highlights some of these applications. The rubbery butadiene impacts toughness of the material and acrylonitrile adds resistance to heat and environmental degradation [23]. This polymer is available in different grades. The form of ABS used in AM is very similar to that used in injection-molded parts such as Lego bricks. The 3D-printed parts of ABS present a reasonable smoothness due to its rheological properties. The temperature of the print head is around 220 °C during the extrusion. The ABS 3D-printed parts are today present in different industrial and research contexts and greatly impact our day-to-day life. One can mention cryogenic applications [22], automotive applications [24, 25], vacuum and pressure tight vessels [26], and several home applications [27]. The relationship between the color of the ABS filament used during 3D printing and the mechanical properties has been established [28].

2.1.2 Polylactic acid

Polylactic acid (PLA) is a biopolymer produced from lactic acid by direct polymerization [29]. PLA has a distinct place among polymers used in FDM because of its various applications. The biomedical field is one domain where PLA is commonly used for implantology, regenerative medicine,

Fig. 3 Creation a life-size 3D model of the manifold using 3D printing technology [20] (a), ABS 3D-printed support in ABS fabricated for the experimental realization of a “magnetic concentrator,” working at 77 K [22] and ABS 3D-printed lightweight pipes [21] (c)



tissue engineering, and drug carriers [30–35]. The reason of its application to biomedical fields comes from its biodegradability, bioresorbability, and biocompatibility [36, 37]. Figure 4 illustrates some applications of PLA 3D-printed structures in medicine. PLA 3D-printed parts are also used in packaging specifically for food [32] and for structural applications [38]. The mechanical properties, the low cost, and the reusability make also PLA a serious alternative to other thermoplastic polymers, mainly ABS [39]. A comparative analysis was performed between ABS and PLA about the influence of process parameters on mechanical behavior. From that study, it appears that PLA parts are more rigid than ABS ones and have greater tensile strength than ABS [40]. Then demand on PLA is increasing regarding its various applications such as packaging, pharmaceuticals, textiles, automotive, aerospace, biomedical, and tissue engineering [41].

In addition to its good mechanical properties [42], PLA is also appreciated because of properties like printability, hydrophobicity, thermoplasticity, and low cost. However, PLA has some disadvantages like brittleness, poor thermal resistance, and low glass transition temperature [43]. PLA has been combined with other materials in order to compensate its drawbacks. Many studies show that the reinforcement of PLA with another materials such as glass fibers or graphene leads to better properties [36, 39, 44, 45]. For example, the elastic modulus is

increased when PLA is reinforced with glass [45]. Garcia et al. show the influence of build parameters on geometry properties of two PLA-based filaments (unreinforced PLA and PLA-graphene composite materials). In conclusion, PLA-graphene filament feature improved mechanical, electrical, and thermal properties and do not affect the geometry quality. All this results in the fact that PLA is very suitable for AM.

2.1.3 Polyether ether ketone

Polyether ether ketone (PEEK) is a suitable thermoplastic polymer which combines good mechanical, chemical, and biological properties [46, 47]. It is used for automotive, aerospace, biomedical, and electrical applications [48, 49]. Because of its mechanical and chemical properties and also its biocompatibility, PEEK is today a center of attraction in research for bone replacement and implant design [46, 50]. PEEK has a high melting point [51] of 343°C and a high glass and transition temperature of 143°C. Today, the use of AM (FDM) in the field of medical manufacturing is growing quickly due to accuracy and flexibility of manufacturing processes [46]. Like many thermoplastic materials, PEEK properties are sensitive to temperature variations in the human body [52]. Recent works focus on improving mechanical properties of PEEK and PEEK composite materials [50, 52, 53]. The compatibility for

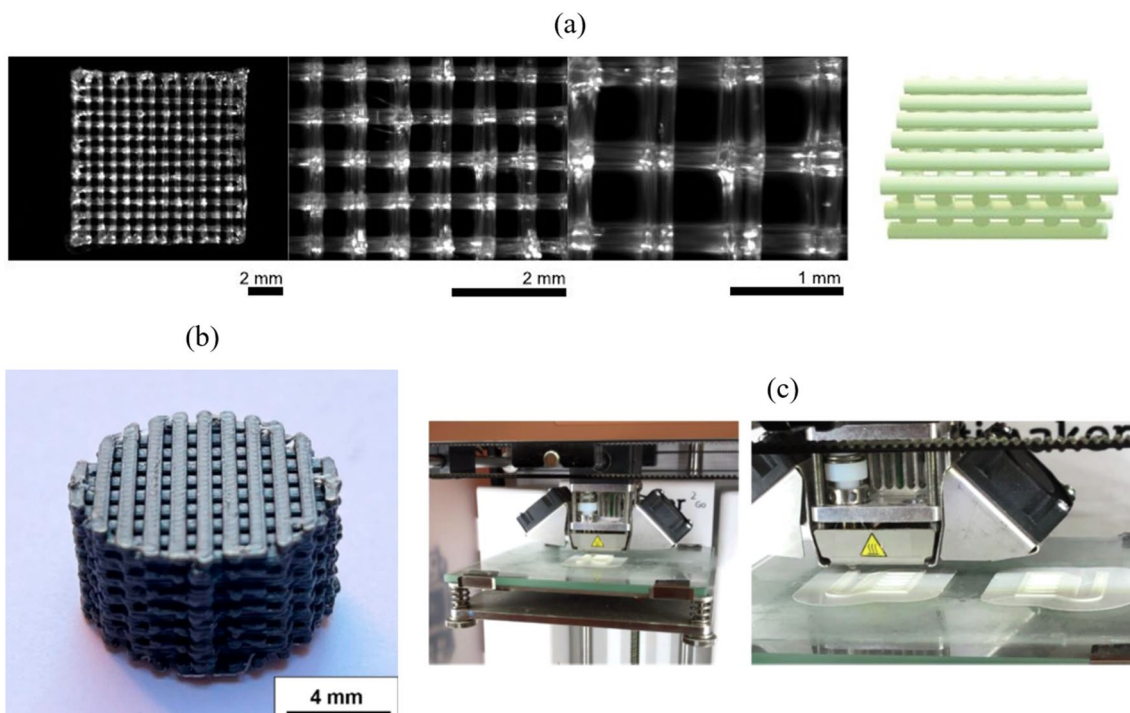


Fig. 4 3D-printed PLGA implant by FDM for drug release [33] (a), macro image of 3D-printed PLA-Gr-Mg composite scaffold [34] (b) and 3D printer performing the fabrication of an object using PLA as the filament for tissue application engineering [35]

bone implants is necessary in order to ensure the interconnections [54]. Oladapo et al. recently used finite element analysis (FEA) for studying and improving the fracture toughness of polyether ether ketone and hydroxyapatite graphene oxide (PEEK-HAP-GO) obtained by 3D printing. PEEK has a good potential for orthopedic applications and could replace other metal alloy implants. Figure 5 shows a typical 3D-printed human bone implant [54]. It is well known that the temperature variations during the 3D printing process can modify greatly the crystallinity of thermoplastic materials [55]. This effect has an important on PEEK 3D-printed parts.

2.1.4 Polymethyl methacrylate

PMMA is a synthetic acrylic polymer [56, 57] which is biocompatible and features suitable mechanical properties and good biostability. Because of its transparency and good durability in environmental conditions, PMMA is widely used in biomedical applications [57]. PMMA is used for dental implants, craniofacial maintenance, reconstructive structures, remodel lost bones, orthopedic surgery [56, 58, 59], and antibacterial effect by coating some nitrides at the structure surface [60]. Figure 6 presents some of the applications of PMMA 3D-printed by FDM. Furthermore, it has been demonstrated that FDM can directly create biocompatible PMMA structures with different controlled and predefined porosities using specifications from medical imaging [58]. Although the materials are available for immediate applications, they require preparation and adaptation. FDM makes it possible to achieve a very high precision in the production of parts [61]. PMMA low cost and transparency make it useful for many microfluidic applications [62]. Furthermore, PMMA is the best material for manufacturing camshaft trough rapid prototyping [63, 64]. To get expected properties, PMMA has been used as polymer matrices with calcium for medical applications; the mechanical properties

obtained by using this composite are comparable to those obtained with glass fiber-reinforced [59]. It may be pointed out that PMMA sheet was introduced by artists in their creations [65]. Polzin et al. have made the characterization of 3D-printed PMMA parts and the results show that the tensile strength is of 2.91 MPa and the elasticity modulus of 233 MPa [66]. The mechanical properties and the surface roughness of the obtained parts can be improved by incorporating other materials like epoxy and wax, respectively, in PMMA matrix.

2.1.5 Polypropylene

Polypropylene (PP) is a commercial material used for feed spacers due to its flexibility and chemical resistance properties [68]. PP powder can be used in 3D printing through SLS technology [68]. Due to its high impact strength, chemical resistance, moisture stability, and low cost, it was present as a potential materials for FDM [69–71]. Moreover, PP is used in many domains like textile, packaging, household furniture, automotive, aeronautics, and biomedical [72]. Figure 7 shows the use of PP for manufacturing protective face mask and in hospital part fabrication. However, it features drawback since PP parts are submitted to dimensional accuracy problems and warpage caused by high crystallinity and the orientation during the printing [69, 73, 74]. In most 3D printing technologies, polymers are used for their excellent mechanical properties [75], but PP parts have a high tendency to warp unlike other materials such as ABS and PLA [76]. Furthermore, it was shown that PP/PC blends and PP/inorganic particles present low shrinkage and little warpage [70]. Another disadvantage of PP is that it has low surface energy and, for that reason, PP does not adhere to the deposition surface [76]. Moreover, PP has the advantage of low-temperature printing despite the fact its properties limit the applications to specific areas.

Fig. 5 Typical 3D-printed human bone implant structure produced **a** knee cup, **b** finger, **c** femur bone, **d** tensile test piece [54]

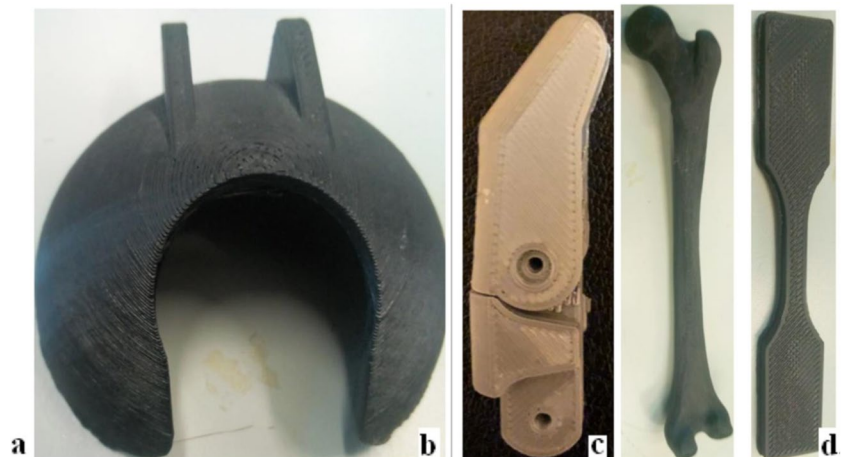


Fig. 6 **a** Microfluidic devices obtained by printing PMMA on PLA top image and the same device now with PMMA micro-channels printed on PMMA slide. This last device presents good transparency when observed in optical microscopy. The image c presents the PLA/PMMA boundary in the first microfluidic device [67]. **b** [58] and **c** [56]

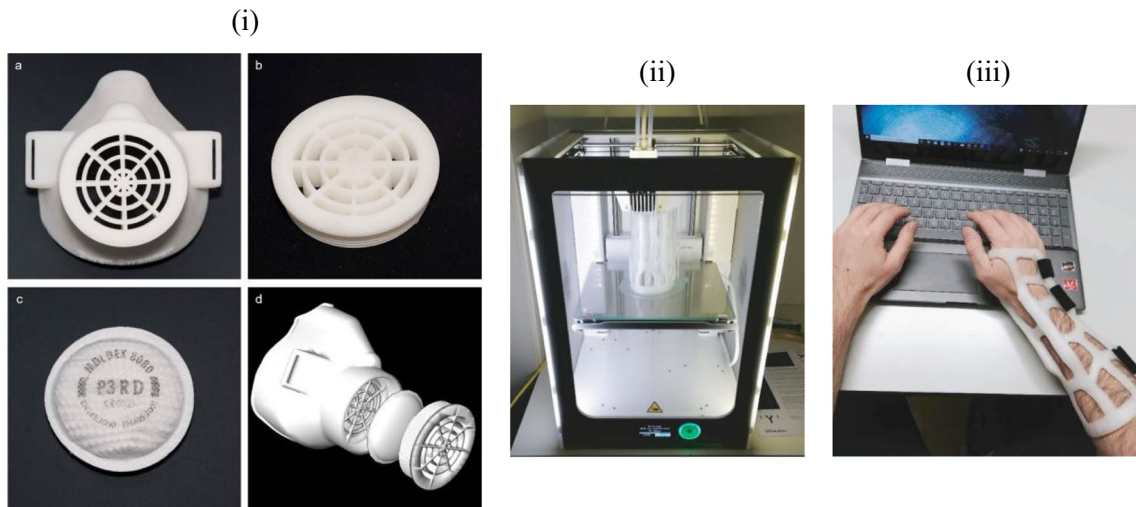
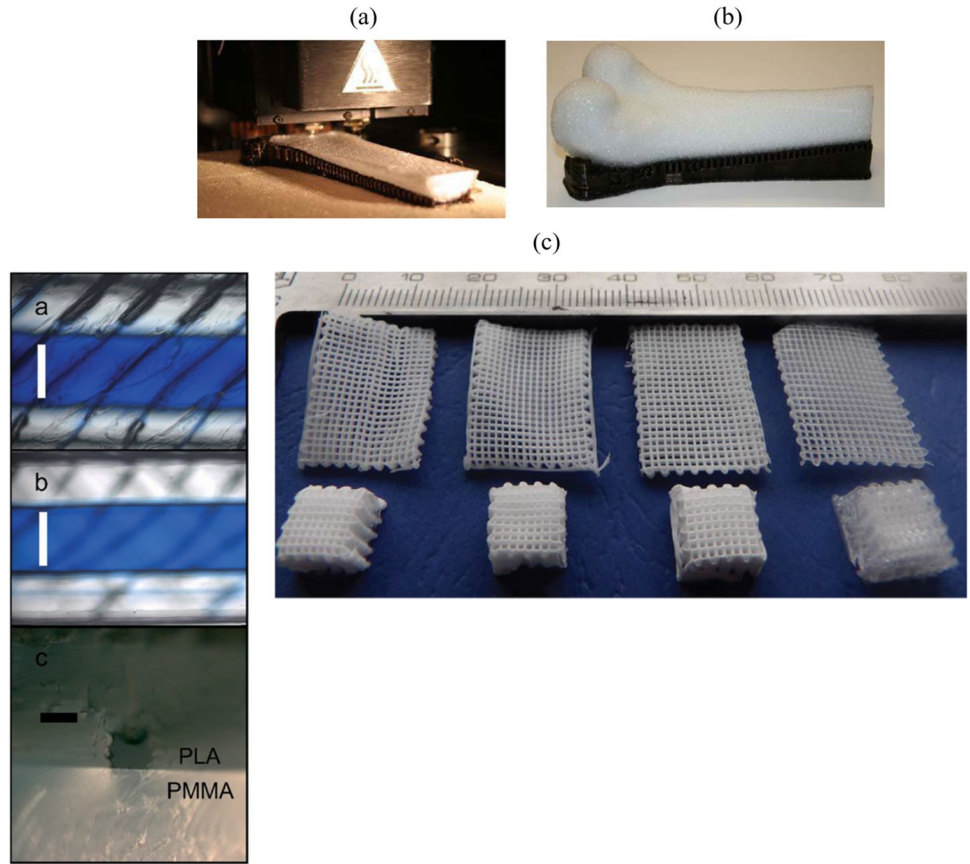


Fig. 7 Custom-made individualized 3D-printed protective face mask: **a** reusable 3D-printed face mask and **b** filter membrane support; **c** polypropylene (PP) non-woven melt-blown particle filter and **d** 3D image of the prototype [77] (i). In-hospital, overnight printing using

an FDM-printer with Polypropylene- (PP-) filament (ii). Fitted customized forearm-cast with ventilation openings and Velcro-Fasteners (iii) [78]

2.1.6 Polycarbonate

PC is a thermoplastic polymer recognized for its good properties like creep resistance, temperature resistance, high

impact strength, and good dimensional stability [79–81]. Due to its high strength, high Z-layer adhesion, high temperature stability, a smooth printed texture, and optical clarity, PC has a huge potential for 3D printing [23]. Another quality

of PC is the fact that it is an amorphous polymer, simple material with a relatively simple rheology [82], then it does not have the complexity of crystallization transition. PC is also one of the most used polymers in the field of engineering in many areas: medical, optical, electronics, aerospace, and indoor home part fabrication [83–85]. Figure 8 represents some of these applications. It was shown that FDM PC parts have a good tensile strength that can reach 58.8 MPa [86]. PC is regularly chosen [83] as a reinforce because of its large range of properties. It has been used like a reinforce of ABS; this reinforcement has improved the mechanical behavior of ABS particularly flexural modulus and hardness [79]. PC has been also used with aluminum to realize built plates through FDM that are less expensive and better to use than bed glass. It has been proven that PC/PP composite is a potential material for FDM part fabrication; the combination of PC/PP and poly (ethylene-co-glycidyl methacrylate) has improved the mechanical properties particularly the toughness [87]. Despite the fact that PC parts are good for functional testing, it also has disadvantages like low fatigue strength, crack easily, and high melt viscosity [87]. PC can be recycled. A research has shown that 3D printing manufactured by recycled PC can have a high strength and heat resistant comparable to commercial PC [88].

2.1.7 Polyamide or nylon

Polyamide, also called Nylon has two variants, nylon 6 and nylon 12. It is a semi-crystalline polymer that belongs good mechanical and electrical properties along with a good resistance to heat and chemicals [89]. Nylon has various applications in automotive industry; those automotive

applications include rear mirror housing, door handles, windscreen wipers or key lock system, bumpers [90, 91]. Furthermore, polyamide is hygroscopic; i.e., it can absorb moisture from the air and thus affect its properties and performance [92]. 3D-printed polyamide also presents good wear properties and can then be used for gear manufacturing [93] (see Fig. 9a). When mixed with PP, polyamide can exhibit shape memory properties that can be used for 4D devices [94] (see Fig. 9b). Many works have been done to determine the properties of PA, the melting temperature is 177°C, and the tensile strength is 42.7 MPa [95] (Table 1).

2.2 Composite materials

As previously mentioned, while polymers and metals are the major material groups for 3D-printing applications, composites have rapidly gained in attention for structural applications. AM industry has now many requirements about mechanical properties of each functional part considering the fact that the mechanical properties of a part essentially derive from the properties of the constitutive material. Most often, polymers are limited in terms of their mechanical properties like the ultimate tensile strength or the ductile feature. Therefore, part performance requirements are not reached by using pure polymer materials for numerous domains like aeronautic or energy. Moreover, recent technologies require materials with unusual combinations of properties: multifunctional structures. The realization of composites through a combination of two or more materials appears to be the best way to get high performance and high mechanical strength for specific applications [105, 106]. Figure 10 illustrates graphically a visualization of the

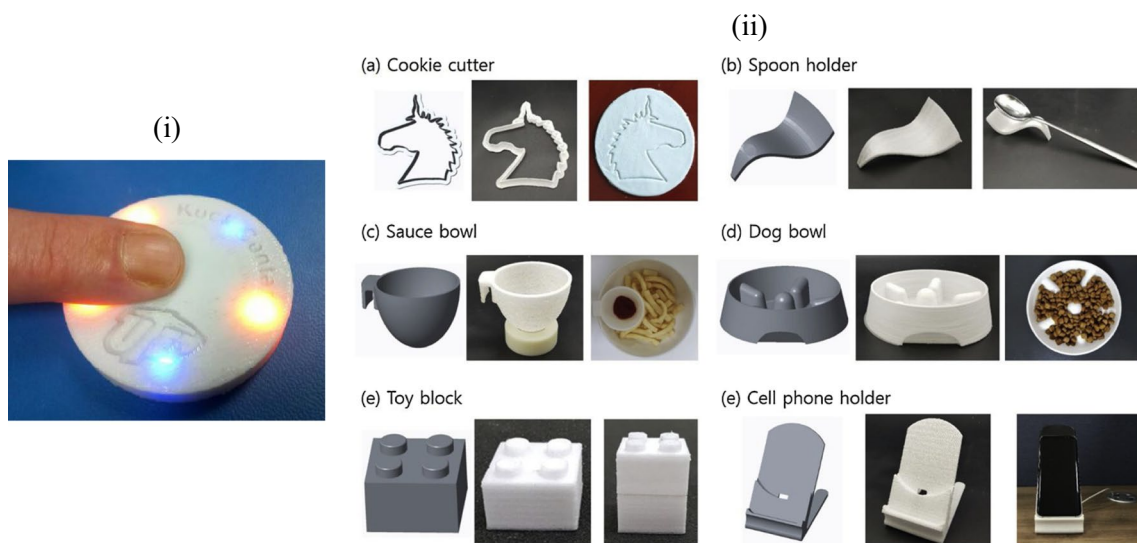


Fig. 8 Capacitive sensor encapsulate in polycarbonate box fabricated by FDM [84] (i). Indoor home devices manufactured with PC [85] (ii)

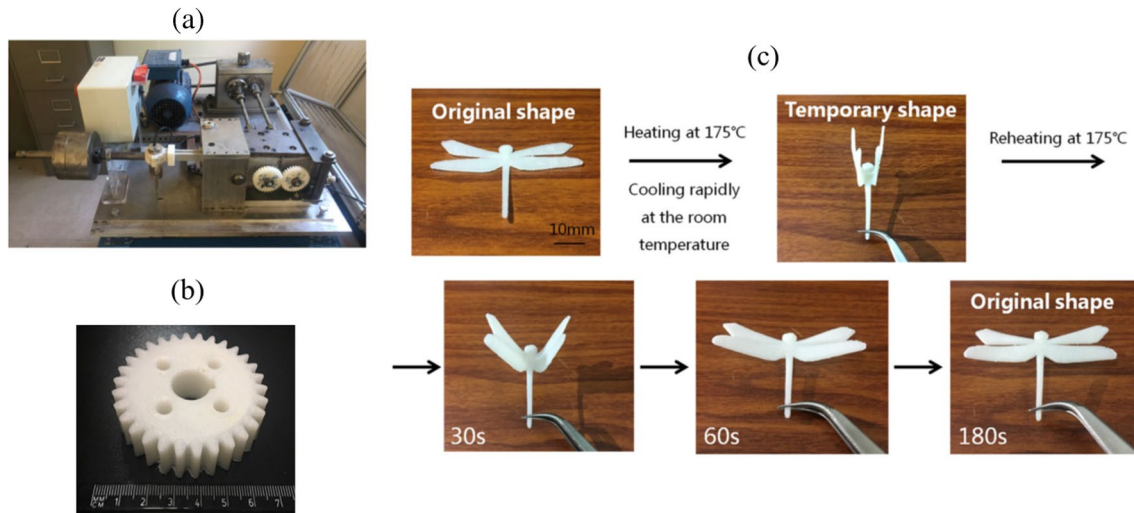


Fig. 9 Schematic of test rig for polymer gears (a), 3D-printed Nylon gear in simplified 3D [93] (b), photographs showing the SME of the 3D-printed product based on PP/PA6 alloy with 30 wt% of PA6 [94]

Table 1 Mechanical properties of FDM polymers

| Polymers | Tensile strength (MPa) | Tensile modulus (GPa) | Elongation % | Density (kg/m ³) | Processing temperature | References |
|----------|------------------------|-----------------------|--------------|------------------------------|------------------------|---------------|
| ABS | 11–65 | 1–2.65 | 8 | 1050 | 230–260°C | [96–98] |
| PLA | 30–65 | 2.3–3.3 | 2.5 | 1240 | 190–230°C | [96, 99–101] |
| PC | 58.6–72 | 1.79–3.24 | 4.8 | 1200 | 150–140°C | [96, 99, 102] |
| PEEK | 32–100 | 3.56–4.00 | 30 | 1300 | 350°C | [96, 103] |
| PMMA | 2.91 | 0.223 | | | | [1, 96, 103] |
| PP | 17–32 | 1–1.05 | | 900 | 220–250°C | [89, 96, 104] |
| PA | 35–186 | 0.45–3.50 | 30 | 950 | 225–265°C | [92, 103] |

requirements for key components with target outcomes of the endeavors around polymer-based composite material development for 3D printing applications.

2.2.1 Polymers matrix composites

Polymers are often used as base matrix materials in composites and carbon fibers, glass fibers, ceramics, and metals or alloys mostly in powder form or pellets are used as reinforcement which results in a material with particular properties from both materials [59, 107–109]. Figure 11 summarizes the different materials which are usually used for reinforcement and the possibilities in optimization of mechanical properties and functionalization. The polymer matrix composites (PMCs) have experienced fast development in recent years due to the need for more advanced engineering materials with high strength and low weight [110]. Properties such as adhesiveness, flexibility, conductivity, process ability, toughness, and strength depend on the composition of the matrix and the reinforcement materials [111].

Figure 12 shows the fabrication of filament of PEEK and PEEK reinforced with carbon and glass fibers and composite structure made with continuous fibers. There are limitations regarding the composition of metal powder in PMC due to its effect on viscosity, but its composition can be improved by using additives such as surfactants and plasticizers [112]. Most commonly used metal powders for PMC are aluminum and iron powders with matrix materials such as ABS, PP, and PA. The thermal properties of the PMC increase with the increase in the size of the reinforcement/filler particles.

2.2.2 Polymers ceramic composites (bio-composites)

Ceramics are very useful in biomedical applications which require materials that are biocompatible, highly corrosion resistant, and flexible [116, 117]. Biocomposite materials are highly compatible with simulated body fluid, similar to those found in human blood plasma. The most preferred materials for bone graft applications are bioceramics, but their uses are restricted due to their brittleness and poor

Fig. 10 FDM polymer filaments [103]

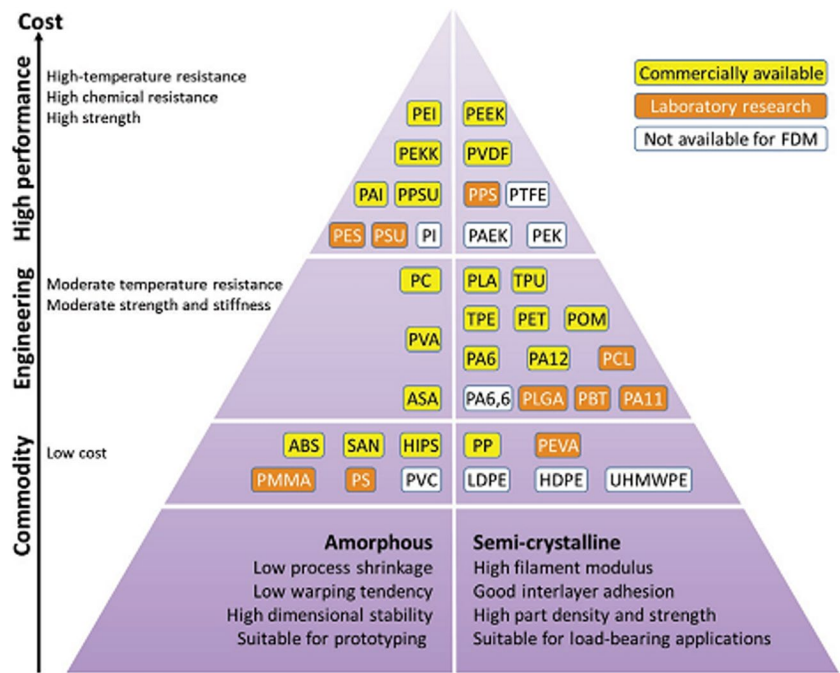
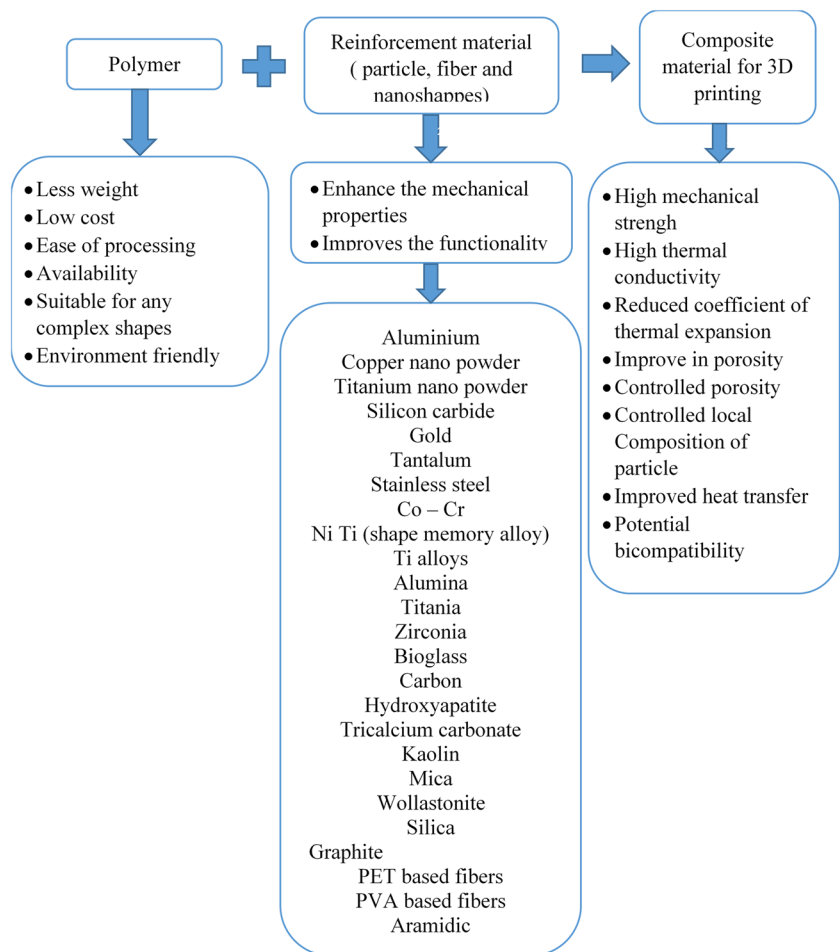


Fig. 11 The polymer-based composite [113]



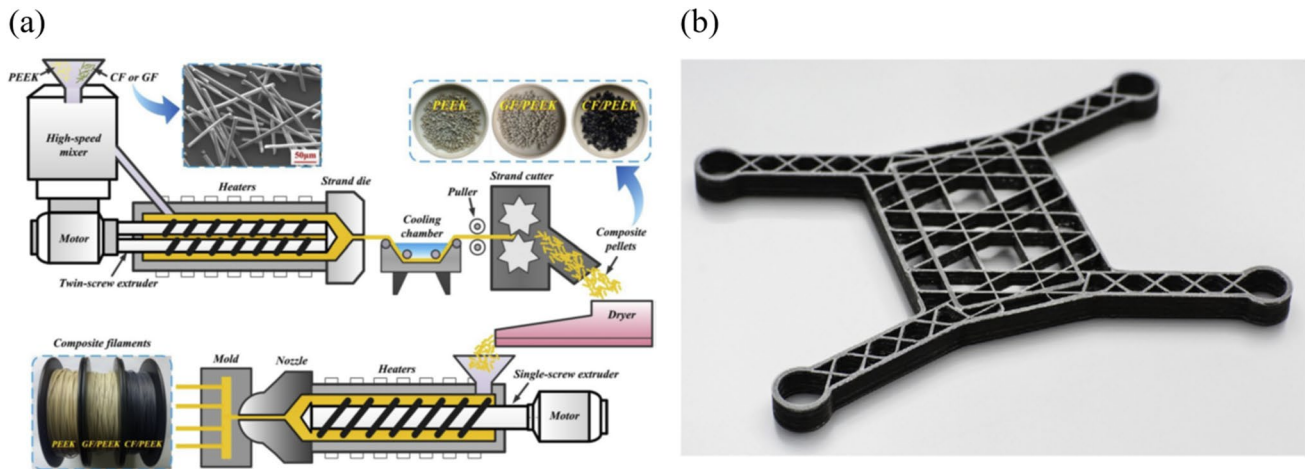


Fig. 12 Preparation process of composite filaments (PEEK, CF/PEEK, and GF/PEEK) [114] (a) and an example of small size structure obtained by 3D printing continuous fiber composite [115] (b)

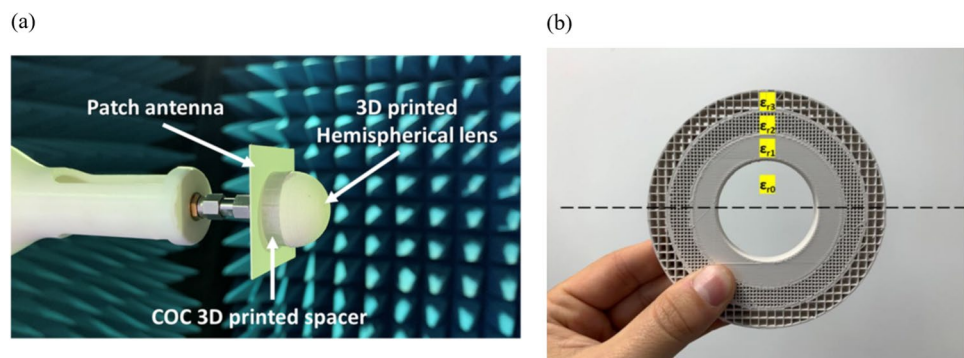
mechanical strength. However, by combining these materials with polymers, they can be used as polymer ceramic composites which bring solution for intrinsic limitations [118]. Figure 13 shows some applications of polymer ceramic composites. Ceramics such as TiO_2 , ZrO_2 , and Al_2O_3 and calcium ceramics are mostly used as reinforcement materials with polymer matrices such as PA, PP, and PLA. Some polymers like polycaprolactone (PCL), PEEK, and PMMA which are biocompatible materials have a place of choice in fabrication of parts for biomedical applications by FDM and can be combined with ceramics. Biocomposites have brought significant advancements in the field of biomedical and modern healthcare sectors and helped in the development of artificial human organs and tissue engineering. The challenges remain in the fact to design parts with enhanced mechanical properties [119]. 3D printing appears to be the ideal manufacturing technique thanks to its multiple process parameters that make it possible to obtain parts with desired properties. Ceramic composites parts obtained by FDM also have

great potential for applications in sensing and aerospace [84] despite existing challenges.

2.2.3 Nanocomposites

Polymer nanocomposites represent a new class of materials that offers an alternative to the conventional filled polymers. In this new class of materials, nanosized reinforcements are dispersed in polymer matrix offering tremendous improvement in performance properties of the polymer [122]. The physical properties of FDM parts can be improved using conductive raw materials or by adding appropriate nanoparticles that improve both mechanical and thermal properties [111] and conductive properties [123]. Addition of nanofillers increases the brittleness of the composite material due to the lack of adhesiveness and interaction between nanofillers and polymer materials [124]. Adding nanomaterials such as carbon nanotubes, nanoceramic particles, and metal nanoparticles to matrices such as polymers and metals has been used in the previous research and provided remarkable

Fig. 13 3D-printed hemispherical dielectric lens using a BST/ABS composite [120] (a) and 3D-printed Fresnel zone plate lens ($\epsilon_{r1} > \epsilon_{r2} > \epsilon_{r3} > \epsilon_{r0}$) with polymer-ceramic composite [121] (b)



improvements in the properties of the final parts [124–127] (see Fig. 14). The FDM of nanocomposites presents also good perspective in fashion industry by the possibility for direct 3D printing onto textile fabric with excellent adhesion properties [128]. This is both ecological friendly by the reduction of the waste of water and of chemical products and also for production time reduction. Because of the wide range of applications and the attracting properties, the optimization of the properties of 3D-printed nanocomposites is still an exciting topic [129, 130]. Lei et al. have studied numerically and experimentally the influence of printing parameters on the mechanical properties of FDM 3D-printed PLA/GNP nanocomposite [130].

2.2.4 Fiber-reinforced composites

There are different kinds of fiber-reinforced polymer (FRP) composites obtained by the combination of polymers and materials like carbon and glass fibers. These last provide to the composite structures with high strength and low weight [131–133]. FRPs are widely used in manufacturing industries particularly in the transportation sector such as aerospace and automobile sectors. These materials aim for replacing the components that were previously made of metals or alloys in order to reduce their weight and then increase their efficiency and performance. The fibers used for the reinforcement can bring to parts in addition to advanced structural properties another functionalities or properties. The possibility of 3D printing FRP composites by FDM has given rise to prolific research areas and numerous industrial applications [133]. For example, carbon fiber-reinforced polymer (CFRP) composites present interesting properties such as wear resistance, corrosion resistance, lightweight structures, high strength-to-weight ratio, and high dimensional stability.

However, the FRPs are non-biodegradable and today their environment impact is not well mastered because of recyclability concerns [134]. Recently, extensive research has been carried out with the purpose of developing another generation of fiber-reinforced polymers with limited environment impact or reduced carbon emission. Natural fibers are potentially the best candidate due to their advantages such as low cost, low abrasive wear, low density, ease of availability, and environmental-friendly and biodegradable nature. There are many natural fibers available such as wood, bamboo, flax, coir, jute, sisal, vegetable fibers, and oil palm [135, 136]. Natural fibers are abundantly available in the subcontinent, China, and southeastern countries which are having the fastest growing economies in the world [137]. Mostly, these fibers are used for conventional purposes in developing countries and hence there is a pressing need to find advanced application areas (such as FDM) to further strengthen their economies and they can possibly become the manufacturing hub for natural fiber products [4, 138] (Fig. 15).

As previously mentioned, there are more and more requirements about functional parts in the industry. In order to improve the mechanical properties of polymers, one of the adopted strategies is the introduction of composite materials by adding fillers in polymer matrix. The filler used can be synthetic or natural and then biodegradable. Table 2 gives an overview of different composite materials with their basic mechanical properties.

2.3 Smart materials

Smart materials are known as materials which are able to respond by changing their shape or another properties due to an external stimuli [8, 149, 150] such as temperature, electricity, light, solvent, moisture, and magnetic fields for

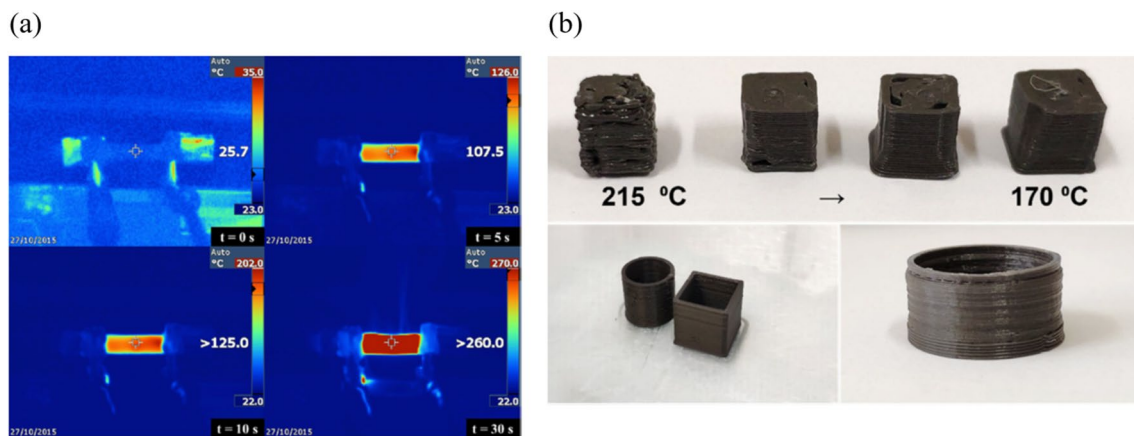


Fig. 14 Infrared thermal imaging of ABS-CNT-06 nanocomposite samples under an applied voltage of 24 V [126] (a) and demonstration of 3D printing of the fabricated magnetic composite filament [127] (b)

Fig. 15 CT images of onyx material printed on the bed: **a** cross-section vertical to printing direction, **b** 3D view, **c** cross-section along printing direction near the upper surface, and **d** near the print bed (i). Bending deformation of a 3D-printed locally bendable CFRP plate specimen (in-phase structure, girder angle $\theta = 60^\circ$) [139] (ii). Cartesian 3D printer modified to print continuous carbon fiber-reinforced nylon filaments (iii) and L-bracket AM part printed with continuous fiber-reinforced composite [140] (iv)

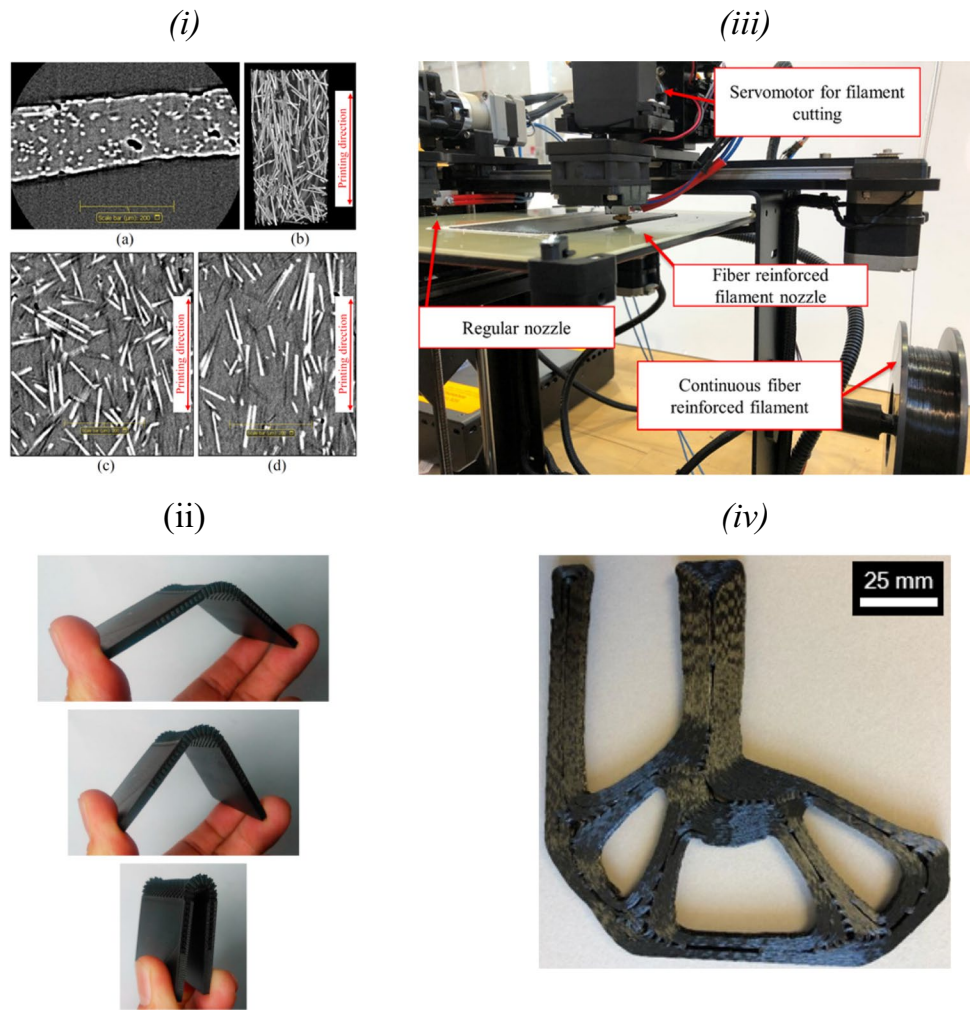


Table 2 Mechanical properties of FDM composite materials

| Polymers matrix | Filler | Tensile modulus | Modulus | References |
|-----------------|--------------------|-----------------|---------|------------|
| ABS | Glass fiber | 58 | – | [141] |
| | Short carbon fiber | 1900 | 28 | [103] |
| | Graphene | 1700 | 31 | [1, 142] |
| | MWCNT | 2000 | 35 | [103] |
| | TiO ₂ | 1708 | 32.2 | [89] |
| | ZrB ₂ | | 32.56 | [103] |
| | Montmorillonite | 3600 | 39.48 | [143] |
| PLA | Jute fiber | 1543 | 25.9 | [89] |
| | Short carbon fiber | 19500 | 185.2 | [144, 145] |
| | Bamboo fibers | | 21.83 | [76, 89] |
| | Graphene | 12.35 | 64 | [96] |
| | MWCNT | 137.4 | 64.0 | [143] |
| PP | Jute fiber | 57.1 | 5110 | [146] |
| | Glass fiber | 50 | 20 | [147] |
| PMMA | Carbon fiber | 1000 | 28 | [72] |
| | Silica | 1160 | 20 | [148] |

example [149]. The smartness of the material makes it able to evolve in a predefined manner over time and has given rise to a new term: 4D printing [150–153]. 4D printing brings the capacity to change the printed configuration with the time, while 3D printing makes static parts [8]. The 4D printing is developed for structures based on both synthetic [149] and natural [153] fillers. Gardan et al. have suggested to classify smart materials in two major groups: advanced structured materials and responsive materials [8]. The advanced structured materials cover complex 3D geometries with predefined or static properties to be attended. The responsive materials can undergo transformations with time and external conditions. The smart materials have brought major improvements and revolutions in terms of applications of FDM. For example, the use of FDM in a (bio) analytical/lab-on-a-chip research laboratory has changed the day-to-day practices [150, 154]. FDM has a key position in comparison to other 3D printing technologies because of its flexibility since it enables combination of several materials and biocompatibility of most of the materials to be used. Salentijn et al. realized microfluidic channel devices with PLA glass and PLA transparent are suitable for microscopic inspection (as shown on Fig. 16).

Another classification of responsive materials consists in dividing them into enhanced smart nanocomposites and shape memory materials (SMM) [150]. Their smartness comes from the fact that they are able to produce electrical charge or voltage when experiencing an externally applied stress and vice versa. Loud speakers, acoustic, imaging, energy harvesting, actuators, transducers, and tissue regeneration are domains where one can find applications of piezoelectric materials. There are recommended for systems that require mechanical flexibility, small active elements, and biocompatibility [150]. There are thermo-responsive materials based on shape memory effect (SME) and have the capacity to return from a deformed temporary shape to an initial shape by the application of external stimulus like

temperature, magnetic fields, light, and moisture. They can be divided into shape memory alloys (SMA), shape memory polymers (SMP), shape memory hybrids (SMH), shape memory ceramic (SMC), and shape memory gels (SMG). Due to their easier printability, light weight, and non-expensive costs compared to other smart materials, SMP are the most popular [7, 149, 155]. Finally, it is important to point out that smart materials start to be deployed in many sectors such as biomedical, textile, electronics, and soft robotics as well as aerospace.

3 Process parameters effect on mechanical properties

FDM is an AM process based on extrusion during which the material is heated and selectively dispensed through a nozzle. In this process, many parameters evolve and the variation of each of them can significantly change the mechanical properties of the obtained parts. These process parameters have been classified in three groups: slicing parameters, building orientation, and temperature conditions [11]. The main challenge that has been investigated by researchers from both academic and industrial areas is to master the tripartite relationship: process-structure-(mechanical) properties. This is necessary for allowing the evaluation of the part suitability for a given application. Figure 17 presents some process variables that can be studied and optimized during part fabrication with FDM process.

Given the significant number of studies dedicated to this issue, some authors tried to summarize the most important research works in this field in the review article such as Mohamed et al. [11], Popescu et al. [12], and Cuan-Urquiza et al. [156] and others [38, 157–159]. In the present work, we focus on the influence of these process parameters on mechanical properties in regard to specific mechanical solicitations (*tensile and compression, flexural and fatigue*)

Fig. 16 **A, B** PLA glass device with sealed fluidic channels, suitable for microscopic inspection. **C** Transparent PLA was used, which gives semitransparency through a limited thickness. **D** The blue solution in the same printed channel can be clearly imaged under the microscope when viewed through the glass bottom

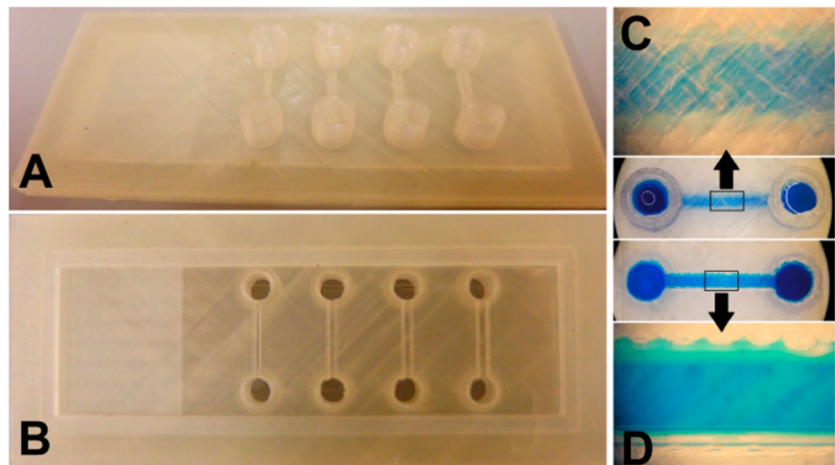
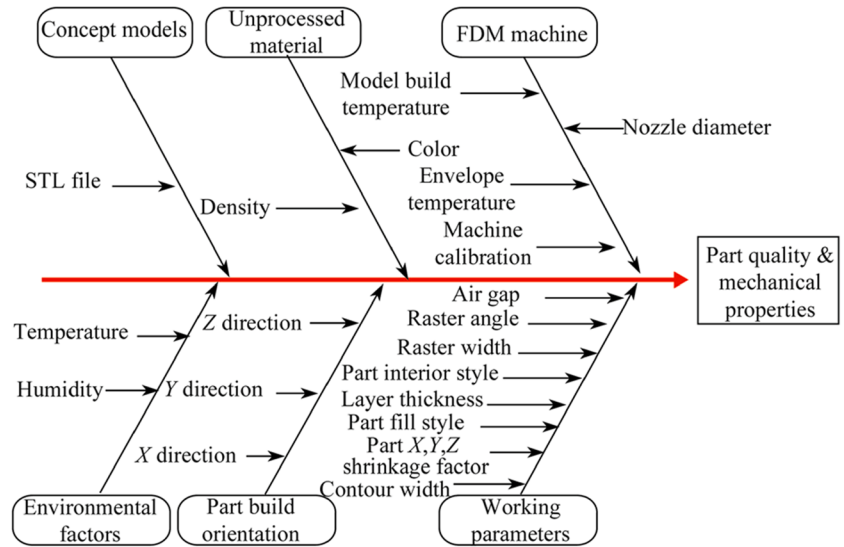


Fig. 17 Cause and effect diagram of FDM process parameters [11]



both in the general considerations and particularly for the materials point of view.

3.1 The effect of the process parameters on the mechanical properties

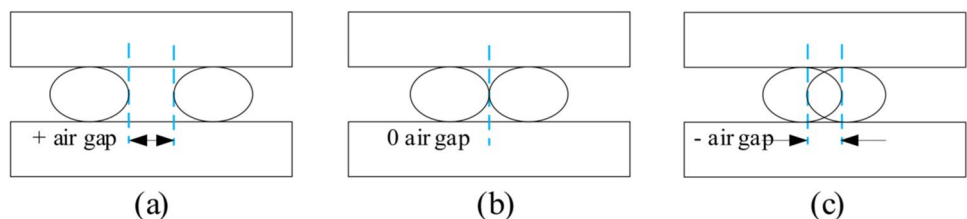
3.1.1 Air gap

The air gap is defect inherent to FDM process and can be defined as the space between two neighboring filaments in a given deposited layer. It results to impossibility to perfectly fill the space by the deposited filament during the 3D fabrication. In the literature, three types of air gap are commonly defined: zero, positive, and negative air gap [160] (see Fig. 18). A zero gap implies that the beads are in direct contact with each other and this type of printing is highly recommended. Positive air gaps allow for spacing between two adjacent layers, resulting in a loose interconnection structure with weak bonding between adjacent filaments, leading to lower strength. A negative air gap refers to the overlap position of two beads with strong interfacial bonding, significantly improving the strength. Depending to the air gap type, the surface quality of the parts can be affected. Negative air gaps lead to *very poor surface quality* compared to their counterparts with positive air gaps that resulted to the overlapping of the filaments and excess material buildup

[161, 162]. The negative air gap also affects the *dimensional tolerance* of the parts [163–165]. In this subsection, the effect of the air gap on each mechanical property is detailed starting with the tensile and compression properties.

Tensile and compression properties Like other process parameters, air gap influences the mechanical properties of the parts [166–168]. The comparison of the effect of different types of air gap on the tensile properties has been made [169, 170]. It was found that the negative air gap significantly enhanced the mechanical properties of 3D-printed ABS parts. However, the positive air gap leads in the alteration of mechanical properties. In another study, the behavior of ABS 3D-printed parts with negative air gap of -0.0762 mm fabricated with different raster orientations (0° , $+45^\circ$, -45° , and 90°) has been studied in tensile strength and compression strength tests. It appears that the negative air gap increases the material strength and stiffness [166]. It has been recommended from this study that the air gap size have to be less than -0.0762 mm. Rayegani et al. have found that ABS printed specimens -0.025 mm present very low surface quality despite the mechanical properties because of overfill [170]. However, the specimens with -0.0025 mm (< -0.0762 mm) present better surface quality and good mechanical properties. Motaparti et al. studied ULTEM 9085 3D-printed specimens with air gap

Fig. 18 Air gap: **a** positive air gap, **b** zero air gap, **c** negative air gap [160]



values of -0.00635 mm, -0.0127 mm, and -0.01905 mm and demonstrate that air gap values have a limited influence on mechanical properties [171]. The printing temperature has a great influence on the porosity ratio and size of air gaps [167]. It has been found that the tensile strength and the elongation at break of PLA tensile specimens were function of printing temperature. The specimens printed at 180°C present the lowest tensile strength while the ones at 260°C have the highest one with the lowest elongation at failure. The bigger air gaps result on very roughness surface in addition of the alteration of the tensile properties [170].

The effect of air gap on compressive strength was studied by Too et al. [172]; it was found that the compression strength decreases with the increasing of air gap. The effect of negative air gap was determined to have no significant effect on the compressive strength [171]. It appears that the impact of air gap both on mechanical properties and surface quality is influenced by other process parameters such as nozzle diameter [173] and layer thickness [164, 174]. The raster orientation has a significant effect on dimensional accuracy compared to surface finishing [174]. These results are also material dependent.

Flexural properties The flexural properties of 3D-printed polymer parts are also affected by the presence of air gap. However, the effect of air gap is moderated compared to the one of other process parameters in the specific case of flexural properties [168, 171]. It has been shown that the negative air gap leads to the improvement of flexural strength of ULTEM 9085 fabricated by FDM [171]. This is justified by the fact that with the negative air gap, the obtained structure is dense and the adhesion between adjacent filaments is also strengthened. It has been also demonstrated that the positive air gap leading to voids in the specimen's volume results in alteration of flexural properties [175, 176]. Mishra has

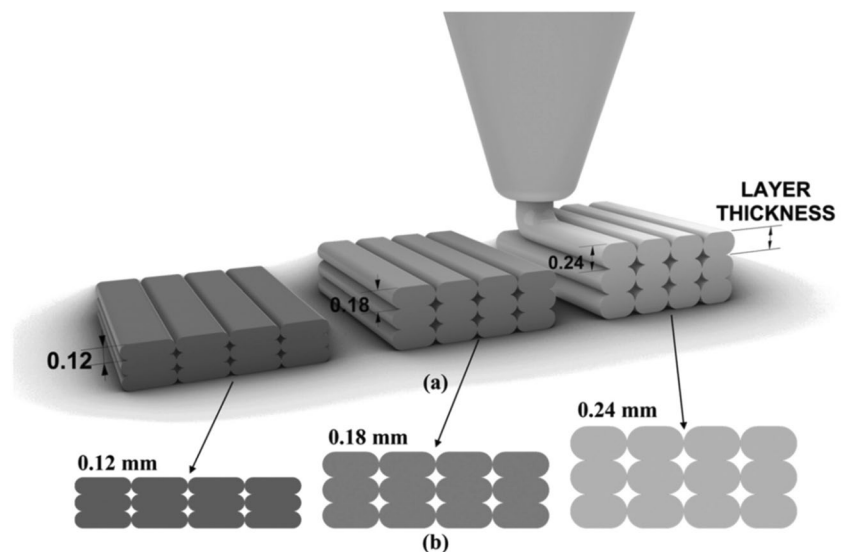
shown that for the optimum set for the process parameter for FDM ABS specimens, the increase of the air gap decreases the flexural strength [176]. Kamoona et al. studied the effect of three process parameters on flexural strength of FDM nylon 12 parts. They conclude that the air gap was one of the parameters greatly decreasing the flexural properties as its values increase [175].

Fatigue properties The impact of air gaps in the fatigue properties of FDM parts has not yet been systematically investigated in the up-to-date literature. The air gaps (voids) are inherent to FDM 3D-printed parts and their consideration in numerical simulation leads to increase the results' accuracy. The influence on fatigue strength reduction factors and fatigue lives has been taken into account in the study of Hassanifard et al. in the case of PLA 3D-printed parts [177]. Mishra et al. have studied the effect of six process parameters on fatigue life of ABS 3D-printed parts under low cycle fatigue tests [178]. Among these parameters, three air gap values 0.0000 , 0.0254 , and 0.0508 mm have been considered in response surface methodology. Air gap and its interactions with the raster width and the raster angle appear like significant parameters affecting the fatigue life, although they are in the second zone of the overall studied parameters. It has been shown that the air gap decreases the fatigue life of the parts.

3.1.2 Layer thickness

Layer thickness also called layer height is the deposited bead cross-section dimension along the vertical axis of the FDM machine (see Fig. 19). The layer thickness is directly related to diameter of the nozzle and the width of the raster. A large number of studies have been made on the influence of layer thickness on the mechanical properties of FDM parts.

Fig. 19 Layer thickness illustration in FDM [179]



Tensile and compression properties Numerous works show that the tensile strength and the young modulus are significantly impacted by layer thickness [4, 79, 180]. Shubham et al. have studied the ABS 3D-printed parts. Five specimens have been printed by FDM following the ASTM D-1708 standard with different layer thicknesses (0.075, 0.10, 0.25, and 0.50 mm). The results show that when the layer thickness increases, the tensile strength is reduced by 46% and impact strength is reduced by 54.5%. However, an exception with layer thickness of 0.5 mm has been observed [4]. Sood et al. [98] have studied the influence of layer thickness by printing ABS specimens following the ASTM: D638 with 0.127-, 0.178-, and 0.254-mm layer thickness and make tensile test. They concluded that the tensile strength was at first lower, but then increased as the layer thickness increased for 0.127, 0.178, and 0.254 mm values. Tymrak et al. [181], from the study did on ABS and PLA by printing through open-source 3D printers and the tensile test perform conforming to ASTM: D638, stated that the lowest layer height resulted in the highest tensile strength for 0.2 and 0.4 mm value of layer thickness for both polymers. Uddin et al. [182] worked on layer thickness effect by studying different values of deposited layer thickness 0.09, 0.19, and 0.39 mm on ABS 100% infilled samples. Thinner layers showed the highest values for stiffness and strength. Globally, the layer thickness up to a certain value (lower than 0.3 mm) can be used to increase the mechanical properties. However, high value of layer thickness (bigger than 0.3 mm) can affect negatively the mechanical properties.

The influence of the layer thickness on the mechanical properties can work in synergy with other process parameters during the part manufacturing. When compared to the layer thickness, the infill showed higher influence [183] because porous structures have lower mechanical properties when compared to their quasi-solid (100% infill) counterparts [40]. A study by Chacon et al. [184] found that the effects of the layer height vary depending on the build orientation of the sample part. In the case of vertical samples, an increase in the layer height resulted in higher strength because of a reduction in the number of layers or, in other words, a reduction in the stress concentration areas. Meanwhile, for vertical and horizontal orientations, variations in the tensile and flexural properties were observed for the layer thickness in the range of 0.06, 0.12, 0.18, and 0.24, indicating that no significant effects were observed. From different studies, it can be concluded that layer thickness is one of the most significant parameter that influences the tensile strength of FDM printed parts [3, 4, 185].

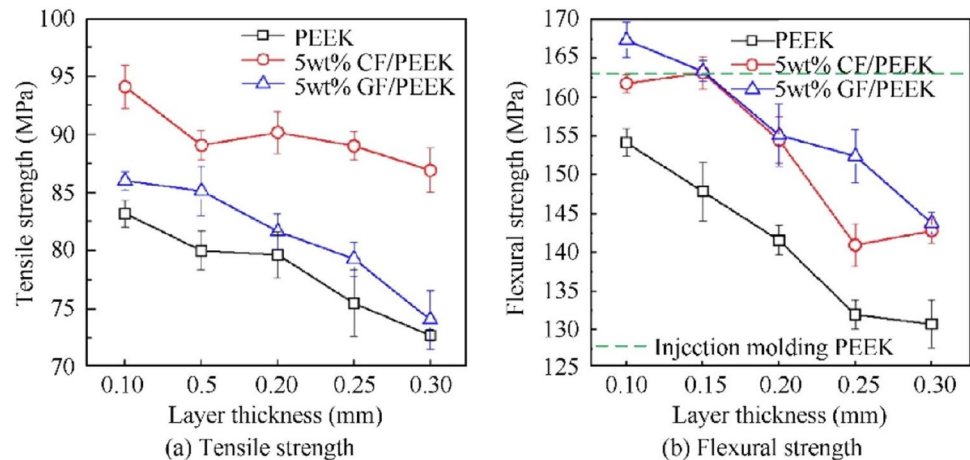
For the compression strength, results show that for compressive behavior, layer thickness is a significant process parameter. Parts fabricated with higher layer thickness present a low compressive strength than that of smaller layer thickness [79].

Flexural properties The flexural strength is greatly influenced by the layer thickness value. Travieso-Rodriguez et al. have shown in their work on 3D-printed polylactic acid parts that the layer height is the process parameter that influence the most the flexural strength [186]. The flexural strength decreases with the increase of the layer thickness for the values from 0.1 to 0.3 mm. Xu et al. have investigated the flexural properties of 3D-printed polyetherketoneketone parts obtained by FDM [187]. The layer thickness considered were from 0.1 to 0.4 mm and both flexural strength and modulus decrease with the augmentation of the layer thickness. However, due to the synergism between process parameters, for the lower infill ratio (0.1 to 0.3), the increase of the layer thickness seems to increase flexural properties [187]. The flexural strength seems also to increase with highest values of layer thickness: 0.5 and 0.6 mm [187]. In their study, Nugroho et al. vary the layer thickness of 3D-printed PLA specimens from 0.1 to 0.6 mm and they observed fluctuation on flexural strength for layer thickness value between 0.1 and 0.4 mm and an increase for the 0.5- and 0.6-mm layer thickness values [188].

Wang et al. delved into the influence of layer thickness, a key FDM-3D printing parameter, on the mechanical properties of fiber-reinforced PEEK composites [189]. To conduct their investigation, filaments composed of 5wt% carbon fiber (CF)- and glass fiber (GF)-reinforced PEEK composite have been prepared. They investigated the tensile strength, flexural strength, and impact strength of PEEK, CF/PEEK, and GF/PEEK printed samples, utilizing layer thicknesses ranging from 0.1 to 0.3 mm. Their findings, depicted in Fig. 20, revealed a noteworthy trend: increasing layer thickness had a pronounced detrimental effect on the mechanical properties of the printed materials, reaching the lowest values for the layer thickness of 0.3 mm. Specifically, the flexural strength of both CF/PEEK and GF/PEEK composites exhibited a reduction of up to 14% as the layer thickness increased from 0.1 to 0.3 mm. Intriguingly, the research underscored that layers thinner than 0.15 mm could significantly enhance the flexural strength of fiber-reinforced PEEK composites, surpassing 163 MPa, which is equivalent to that achieved through injection modeling of PEEK.

Fatigue properties The layer thickness strongly influence the fatigue properties of polymeric parts obtained by FDM [178, 190, 191]. Alshammari et al. have studied the influence of four process parameters on the fatigue crack growth rate of ABS FDM parts with the *dynamic bending vibration tests* [192]. They show that the simultaneous increase of the layer thickness and nozzle diameter could attenuate the fatigue crack growth rate due to micro air void reduction. He et al. found similar results by studying the *bending fatigue performance* of ABS FDM samples under thermo-mechanical loadings with different process parameters [193].

Fig. 20 Effects of layer thickness on mechanical properties [189]



It appears in this study that fatigue life can be increased by using a larger nozzle diameter and thicker layer height. It has been demonstrated in the study of Mishra et al. that the layer thickness has considerable influence after the contour numbers on fatigue properties during the *low cycle fatigue tests* [178]. The interactions of the layer thickness with other parameters like the part orientation and raster orientation cannot be neglected. However, the fatigue life increases with the minimum values of layer thickness and part orientation. The influence of four process parameters (layer height, nozzle diameter, infill density, and printing speed) on lifespan of cylindrical ABS FDM samples during *rotating bending fatigue tests* has been studied [194]. Logically, infill density presents the highest influence on fatigue lifespan. The interaction of the layer height with the nozzle diameter on fatigue properties has been underlined like in the study of Alshammari et al. The fatigue life of PLA FDM samples with rotating fatigue bending machine has been studied [190]. The layer thickness has been shown to be second parameter having the most influence on the number of cycles to failure after the fill density. It is worth noting the strong interaction of layer height and the nozzle diameter and their influence on fatigue properties. Among the studied infill patterns, the honeycomb infill presents the better fatigue lifespans compared to rectilinear infill. A similar study has been conducted with PLA-wood FDM samples [195]. However, the layer thickness was found to be the parameter with the greatest influence on fatigue life for this wood-reinforced PLA composite. The fatigue life increases as the layer height increases. The limitation herein was found by the population of the defects resulting on the increasing of the layer height and nozzle diameter. The influence of process parameters on fatigue properties of PLA FDM samples has been studied in four-point bending and rotating bending tests [191]. It appears that the higher layer height may not consistently improve the fatigue life. According to these studies, it can be concluded that the effect of the layer

thickness on the fatigue properties strongly depends on the nature of the material.

3.1.3 Build orientation

The build orientation defines the part position on the platform in respect of the X, Y, and Z axes and can be presented as a quantitative parameter (angle of axis) or a categorical parameter (ZX-upright, XZ-edgewise, and XY-flatwise) (see Fig. 21). The build orientation leads to anisotropic of mechanical properties of parts obtained by FDM. The influence of the build orientation on mechanical properties of parts has been investigated in the literature and the major findings are summarized in this subsection.

Tensile and compression properties The tensile strength and the strain at failure are greatly dependent on the build orientation [182, 196–198]. According to Zaldivar et al. [197], the tensile strength of ULTEM 9085 3D-printed dogbone specimens is greatly dependent on the build orientation. In addition, specimens with the deposited layers oriented along the tensile direction result in optimum tensile strength. Cantrell et al. [199] and Abbott et al. [200] reiterated the previously mentioned studies and concluded that the impression in the P direction (on-edge) gives the highest tensile strength followed by PTB direction (flat orientation).

The confirmation of these findings can be observed in the research conducted by Gonabadi et al. [201], which investigated the influence of build orientation on the tensile properties of PLA produced using a 3D FFF printer. They revealed a notable fluctuation in tensile strength, elastic modulus, Poisson's ratio, and elongation depending on the build orientation. In Fig. 22, a concise summary of the mechanical test outcomes illustrates the significant variability in PLA's mechanical behavior based on its build orientation. Notably, the "on-edge" build orientation exhibited the highest ultimate tensile strength ($\sigma_{UTS} = 55$ MPa) and elastic

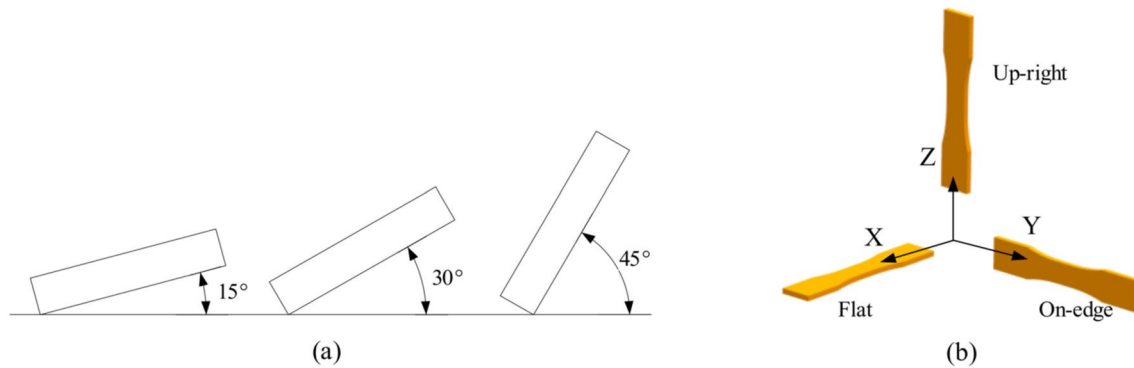


Fig. 21 Build orientation: **a** arbitrary angle, **b** certain angle [160]

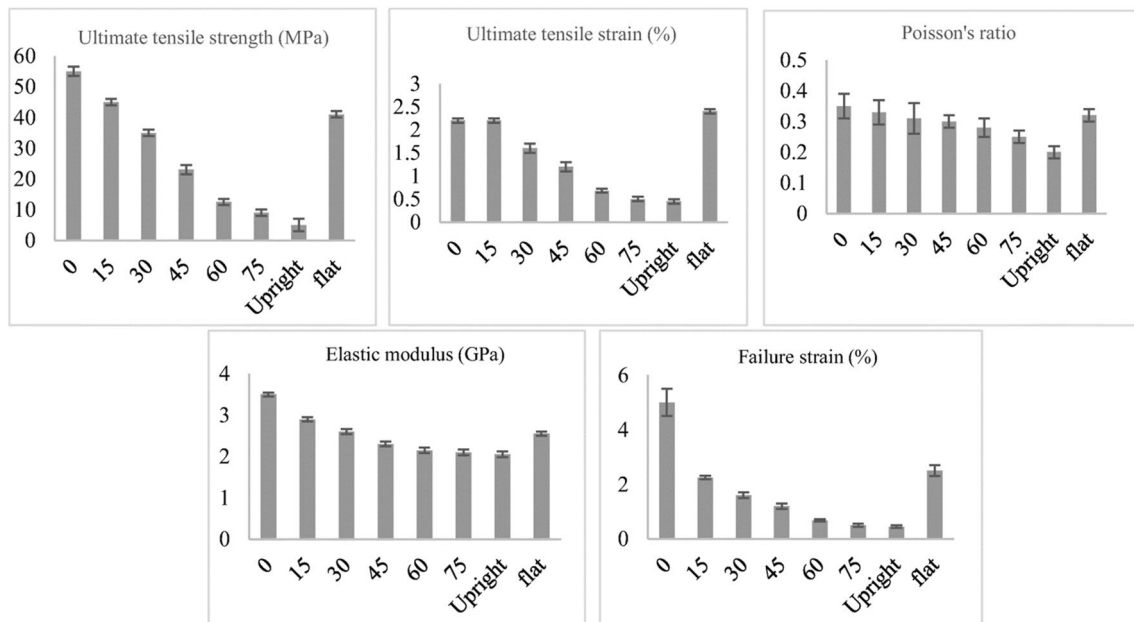


Fig. 22 Tensile properties of 3D FFF-printed PLA as a function of build orientation [201]

modulus ($E_y = 3.5$ GPa) among all orientations tested. Conversely, the “upright” orientation yielded the lowest values, with tensile strength and elastic modulus measuring approximately $\sigma_{UTS} = 5$ MPa and $E_y = 2$ GPa, respectively. Additionally, the “on-edge” orientation demonstrated the highest elongation and Poisson’s ratio, averaging about $\epsilon_{max} = 5\%$ and $\nu_m = 0.35$, respectively. This surpassed both the “flat” ($\epsilon_{max} = 2.5\%$ and $\nu_m = 0.32$) and the “upright” ($\epsilon_{max} = 0.45\%$ and $\nu_m = 0.2$) orientations, signifying a significant enhancement in mechanical properties for the “on-edge” orientation compared to the others.

Furthermore, as the angle of the “on-edge” orientation increased from 15° to 75° , a decrease was observed in tensile strength, elastic modulus, Poisson’s ratio, and elongation (see Fig. 22).

Dul et al. [142] have studied the effect of graphene nanoplatelets in ABS matrix in function of the build orientation. They reported that specimens built in the horizontal direction has the highest tensile properties, followed by the specimen built in the vertical direction and, lastly, in the perpendicular direction. The same finding was reported by Smith et al. [202].

For the uniaxial solicitation, the mechanical properties observed can be affected by the tensile direction depending on the build orientation. Dorigato et al. [126] found that the material exhibited a greater strength in the vertical configuration due to the direction of the sample being pulled along the cross-section of the deposited roads. In another study, Jin et al. [203] claimed that building the samples in the horizontal or vertical directions rarely has an influence on the

resultant tensile strength if the perpendicular or z -directions are not involved. When the deposited layer is perpendicular to the direction of stress, the sample becomes brittle and breaks easily, thus reducing the resulting tensile strength [204]. Chacon et al. [184] also observed that the highest strength and stiffness are obtained in the horizontal and vertical directions compared to the perpendicular direction, which results in brittle behavior. From all these reports, there is, at least, a consensus among researchers that the upright built specimen would have a lower mechanical property compared to an on-edge built or flat orientations.

Flexural properties Several studies showed that the build orientation has an important impact on the flexural properties of FDM parts; the on-edge and flat build orientations present better flexural properties than up-right build orientation [205, 206]. Taylor et al. [206] have studied the effect of build orientation on flexural properties of ULTEM 1010 coupons fabricated by FDM and they evidenced the important interaction of the build orientation and the raster angle on the flexural properties. In this study, the XZY (on edge build orientation) with $\pm 45^\circ$ raster orientation gives the highest modulus and yield strength. Raut et al. [207] have also showed that the maximum flexural strength is achieved with specimens placed at the x -axis 0° build orientation with ABS 3D-printed samples.

These findings align with research previously conducted by Beattie et al. [208]. Figure 23 provides a comprehensive overview of the average flexural modulus, average flexural strength, and elongation at break for each build orientation, accompanied by the standard deviation calculated from five specimens per orientation. One standout observation from this study pertains to the considerable difference in flexural strength among parts printed in the vertical orientation. In comparison to other orientations, the flexural strength of vertically printed parts was notably lower, exhibiting a reduction of approximately 35%. Xu et al. have studied the flexural properties of FDM-printed PEKK specimens. They

showed that the on-edge orientation samples give higher flexural performance than the flat and the upright orientations. The last one presents the lowest flexural properties. The failure modes were also dependent to the build orientation. The influence of build orientation has been studied with Nylon 12 FDM-3D-printed samples. The samples with 0 mm air gap, 30° raster orientation, and 45° Y -orientation (flat) present the highest flexural strength [187].

Fatigue properties The impact of the build orientation on the fatigue properties of FDM parts [209–212] has been found to be considerable. Fischer et al. have studied the fatigue behavior of FDM samples fabricated with Ultem 9085 during tensile fatigue tests [212]. In this study, the effect of build orientation on fatigue properties have been analyzed. For the higher loads, the lifetime of different samples is influenced by the anisotropy resulting to the build orientation similarly to the static tensile bar response. The samples printed in X -direction (edge) presented the longest fatigue lifetime for the maximum stresses (> 15 MPa), followed by the one in Y -direction and Z -direction respectively. For the lower loads which lead to higher fatigue lifetime, the S – N curves of different build orientations converge. The chemical treatment applied in order to ameliorate the surface roughness of the samples improves the tensile strength and has no influence on fatigue behavior. The effect of build orientation on fatigue behavior of PLA 3D-printed samples has been studied during tensile cyclic loading conditions [209]. The stress–strain behavior obtained under cyclic loading is quite different from that under static loading. The samples with the X -orientation (PLA- X) present the highest ultimate tensile strength followed by PLA-45 and PLA- Y . However, the parts with 45° build orientation achieved the highest fatigue life compared to those with X -orientation and Y -orientation. A similar trend was obtained in the capacity to store strain energy. Azadi et al. have studied the influence of printing direction on the bending fatigue

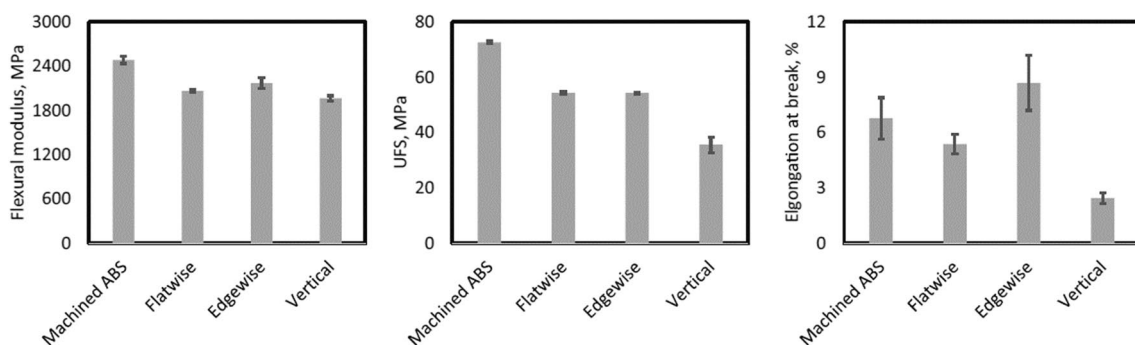


Fig. 23 Comparison of flexural modulus, ultimate flexural strength (UFS), and elongation at break with deviation for three printed orientations and machined [208]

properties of ABS and PLA 3D-printed samples [213]. Standard dog-bone samples were printed in both horizontal and vertical directions and tested during rotating bending fatigue tests. It is worth noting that under low stress levels, the author shows that the bending fatigue lifetime of horizontally 3D-printed ABS samples was higher than that of vertical samples, while under high stress levels, the flexural fatigue behavior is similar for samples printed in both directions for the two materials. For the PLA samples printed in horizontal direction, the average fatigue lifetime is improved at different stress levels 5, 10, and 15 MPa compared to vertical ones of 813%, 557%, and 1104% respectively. The PLA samples present better fatigue lifetime compared to the ABS samples. It appears that the significant parameters influencing the fatigue lifetime in addition to the printing direction are the material used and the stress levels. The influence of build orientation on the flexural fatigue behavior of PC FDM samples has been investigated experimentally and numerically [210]. It appears that the build orientation influences significantly the fatigue behavior. This could be explained by the inner anisotropy generated by the build orientation. The samples printed in the YZ orientation present the highest fatigue lifetime. It has been also demonstrated that the variations of stress ratio (R-1 or R-0.5) impact the numbers of cycles to failure. For the low stress levels, the fatigue lifetime of the samples of XY and YZ directions is similar. However, the observed failure behaviors were clearly different. Hassanifard et al. have studied the influence of build orientation based on the Ramberg–Osgood model of stress–strain curves of type C for FDM parts of different materials [214]. The fatigue parameters have been calculated from original data of Ultem 9085 [212], PC [210], and PLA [209]. The effects of build direction (XY, YZ, and XZ) on fatigue parameters have been implemented for Ultem 9085 and PC. It appears that regardless to the differences of experimental conditions and specifications of these two materials, the XY and XZ build directions respectively

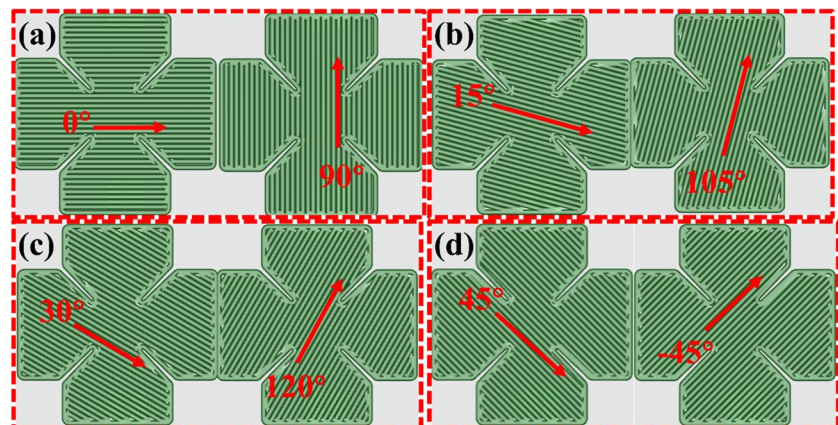
present the strongest and weakest fatigue strength in both low and high cycle fatigue regimes. However, the variation of stress ratio (R-1 and R-0.5) do not impact the fatigue strength or the ductility exponents of the PC FDM samples. Terekhina et al. have investigated the influence of build orientation on the flexural quasi-static and fatigue behavior of PA6 FDM samples [211]. The anisotropy of the fatigue properties follows similar trends to the ones of the quasi-static properties. The samples with the XZ build orientation present the highest fatigue properties.

3.1.4 Raster angle

Raster angle, also called raster orientation, plays an important role in improving the mechanical properties of FDM 3D-printed parts. The raster angle defines how each layer is oriented while printing the desired shape [215]. Figure 24 shows examples of raster orientation. Commonly, the default orientation angles of FDM printed parts are made at 0° , 90° , -45° , and 45° alternately, layer by layer. Raster orientation may contribute to the anisotropic behavior of FDM parts, where the properties of the parts depend largely on the chosen raster orientation [38].

Tensile and compression properties Many studies have been done in order to investigate the effect of raster orientations on tensile strength. Commonly, 0° raster orientation is considered aligned to tensile direction. It has been proved that 0° raster orientation produces the maximum tensile strength [216]. Es-Said et al. [217] have analyzed the influence of raster angles on tensile properties of ABS parts manufactured by FDM; it was shown that the raster angle of 0° leads to the best tensile strength. The ductility is also closely related to the raster orientation, and the $\pm 45^\circ$ raster orientation samples exhibit the highest fracture strain values. The failure mechanism of a part under tensile loading depends on the raster angle. It was demonstrated that the failure of samples made with 0° raster angle occurred from the raster fracture

Fig. 24 Raster orientations of samples **a** $0^\circ/90^\circ$, **b** $15^\circ/105^\circ$, **c** $30^\circ/120^\circ$, **d** $\pm 45^\circ$



while an interlayer failure is observed on samples made with 90° raster angle. The failure mechanisms of 3D-printed specimens in tensile loading are mainly driven by the raster angle and the build orientation [38].

Beyond the failure mode which strongly depends on the raster angle, the effect of the latter on the mechanical properties may be lower. In fact, many studies claim a limited influence of raster angle on the elastic properties (elastic modulus) [199, 216, 218]. Cantrell et al. proved that the effect of raster orientation on 3D-printed ABS specimens is limited compare to similar 3D-printed PC samples [199]. It has been also mentioned the limited effect of the printing angle on mechanical properties of 3D-printed PLA [199]. Similar observations can be followed on the study of B. Gülçimen Çakan where four different materials are 3D printed [216]. It can be concluded that the effect of raster orientation on mechanical properties depends on the used material.

Flexural properties The flexural properties of FDM parts can be modified by the raster orientation. The flexural strength of 3D-printed PLA parts shows the best values for the raster orientation of 0° [219]. Christiyan et al. [220] have studied the flexural properties of PLA 3D-printed samples with an infill density of 40%. Similar results were obtained; the highest value of the flexural strength was obtained at the raster orientation of 0°. This performance was explained by the good layer bonding due to the small value of deposited

layer thickness. The flexural properties of ABS 3D-printed samples have been studied and similar trends observed in PLA 3D-printed samples have been obtained. The influence of the raster angle has been evaluated on the in-plane and edgewise flexural properties of ABS samples [221] and the best performance have been obtained with the samples with 0° raster angle. The same trends have been obtained in the case of samples fabricated with layers of composite materials. These materials are obtained from industrial wastes and the matrix is constituted of recycled ABS. The flexural properties of composite material constituted with ABS matrix reinforced with carbon fiber seems to less depending to the raster angle [222]. The impact of the raster angle of ULTEM 9085 3D-printed samples on the flexural properties has been evaluated [161]. The works of Gebisa et al. [161] using the design of experiment method showed that the best flexural properties are obtained with a 0° raster and that flexural strength, flexural modulus, and flexural strain tend to decrease with the raster angle evolution from 0° to 90°.

In a recent study conducted by S. Srinivasan Ganesh Iyer and O. Keles, they explored how varying the raster angle affects the mechanical properties of short-carbon-fiber reinforced (SCFR) thermoplastics [223]. The study included a range of raster angles, counting 0°, 15°, 30°, 45°, 60°, 75°, and 90°, and involved conducting tests for tensile strength, flexural strength, and fracture toughness on the SCFR ABS material. The findings, as illustrated in Fig. 25, revealed noteworthy trends. When transitioning from a 0° to a 15°

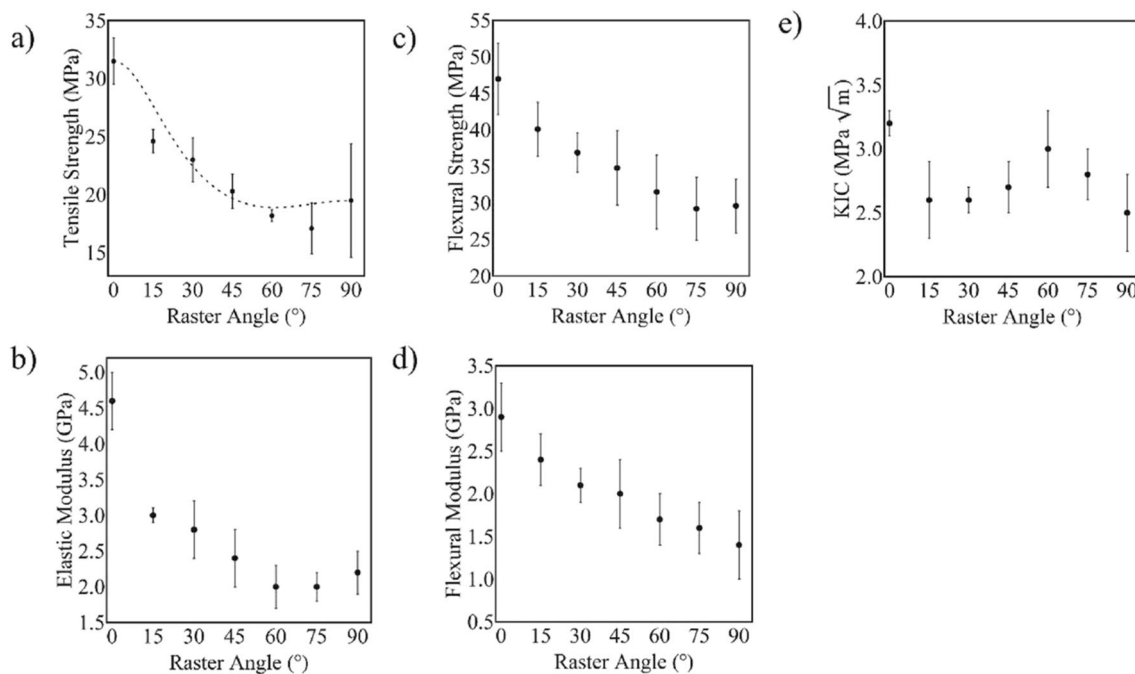


Fig. 25 Variation of mechanical properties with raster angle: **a** tensile strength, **b** elastic modulus, **c** flexural strength, and **d** flexural modulus [223]

raster angle, both tensile strength and elastic modulus experienced a reduction ranging from 22 to 35%. Conversely, flexural strength demonstrated a higher tolerance to changes in raster angle, consistently surpassing tensile strength by at least 50% across different raster angles. Meanwhile, flexural modulus consistently lagged behind elastic modulus by approximately 15%. The relationship between fracture toughness and raster angle was non-linear. Maximum fracture toughness was observed at raster angles of 0° and 60°, indicating a unique pattern. This increase in toughness was attributed to crack deflection mechanisms.

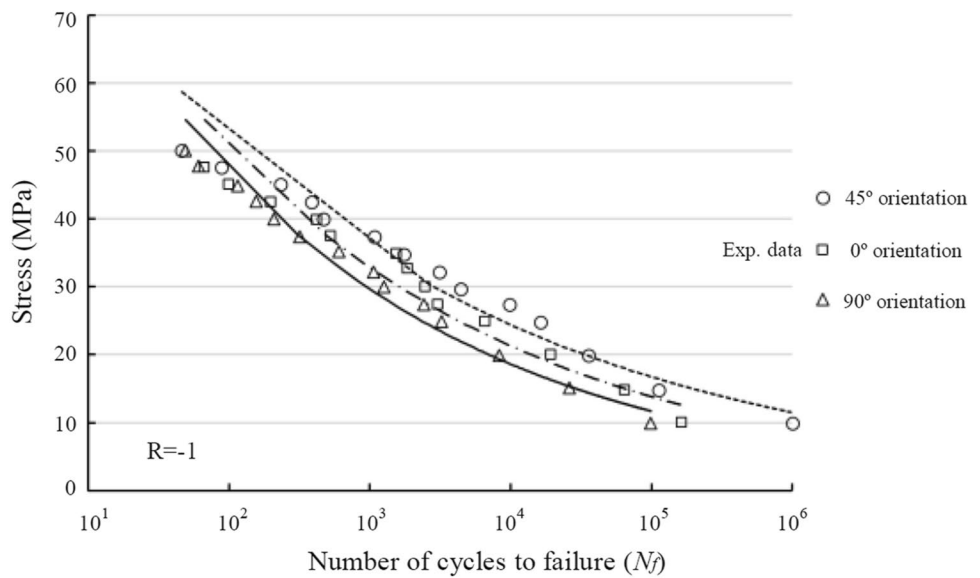
Fatigue properties Among the printing parameters, raster orientation has a considerable impact on the fatigue behavior of FDM samples [177, 224–226]. Ziemian et al. have studied the effect of raster orientation on the tensile behavior and the fatigue performance of ABS FDM samples during tension-fatigue tests [224]. Anisotropic behavior was found in both tensile strength and fatigue performance. Although the highest tensile strength was obtained with 0° raster orientation, the $\pm 45^\circ$ raster orientation presents the largest number of fatigue cycles to failure on average at each normalized stress level. This fatigue life performance of $\pm 45^\circ$ raster orientation was followed by the 0°, 45°, and 90° raster orientations. It also appears that the direction of the layers in regard to the stress axis and the defect orientations (air gaps and porosities) have an influence both on tensile properties and fatigue performances. The fatigue performance of ABS FDM samples was studied during sinusoidal tension-tension fatigue loading with the applied stress normalized to the ultimate tensile strength (UTS) of each raster orientation [226]. At the same percentage of UTS, the studied raster orientations ($\pm 45^\circ$ and 0°/90°) failed approximately at equivalent number of cycles. The author concluded that a failure mechanism inherent to FDM process may explain these observations. However, at the same absolute stress, the $\pm 45^\circ$ raster orientation shows a higher number of cycles to failure. This result is consistent compared to the one obtained in [224]. Hassanifard et al. have investigated the influence of fatigue crack growth (FCG) rate of ABS 3D-printed parts during dynamic bending vibration tests [227]. In this study, the effect of environmental temperature on FCG rate has also been investigated. It was found that the raster orientation affects both the fatigue life and the Paris power law constant C and m. The FCG rate is accelerated in samples with 90° raster orientation and also with the increased of temperature. The fatigue performance of ABS 3D-printed samples have also been evaluated during bending fatigue tests in different environmental temperatures (between 50 and 70°C) by varying the printing parameters [193]. It has been shown that the raster

orientation influence on fatigue properties was at the second level after the thermomechanical loading among the considered parameters. The longest fatigue lifetime was obtained with the samples fabricated with 0° raster orientation. The printing defects have been found to greatly affect the fatigue lifetime. Ezech et al. have investigated the fatigue strength of PLA 3D-printed samples fabricated flat on the build-plate by varying the raster orientations and the superimposed static stresses [228, 229]. It has been found that the raster orientation influence on fatigue strength of PLA FDM samples can be neglected in regard to the relative low values of scatter ratio of the endurance limit for different raster orientations. It also appears that the effect of non-zero mean stresses on AM PLA can be access by performing the fatigue assessment in terms of maximum stress in the cycle. The related failure mechanisms to the fatigue behavior of PLA 3D-printed samples are filaments cracking, filament debonding, and layer debonding. Then, in regard to fatigue design, AM PLA can be considered like a homogeneous and isotropic material. In the two previous studies of fatigue performance of FDM PLA, the interactions of raster orientation with other printing parameters have not been considered. The fatigue life of PLA 3D-printed samples has been analyzed experimentally and numerically by considering the raster orientation and printing defects [177]. For doing that, the notched and un-notched samples have been studied during the cyclic tensile tests. It has been shown that the raster orientation had a considerable impact on fatigue reduction factors and fatigue lives. The un-notched samples printed with 0° raster orientation presented higher fatigue lives as compared with the notched ones. However, for the samples with 90° raster orientation, there is no significant difference in fatigue life between the notched and un-notched samples. This is because the stress concentration resulting from the FDM process reacts as sharp notches. By considering the voids between the filaments, the fatigue life predictions obtained with the volumetric approach agreed with the experimental results.

Another study has demonstrated that, when designing for fatigue life, the 45° raster orientation is advisable, especially for extended fatigue life in PLA 3D-printed samples [214]. Conversely, the 90° raster orientation exhibited the lowest fatigue strength in this particular configuration (see Fig. 26).

The fatigue life and the fatigue crack rate have been studied for PLA samples obtained by FDM during the rotating bending fatigue tests combined the variation of environmental temperature [225]. It has been shown that the raster orientation has a great impact on fatigue properties. In fact, the fatigue life depends on infill pattern or the defects related to the infill pattern rather than the thickness of the outer wall of the printed samples.

Fig. 26 Fatigue test data of 3D-printed FDM-processed parts of PLA. The S–N curves have been reproduced by Soran Hassani Fard and Seyed M. Hashemi [230] based on the data available in Todd Letcher and Megan Waytashek works [231]



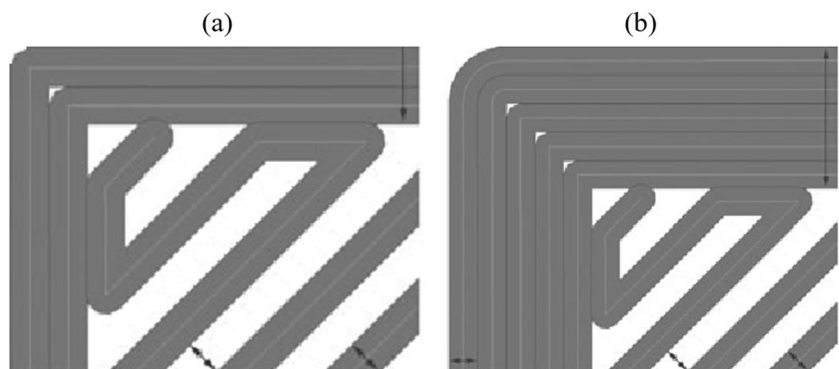
3.1.5 Contours number

The number of contours represents the number of closed roads that are deposited along the edge of the part (see Fig. 27). The contours can be considered the exterior structure and the infill like the inner structure of the part [232]. Like other process parameters, the number of contours affects the mechanical properties of FDM parts.

Tensile and compression properties It appears that there is a consensus between most of the studies that the increase of the number of contours is beneficial for the tensile properties of the FDM 3D-printed parts [233–235]. Croccolo et al. [236] have studied the effect of the number of contours on static strength and stiffness of ABS parts. They showed that, as the number of contours increased, greater elastic modulus and higher maximum strength are obtained. However, increasing the number of contours decreased the percentage of elongation to failure. They have also proposed an analytical model considering the number of contours in the prediction of strength and stiffness properties. The

mechanical performance of PLA 3D-printed samples has been assessed through experimental and numerical methods, considering both the external contours (number of contours) and the inner structure. The correlation between experimental and numerical results has been achieved by considering isotropic and anisotropic the behavior of external contour and inner structure respectively [232]. In another study on PLA 3D-printed samples, Taguchi method has been used to investigate the tensile properties [237]. The authors found that the number of contours impacts the tensile properties at the second level after the build orientation, the nozzle diameter, and the infill density. Despite this observation, the tensile strength increases with the number of contours until a certain value and starts to slightly decreases. Artificial neural network has been used for predicting the effect of process parameters on tensile strength, build time, and surface roughness of PLA 3D-printed samples [235]. It has been found that the build orientation leads to the highest modifications in tensile strength followed by the number of contours. As the number of contours increases, the tensile strength also increases. The interactions of these process

Fig. 27 Contour number: two contour (a) and five contour (b) [231]



parameters with the layer thickness and the raster angle have been evidenced. Similar observations have been obtained by Rashed et al. with the PEKK 3D-printed samples [234]. In the studied process parameters, the build orientation and the number of contours present the most significant impact on tensile strength. In the case of soft-elastomers, the number of contours seems to influence the tensile properties of the FDM 3D-printed parts at the second level [238]. The barrel temperature and the raster orientation have been found to have most significant influence on the ultimate tensile strength and percentage of elongation of the ethylene vinyl acetate (EVA) 3D-printed samples. However, the UTS increases with the increase of the number of contours until a certain value; a small decrease is observed. The elongation is altered with the addition of the number of contours. In the case of 3D-printed TPU-based elastomers, the number of contours played an important role in the integrity and strength of the parts [239]. It is clear that among the large number of process parameters, the number of contours is one of the most impacting the tensile strength of the FDM 3D-printed samples.

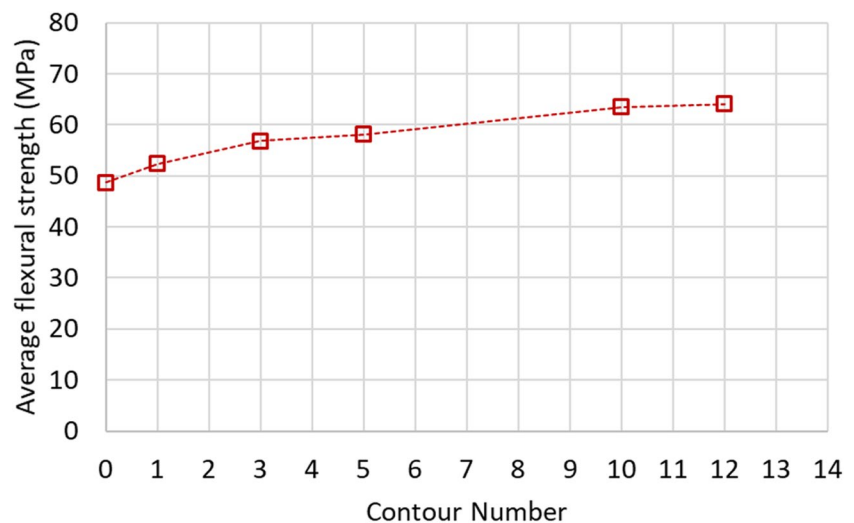
Flexural properties The study of Wagari et al. [161] shows that the contour number has a strong effect on the flexural properties, flexural strength, and flexural strain, of the material. Their result shows that increasing the number of contours from low (one) to high (five) significantly increases the flexural properties of the material. This is due to the fact that by increasing the number of contours, the length and number of rasters are reduced. Thus, the load applied is mainly supported by the contours rather than the raster (inner infill), which improves the performance of the material. The effect of the number of contours is much more visible on parts produced with a 90° raster angle than on parts in the other direction [161]. Similar results were obtained by Mohamed et al. by varying the number of contours. It was increased from

one to ten in the PC/ABS blend 3D-printed samples [240]. The PLA–alumina composite was used to fabricate samples by FDM and the impact of the process parameters both in tensile and in flexural properties has been studied [241]. It has been observed that the number of contours is the second most important parameter which affect the ultimate flexural strength (UFS). As the number of contours increases, the UFS also increases due to the reduction of defects and the improvement of bonding between adjacent contours. However, in the case of high-performance thermoplastic, PEKK, nonlinear variations were observed in flexural properties by changing the number of contours [242].

In their study, Mishra et al. emphasized that the number of contours is the most influential parameter impacting the flexural properties of ABS 3D-printed samples [176]. To investigate the effect of varying the contour number, all other process parameters, including layer thickness, part orientation, raster width, air gap, and raster angle, were held constant at 0.254, 0°, 0.4814, 0.000, and 0°, respectively. A total of six experimental sets, each comprising three test samples, were meticulously executed to analyze the correlation between contour number and flexural strength. As illustrated in Fig. 28, the findings reveal that an increase in contour number corresponds to a notable enhancement in flexural strength. This positive effect can be attributed to the addition of an external perimeter, which effectively relocates the stress concentration zone from the outer edge to the center of the specimen, resulting in increased stiffness and consequently improved flexural strength.

Fatigue properties Until now, very little attention has been given to studying the influence of the number of contours on the fatigue properties of 3D-printed parts. Mishra et al. studied the influence of the contour number on fatigue life of ABS 3D-printed parts during low cycle fatigue tests [178]. The contour number appears like the most significant

Fig. 28 Effect of the number of contours on the flexural strength of FDM 3D-printed ABS. This curve has been reproduced using the data from the studies conducted by Mishra et al. [176]



parameter affecting the fatigue life. The interaction of the contour number with raster angle affects also the fatigue properties. Similar results in the significance effect on contour number have been obtained by Chowdary et al. with PLA [243]. These observations can be explained by the fact that the increase of the contour number reduces the inner infill length, then the defects and shifts the stress concentration from the outer boundary of the parts to the center. The risk of the earlier failure of the samples is then reduced.

The influences of FDM process parameters depends also on type of materials that is used. In the following paragraphs, we will look at their impact on standard materials firstly, secondly on composites materials, and finally on smart materials.

3.2 The effect of the process parameters on mechanical properties of materials groups

3.2.1 Process parameters effect on mechanical properties of standard materials

Thermoplastic materials are used for part fabrication via fused deposition modeling (FDM) process. The mechanical properties of the obtained parts are greatly influenced by the process parameters during the fabrication. To optimize the fabrication process and part engineering, it is crucial to understand the relationship between part fabrication (process parameters), part structure, and mechanical properties. During the last decades, several studies aim to elucidate this subject [3, 12, 160, 184, 215, 244–249]. Many reviews articles also bring some insights in this topic [38, 160]. The primary process parameters influencing the mechanical properties of the FDM parts have been identified and are now well-established: air gap, build orientation, extrusion temperature, infill density, infill pattern, layer thickness, raster width, raster angle, and print speed [160]. The classification of these parameters in regard to their influence in mechanical properties has been proposed in several studies [3, 12, 52, 160, 248]. For instance, build orientation has a more significant influence on mechanical properties compared to other parameters like air gap or raster angle [52, 244]. In another study, it has been concluded that the layer thickness is the parameter having the most important influence on strength properties [248]. However, it is worth noting that there is an interdependence between process parameters. The influence of these parameters is almost analyzed separately; the evolutions of two or more parameters are not often considered.

Some studies have focus on specific thermoplastics, in order to synthetize the effect of the process parameters on their mechanical properties. The impact of process parameters on mechanical properties of ABS has been analyzed [245, 250]. Kaur et al. have reviewed the impact of process

parameters on the tribological properties of ABS parts obtained by FDM [251]. Other review articles have been conducted in the case of PLA [184, 246].

The most investigated polymers in the studied literature are in this order: ABS, PLA, PEEK, PC, and PEI [12]. ABS and PLA are the most used polymers in FDM. The results with ABS exhibit less variability compared to PLA. The parts made from PLA behave more rigidly than ABS. However, there is no clear trend regarding the influence of the parameter's choice on the strain at failure, unlike ABS, which exhibits ductility sensitive to printing parameters. Some of experimental results for tensile strength and tensile modulus are summarized in Table 3. It shows clearly that 3D printing process parameters have a significant effect on the tensile properties of the obtained materials.

3.2.2 Process parameters effect on mechanical properties of composite materials

Incorporating reinforcements like fibers, pellets, particles, or powders into a thermoplastic matrix can enhance the

Table 3 Influences of FDM process parameters on tensile properties

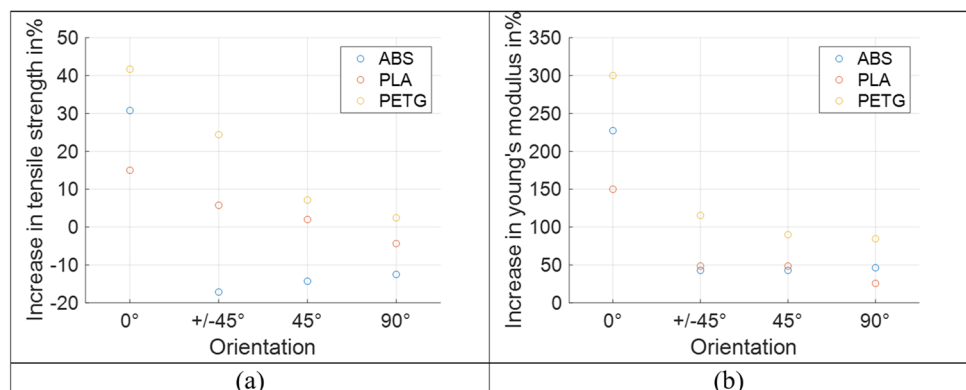
| Material | Process parameters | Tensile strength (MPa) | Tensile modulus (GPa) | Reference | |
|----------|--------------------|------------------------|-----------------------|-----------|-------|
| ABS | Layer thickness | 00 | 36 | [4] | |
| | | 0.75 | 27.5 | | |
| | | 0.1 | 24.9 | | |
| | | 0.25 | 21.0 | | |
| | | 0.5 | 19.2 | | |
| | Raster angle | ± 45° | 38 | [252] | |
| | | 0°/90° | 41 | | 0.712 |
| PLA | Raster angle | 0° | 68 | [253] | |
| | | 45° | 67.12 | | 5.08 |
| | | ± 45 | 62.11 | | 4.98 |
| | | 0°/90 | 57.89 | | 4.86 |
| PC | Raster angle | 0° | 19 | [204] | |
| | | 90° | 59.7 | | |
| | Part orientation | X | 45.9 | | 2.1 |
| | | Y | 54.6 | | 2.41 |
| | | Z | 45.6 | | 2.26 |
| | | X + 45° | 45.5 | | 2.13 |
| | | Y + 45° | 53.3 | | 2.32 |
| Z + 45° | 36.0 | 2.18 | | | |
| PP | Raster angle | 0° | 34 | [42] | |
| | | 90° | 26 | | |
| PEEK | Part orientation | H-0° | 82.58 | [104] | |
| | | H-90° | 72.88 | | 3.54 |
| | | V-90° | 9.99 | | 3.03 |

tensile properties of printed parts [107, 108, 138]. Fibers of different natures such as carbon fibers, glass fibers, natural fibers or others with different lengths (nano, short, or continuous) can be incorporated in the matrix [254]. The mechanical properties of the obtained parts are once again strongly dependent on the parameters used during the 3D printing process [59, 108, 254, 255]. Reports indicate that part anisotropy is closely linked to the alignment of fibers with the printing direction [256–258]. It was shown that improvement can be made by working on the printing orientations [256, 258]. Tekinalp et al. found that the FDM process produces parts with high fiber alignment along the print direction and with better tensile properties [258]. In this case, the high tensile strength of the carbon fiber greatly contributes to the increase in the mechanical properties of the carbon fiber (CFF) polymer test coupons. Jiang et al. [256] studied the effect of the addition of carbon fibers on the tensile properties of PLA, ABS, and PETG test samples as function of print orientation. This shows that when the print orientation aligns with the tensile axis, the addition of carbon fiber leads to the most significant improvement in mechanical properties. Figure 29 is made using the results for tensile strength and tensile modulus found by Jiang et al. [256]. This figure shows the relative increase in percentage of CFF polymer test samples compared to the unfilled polymer test samples. CFFPLA at 0° print orientation have the greatest strength and modulus values, and CFF PETG at 0° print orientation yields the greatest strength and modulus improvement. In general, CFF test samples at the 0° print orientation give the greatest strength and modulus improvement relative to their unfilled counterparts, for all the tested materials. CFF polymer test samples at 90° print orientation gives the least improvement, for all the tested materials. It has been found that the tensile strength can be improved by using an important number of contours and maximum infill percentage in addition with a good combination of other parameters such as printing speed, raster distance in order to reduce the air gap population, and nozzle and bed temperature [254]. It should be noted that the additional physical

properties brought by the presence of the reinforcements are also impacted by the fabrication parameters. It has been also demonstrated that the parts with continuous carbon fibers exhibit better mechanical properties than their counterpart with short carbon fibers [255]. However, the parts with the continuous fibers present more difficulties during the 3D printing process.

Glass fibers are also used to reinforce thermoplastic polymers in order to improve their mechanical properties and lead to lightweight structures [109, 259]. The composites with glass fiber present excellent resistance effect [260]. The impact strength of onyx glass fiber–reinforced composites manufactured by FDM has been studied [260]. The printing pattern and the infill density influence on the mechanical properties have been evaluated. The parts with hexagonal pattern present the maximum energy absorption compared to their counterparts with triangular and rectangular patterns. By adding glass fibers into the polymer matrix, the tensile properties can be improved. The impact of some process parameters on the tensile properties has been investigated [45, 259]. It has been evidenced that the addition of glass fibers in nylon matrix improved the strength and stiffness of the obtained composites [259]. These mechanical properties are enhanced with the increase of fiber content until a certain limit. Moreover, contrary to parts made with pure thermoplastic polymers, the layer thickness influence on mechanical properties has been found minor. Another study reported remarkable mechanical properties for 50% of glass fiber yarn content in PLA matrix [45]. The incorporation of glass fiber in ABS polymer has shown an increasing of strength and tensile strength [261]. For example, in this study, the tensile strength was increased to 57% by adding 30% in weight percentage of short glass fiber in ABS compared to pure samples made with pure ABS. A similar result was found when adding glass fiber to PP [71, 147]. The influence of the recycling in short glass fiber–reinforced polypropylene composites has been investigated. It has been demonstrated that the mechanical properties

Fig. 29 Tensile properties improvement as function of print orientation: **a** tensile strength, **b** tensile modulus. (This figure is made by using Jiang et al. [256] experimental results)



of 3D-printed parts obtained from recycled materials are lower compared to the counterpart made with virgin materials [262]. Carbon fiber and glass fiber have been used in polyamide matrix. It has been shown that the mechanical properties of printed parts incorporated with CF fiber were higher than GF [263]. The flexural properties of glass fiber-reinforced polymer composites are strongly improved [264, 265]. The tensile and flexural properties of continuous glass fiber-reinforced PLA composites have been enhanced for more than 200% with a fiber content inferior to 7% [265]. The comparisons were made with the mechanical properties of PLA samples. The flexural properties of carbon fiber- and glass fiber-reinforced polymer have been evaluated by I. M. Alarifi [264]. He found that glass fiber-reinforced nylon composite exhibits highest stiffness at room temperature. Furthermore, the effect of the fiber reinforcement on mechanical properties of composite materials is highly sensitive to the length of the fiber: short, long, or continuous fibers [266, 267]. The reinforcement with short fiber is made by adding the fiber particule into the molten thermoplastic polymer. The fiber orientation has in this case an effect on the mechanical properties [267]. The orientation of fiber in the filament is dependent on the printing parameters. For continuous fiber, the printing is done by co-extrusion method or uses dual-head printers [268]. It has been proved that continuous fibers significantly improve the mechanical properties than short fibers and are widely used in aerospace industry [215, 269].

Despite the difficulties in the printing process and the limitation in mechanical properties [270–272], *natural fibers* present many advantages like biodegradability, renewability, and low cost. The natural fibers constituted good candidate for sustainable manufacturing and are then used for the fabrication of 3D-printed biocomposites [272–274]. The main challenge in 3D-printed biocomposites is the optimization of mechanical properties [271, 275] by insuring the good adhesion between the natural fibers and polymeric matrix and by considering the physical properties of the fibers like hydrophilic characteristics and chemical sensibility [135, 270]. The fabrication of biocomposites reinforced with natural fibers by FDM is at the stage of development. Actually, most of studies focus on the printing feasibility depending on filler used [276, 277]. Then, important attention has been concentrated in the investigation of the influence of fiber treatment, of the filament fabrication process, and of the addition of agents in the printability and mechanical properties [278–280]. The effect of natural fibers ratio in the mechanical properties of the biocomposites has been studied [276, 277, 281, 282].

However, systematic studies of the effect of the process parameters on the mechanical properties are limited in the

literature [271, 283–285]. It is worth noting that PLA is the most used polymer in biocomposites materials [286].

3.2.3 Process parameters effect on mechanical properties of smart materials

Smart materials development can lead to programmable material for actuation or motion following a pre-determined sequence, which could be defined through a physics-based model to act accordingly of external stimuli. Numerous additive manufacturing techniques have been employed in the literature for the fabrication of smart materials. Beyond these techniques, FDM occupies a prime position thanks to its many advantages. FDM allows, for example, a pre-programmable step which can be tuned by varying process and design parameters. Some studies have investigated the influence of FDM process parameters on these dynamic properties. The process parameters which are able to modify the response or the actuation of smart materials during their fabrication depend on the specific response of the structure and also to the material(s) used [287–289].

Shape memory materials constitute an important range of materials used in the fabrication of smart materials. *Shape memory copolymers* can be used for the 3D manufacturing of smart materials which display interesting shape memory properties [287]. C.-Y. Cheng et al. fabricated a copolymer constituted by PLA and PLC. They demonstrate that the quality of shape-memory properties can be tuned by the composition of the copolymer and the printing speed. Son Thai Ly and Joo Yong Kim [290] have worked on FDM process with thermal-responsive shape memory polymers (SMP). They have shown that the behavior of shape memory polymer composite constituted by polyurethane-based carbon nanotube is influenced by some process parameters like layer thickness and printing temperature [290].

4D bioprinting has gained important attention in the development of *smart biomedical devices* [291–296]. The main advantage of the development of 4D bioprinting is the facility to propose well-adapted patient-specific equipment devices. In their review, after presenting the principal materials sensitive to different external stimuli, the authors discussed their applications in tissue engineering, drug delivery systems, and medical devices [291]. In another review, the 4D bioprinting applications have been discussed and classified in five categories like cell growth and tissue engineering, antimicrobial, drug delivery, stimulus response, and theragnostic [292]. Shape memory polymers can be also employed for manufacturing smart biomedical devices [291]. V. K. Tiwary et al. have studied the combined effect of process parameters like layer thickness, the infill strategy and the printing in the surface quality of 3D-printed medical implants. The effect of three different post-treatment have also investigated, chemical vapor bath, sand paper polishing

and chemical treatments [297]. S. Boularaoui et al. have investigated the effect of printing parameters on cell viability during the extrusion-based bioprinting. The mechanical force specifically shear stress and the dimensions of the nozzle (needles) are the parameters impacting the most the cell viability during the fabrication process. Other parameters like the pressure, the temperature, and the printing speed can also affect the bio-printed devices [292]. Like FDM parts obtained in other industrial applications, the medical devices manufactured by FDM suffer the interdependence and influence of the process parameters on the parts properties. Some of the parameters called critical process parameters are determined like those that have more influence on the final properties of parts [298]. One of the main challenges in the field of FDM today is the control of the properties of the parts and their repeatability.

Smart materials based on the modifications of properties due to an external applied magnetic stimulus are developed and find applications in medicine, soft robotic, and others [299–301]. These devices are often made by composited materials in which magnetic materials have been incorporated like fillers, powder, and particles [301]. FDM is one of the process used for smart magnetoactive soft materials fabrication [301]. Their properties can be affected during the printing process or with an application post-treatment. Shape memory polymers can be used in *magnetoactive smart materials*. N. A. Fisher et al. have shown that the resulting magnetic and the magnetoactive properties of magnetorheological elastomers can be modified during magnetic annealing. In fact, depending on the nature of magnetic field, no field, uniform field, or non-uniform field during the heat treatment can improve or degrade the magnetoactive response of this smart material which can undergo mechanical deformation in the presence of magnetic field [288]. S. Kumar et al. fabricated a thermoplastic (PLA–PVC)-based composite filament with wood dust and magnetite (Fe_3O_4) for FDM. The parts obtained exhibit superparamagnetic properties that can be used for self-assembly applications [302]. They have determined the composition of the filament in order to obtain the optimized magnetic properties. The mechanical properties have been also characterized in function of the printing parameters: infill density, infill angle, and infill speed [303]. And the mechanical and magnetic properties were found not to be in correlation. Thermoplastic polyurethane with either iron, carbonyl iron, or magnetite particles has been used to fabricate 3D-printed parts [304]. The structure of the parts presents the directional magnetic properties that is often obtained after magnetic annealing post-treatment. The properties of these magnetic elastomer materials can be adjusted by altering the infill density and infill orientation.

The additive manufacturing of *electronically smart devices* presents a great potential for flexible and stretchable electronics. Among the AM processes usually employed

like inkjet printing, aerosol printing [305–307], and direct ink writing [308], FDM is also used [309, 310]. The materials used herein are conductive elements associated with soft polymers. Shape changing materials can be employed for the fabrication of electronically smart materials [311, 312]. The effect of printing parameters on the shape memory effect of PLA have been studied [311]. They found that the shape memory effect evaluated by the shape-recovery ratio and maximum shape recovery rate of 3D-printed PLA is mainly influenced by the recovery temperature. However, the deformation temperature and the printing parameters (layer thickness, raster angle) have a very limited impact on this shape memory effect. Lukas Kačergis et al. have investigated the influence of the printing speed, the temperature of the build plate, and the number of active layers on a smart material obtained from 3D printing of PLA and TPU. They have showed that deformation and bending degrees of the structures can be turned by adjusting these printing parameters [289]. Another's shape memory materials made by the combination of PLA with carbon black have been studied by Lee et al. [312]. In their study, they demonstrate that the bending angle achieved by the actuators 3D printed increased with the applied printing speed. 3D-printed photoresponsive shape memory devices constituted by the combination of shape memory polymer with carbon black have been implemented [313]. The influence of the printed material thickness and the sunlight intensity has been evaluated. As the material thickness increases, the illumination time should be increased in order to allow the material deformation. The deformation angle is more significative for the smallest thickness.

Another area of research is the development of *natural fiber-based 4D printed biocomposites* for the fabrication of sustainable smart materials. In the smart biocomposite devices, the inorganic reinforcements are replaced by natural fillers (fibers, pellets, wood, ...) in the thermoplastic matrix. Many achievements have been accomplished and huge efforts are investigated by researchers from both academic and industrial sectors in order to push actual scientific and technological limitations [135, 314, 315]. Most of natural fibers are sensitive to moisture and present a pronounced anisotropy. These properties can be considered like drawbacks or take in advantage in order to implement smart biocomposite devices. In their review, Le Duigou et al. have investigated the 3D/4D of natural fiber biocomposites [135]. Concerning the smart devices with natural fillers, the two categories of shape-transformation materials in 4D printing have been discussed: shape memory materials and shape-changing materials. The hygromorphing properties of natural fiber-based 4D printed biocomposites have been presented and also the perspectives. The use of natural fillers also results in the attenuation of mechanical properties which are also sensitive to the process parameters. The printing

parameters effect on the FDM wood fiber–reinforced composites have been studied [316]. It has been shown that the printing orientation, the printing width, and the important resulting porosity greatly influenced the mechanical properties of the printed biocomposites. The hydromorphic have been increased in composite constituted by wood and polymer with accurate printing parameters. They found that the height of the layer and the part were decisive in the optimization of the self-transformation capacity of the obtained structures [317]. Another smart bio-based device used for the space design was made by the combination of flax yarn with PLA and was triggered-induce by moisture. The reduction of layer thickness and the increase of the width result in the reduction of the porosity ratio and then optimization of mechanical properties [318, 319].

4 Conclusions and outlooks

This article presents a review of materials and the influence of process parameters on the mechanical properties of parts fabricated by FDM. FDM materials have been classified into three categories: standard materials, composite materials, and smart materials.

Standard materials used in FDM have found numerous applications across various engineering domains. However, their main limitations are related to “low” printing speed and to their mechanical properties, which are not suitable for applications requiring high strength and stiffness for example. Different ways to overcome these drawbacks are investigated by researchers such as elaborating polymers with higher mechanical properties often called “high performance” polymers. This materials group has not been treated in this review. Another way consists to combine the standard polymer with one or more other materials in order to obtain a composite material with improve properties. This often leads to the development of new materials that exhibit not only enhanced mechanical properties but also additional functionalities such as optical, electrical, thermal, or other physical properties. The common materials added to standard polymers in order to fabricate composite materials are carbon or glass fibers, graphene, alloys, or ceramics in the form of pellets or grains and other polymers. Then, the parts made from polymer-reinforced composite can take advantages of both 3D printing and fiber addition. Depending on the nature of the fillers, the fabricated parts can present multifunctional properties. For example:

- Carbon fiber–reinforced polymer composites have better properties like wear resistance, corrosion resistance, lightweight structures, high strength-to-weight ratio, and high-dimensional stability. Studies have shown that carbon fiber added to a polymer can increase the tensile

strength and the Young modulus, but ductility, toughness, and yield stress may decrease. Glass fiber–reinforced polymer composites increase the tensile strength but decrease the flexibility of the composite part.

- Ceramic-reinforced polymer composites are widely used in bio-medical application. Their application is limited in other sectors due to their brittleness and poor mechanical strength.
- Other materials used for reinforcing polymers, such as graphene, carbon nanotubes, or carbon fibers, enhance their mechanical, electrical, and thermal performance.

In addition to the development of composite materials in the field of additive manufacturing, research around smart materials have grown significantly. These materials are defined as designed materials that have one or more properties that can be significantly changed in a controlled way by external stimuli. The developments of smart materials are important and promising.

FDM remains an active research area with many challenges, particularly in the quest to fabricate more functional parts with enhanced mechanical properties. The understanding and optimization of the mechanical properties of the various materials (polymer, carbon, or responsive) have been well established in literature. But several questions remain open and many technological and scientific challenges need also to be addressed in the future. Some orientations can be mentioned here in function of different group of materials previously considered:

- Huge efforts have been made in the investigations of the mechanical properties of parts of standard polymers obtained by FDM. It appears that process parameters greatly influence mechanical properties when conventional mechanical tests are implemented (like tensile or creep, flexural tests). However, less studies have been devoted to more complex tests such as multiaxial tests and dynamic tests. These tests could bring more insights in the understanding of these materials in regard to their architectural structure. This remark is valuable for structures with other FDM materials.
- The void population and their alignment in regard to the tensile direction have considerable impact on the fatigue properties. Very less studies intend to study systematically the effect of voids or air gaps on the fatigue performance of polymeric FDM samples. The effect of contour numbers has also received very less attention.
- One way to take advantage of the rich research work around the impact of printing parameters on mechanical properties is to provide charts or a guide for part designers.
- Models describing the FDM process itself and the behavior of the materials need to be developed.

- Further work is now coming about the use of artificial neural networks (ANN) for optimizing these current manufacturing processes. In P. D. Nguyen et al., a data-driven machine-learning-based approach is investigated in order to deal with adjustment of printing parameters and process evolution trends [320]. Data coming from experiments and property characterization measurements may be used in order to fit large databases which can be very efficient as data sets for learning in the context of machine learning. Artificial intelligence (AI) may play a significant role as a tool for reverse engineering to optimize processes according to the intended material applications, especially with the increasing availability of real-time in situ measurements of “material health.”

Author contribution Silvain William TIEUNA TIENTCHEU: formal analysis; writing—original draft; writing—review and editing.

Joseph MARAE DJOUDA: conceptualization; methodology; writing—original draft; writing—review and editing; supervision.

Mohamed Ali BOUAZIZ: methodology; writing—original draft; writing—review and editing.

Elisabeth LACAZEDIEU: review and editing.

Declarations

Conflict of interest The authors declare no competing interests.

References

1. Ngo TD, Kashani A, Imbalzano G, Nguyen KTQ, Hui D (2018) Additive manufacturing (3D printing): a review of materials, methods, applications and challenges. *Compos Part B Eng* 143:172–196. <https://doi.org/10.1016/j.compositesb.2018.02.012>
2. Mohamed OA, Masood SH, Bhowmik JL, Nikzad M, Azadmanjiri J (2016) Effect of process parameters on dynamic mechanical performance of FDM PC/ABS printed parts through design of experiment. *J Mater Eng Perform* 25:2922–2935. <https://doi.org/10.1007/s11665-016-2157-6>
3. Dey A, Yodo N (2019) A systematic survey of FDM process parameter optimization and their influence on part characteristics. *J Manuf Mater Process* 3. <https://doi.org/10.3390/jmmp3030064>
4. Shubham P, Sikidar A, Chand T (2016) The influence of layer thickness on mechanical properties of the 3D printed ABS polymer by fused deposition modeling. *Key Eng Mater* 706:63–67. <https://doi.org/10.4028/www.scientific.net/KEM.706.63>
5. Dilberoglu UM, Gharehpapagh B, Yaman U, Dolen M (2017) The role of additive manufacturing in the era of Industry 4.0. *Procedia Manuf* 11:545–554. <https://doi.org/10.1016/j.promfg.2017.07.148>
6. Gibson I, Rosen D, Stucker B (2014) Additive manufacturing technologies. <https://doi.org/10.1007/978-1-4939-2113-3>
7. Boparai KS, Singh R (2017) Advances in fused deposition modelling. *Ref Modul Mater Sci Mater Eng* 1–10. <https://doi.org/10.1016/b978-0-12-803581-8.04166-7>
8. Gardan J (2019) Smart materials in additive manufacturing: state of the art and trends. *Virtual Phys Prototyp* 14:1–18. <https://doi.org/10.1080/17452759.2018.1518016>
9. Crump SS (1992) U.S. Patent No. 5,121,329. Patent and Trademark Office, Washington, DC
10. Jha K, Narasimhulu A (2018) A critical review of process parameters of fused deposition modelling. *J Mater Sci Mech Eng* 5:138–141
11. Mohamed OA, Masood SH, Bhowmik JL (2015) Optimization of fused deposition modeling process parameters: a review of current research and future prospects. *Adv Manuf* 3:42–53. <https://doi.org/10.1007/s40436-014-0097-7>
12. Popescu D, Zapciu A, Amza C, Baciu F, Marinescu R (2018) FDM process parameters influence over the mechanical properties of polymer specimens: a review. *Polym Test* 69:157–166. <https://doi.org/10.1016/j.polymertesting.2018.05.020>
13. Li N, Huang S, Zhang G, Qin R, Liu W, Xiong H, Shi G, Blackburn J (2019) Progress in additive manufacturing on new materials: a review. *J Mater Sci Technol* 35:242–269. <https://doi.org/10.1016/j.jmst.2018.09.002>
14. Fuenmayor E, Forde M, Healy AV, Devine DM, Lyons JG, McConville C, Major I (2018) Material considerations for fused-filament fabrication of solid dosage forms. *Pharmaceutics* 10:1–27. <https://doi.org/10.3390/pharmaceutics10020044>
15. Condruz MR, Paraschiv A, Puscasu C (2018) Heat treatment influence on hardness and microstructure of ADAM Manufactured 17–4 Ph, Turbo. V 4–11. <https://www.researchgate.net/publication/332423408>
16. Galati M, Minetola P (2019) Analysis of density, roughness, and accuracy of the atomic diffusion additive manufacturing (ADAM) Process for metal parts. *Materials (Basel)* 12:4122. <https://doi.org/10.3390/ma12244122>
17. Bouaziz MA, Marae Djouda J, Chemkhi M, Rambaoudon M, Kauffmann J, Hild F (2021) Heat treatment effect on 17–4PH stainless steel manufactured by atomic diffusion additive manufacturing (ADAM). *Procedia CIRP* 104:935–938. <https://doi.org/10.1016/j.procir.2021.11.157>
18. Chemkhi M, Djouda JM, Bouaziz MA, Kauffmann J, Hild F, Retraint D (2021) Effects of mechanical post-treatments on additive manufactured 17–4PH Stainless steel produced by bound powder extrusion. *CIRP Ann – Manuf Technol* 00:0–4
19. Diamant J, David S, Williams MC (1982) The mechanical properties of styrene-butadiene-styrene (SBS) triblock copolymer blends with polystyrene (PS) and styrene-butadiene copolymer (SBR). *Polym Eng Sci* 22:673–683
20. Sidorowicz M (2017) Verification of the prototype: fire engine’s manifold 3D printout, 3Dgence. [3dgence.com](https://www.3dgence.com)
21. Ergene B, Şekeroğlu İ, Bolat Ç, Yalçın B (2021) An experimental investigation on mechanical performances of 3D printed lightweight ABS pipes with different cellular wall thickness. *J Mech Eng Sci* 15:8169–8177. <https://doi.org/10.15282/jmes.15.2.2021.16.0641>
22. Bartolomé E, Bozzo B, Sevilla P, Martínez-Pasarell O, Puig T, Granados X (2017) ABS 3D printed solutions for cryogenic applications. *Cryogenics (Guildf)* 82:30–37. <https://doi.org/10.1016/j.cryogenics.2017.01.005>
23. Bates-Green K, Howie T (2017) Materials for 3D printing by fused deposition. *Technical education in additive manufacturing and materials* 1–21
24. Schmitt M, Mehta RM, Kim IY (2020) Additive manufacturing infill optimization for automotive 3D-printed ABS components. *Rapid Prototyp J* 26:89–99. <https://doi.org/10.1108/RPJ-01-2019-0007>
25. Yadav DK, Srivastava R, Dev S (2019) Design & fabrication of ABS part by FDM for automobile application. *Mater Today*

- Proc 26:2089–2093. <https://doi.org/10.1016/j.matpr.2020.02.451>
26. AL-Hasni S, Santori G (2020) 3D printing of vacuum and pressure tight polymer vessels for thermally driven chillers and heat pumps. *Vacuum* 171:109017. <https://doi.org/10.1016/j.vacuum.2019.109017>
 27. Jain PK, Jain PK (2020) Use of 3D printing for home applications: a new generation concept. *Mater Today Proc* 43:605–607. <https://doi.org/10.1016/j.matpr.2020.12.145>
 28. Gao G, Xu F, Xu J, Liu Z (2022) Study of material color influences on mechanical characteristics of fused deposition modeling parts. *Materials (Basel)* 15:1–15. <https://doi.org/10.3390/ma15197039>
 29. Taubner V, Shishoo R (2001) Influence of processing parameters on the degradation of poly(L-lactide) during extrusion. *J Appl Polym Sci*. [https://doi.org/10.1002/1097-4628\(20010321\)79:12%3c2128::AID-APP1020%3e3.0.CO;2-#](https://doi.org/10.1002/1097-4628(20010321)79:12%3c2128::AID-APP1020%3e3.0.CO;2-#)
 30. Baptista R, Guedes M (2021) Morphological and mechanical characterization of 3D printed PLA scaffolds with controlled porosity for trabecular bone tissue replacement. *Mater Sci Eng C* 118:111528. <https://doi.org/10.1016/j.msec.2020.111528>
 31. Serra T, Mateos-Timoneda MA, Planell JA, Navarro M (2013) 3D printed PLA-based scaffolds: a versatile tool in regenerative medicine. *Organogenesis* 9:239–244. <https://doi.org/10.4161/org.26048>
 32. Joseph TM, Kallingal A, Suresh AM, Mahapatra DK, Hasannin MS, Haponiuk J, Thomas S (2023) 3D printing of polylactic acid: recent advances and opportunities. *Int J Adv Manuf Technol* 125:1015–1035. <https://doi.org/10.1007/s00170-022-10795-y>
 33. Bassand C, Benabed L, Charlon S, Verin J, Freitag J, Siepmann F, Soulestin J, Siepmann J (2023) 3D printed PLGA implants: APF DDM vs. FDM. *J Control Release* 353:864–874. <https://doi.org/10.1016/j.jconrel.2022.11.052>
 34. Mohammadi-Zerankeshi M, Alizadeh R (2023) 3D-printed PLA-Gr-Mg composite scaffolds for bone tissue engineering applications. *J Mater Res Technol* 22:2440–2446. <https://doi.org/10.1016/j.jmrt.2022.12.108>
 35. DeStefano V, Khan S, Tabada A (2020) Applications of PLA in modern medicine. *Eng Regen* 1:76–87. <https://doi.org/10.1016/j.engreg.2020.08.002>
 36. Caminero MÁ, Chacón JM, García-Plaza E, Núñez PJ, Reverte JM, Becar JP (2019) Additive manufacturing of PLA-based composites using fused filament fabrication: Effect of graphene nanoplatelet reinforcement on mechanical properties, dimensional accuracy and texture. *Polymers (Basel)* 11. <https://doi.org/10.3390/polym11050799>
 37. Zhang H, Wang M, Wu R, Guo J, Sun A, Li Z, Ye R, Xu G, Cheng Y (2023) From materials to clinical use: advances in 3D-printed scaffolds for cartilage tissue engineering. *Phys Chem Chem Phys*. <https://doi.org/10.1039/d3cp00921a>
 38. Cojocar V, Frunzaverde D, Miclosina CO, Marginean G (2022) The influence of the process parameters on the mechanical properties of PLA specimens produced by fused filament fabrication—a review. *Polymers (Basel)* 14. <https://doi.org/10.3390/polym14050886>
 39. García E, Núñez PJ, Chacón JM, Caminero MA, Kamarthi S (2020) Comparative study of geometric properties of unreinforced PLA and PLA-graphene composite materials applied to additive manufacturing using FFF technology. *Polym Test* 91. <https://doi.org/10.1016/j.polymertesting.2020.106860>
 40. Rodríguez-Panes A, Claver J, Camacho AM (2018) The influence of manufacturing parameters on the mechanical behaviour of PLA and ABS pieces manufactured by FDM: a comparative analysis. *Materials (Basel)* 11. <https://doi.org/10.3390/ma11081333>
 41. Bustillos J, Montero D, Nautiyal P, Loganathan A, Boesl B, Agarwal A (2018) Integration of graphene in poly (lactic) acid by 3D printing to develop creep and wear-resistant hierarchical nanocomposites. *Polym Compos* 39:3877–3888
 42. Song Y, Li Y, Song W, Yee K, Lee K-Y, Tagarielli VL (2017) Measurements of the mechanical response of unidirectional 3D-printed PLA. *Mater Des* 123:154–164
 43. Harris M, Potgieter J, Ray S, Archer R, Arif KM (2020) Polylactic acid and high-density polyethylene blend: characterization and application in additive manufacturing. *J Appl Polym Sci* 137:1–18. <https://doi.org/10.1002/app.49602>
 44. El Magri A, El Mabrouk K, Vaudreuil S, Ebn Touhami M (2019) Mechanical properties of CF-reinforced PLA parts manufactured by fused deposition modelling. *J Thermoplast Compos Mater*. <https://doi.org/10.1177/0892705719847244>
 45. Akhouni B, Behravesh AH, BagheriSaed A (2019) Improving mechanical properties of continuous fiber-reinforced thermoplastic composites produced by FDM 3D printer. *J Reinf Plast Compos* 38:99–116. <https://doi.org/10.1177/0731684418807300>
 46. Haleem A, Javaid M (2019) Polyether ether ketone (PEEK) and its 3D printed implants applications in medical field: an overview. *Clin Epidemiol Glob Heal* 7:571–577. <https://doi.org/10.1016/j.cegh.2019.01.003>
 47. Tseng JW, Liu CY, Yen YK, Belkner J, Bremicker T, Liu BH, Sun TJ, Wang AB (2018) Screw extrusion-based additive manufacturing of PEEK. *Mater Des* 140:209–221. <https://doi.org/10.1016/j.matdes.2017.11.032>
 48. Zhang H, Hui J, Lv J, Lee CH, Yan Z, Jie Wang J, Guo L, Xu Z (2023) A novel method to combine fused deposition modelling and inkjet printing in manufacturing multifunctional parts for aerospace application. *J Mater Res Technol* 24:4405–4426. <https://doi.org/10.1016/j.jmrt.2023.04.059>
 49. Shi Y, Deng T, Peng Y, Qin Z, Ramalingam M, Pan Y, Chen C, Zhao F, Cheng L, Liu J (2023) Effect of surface modification of PEEK artificial phalanx by 3D printing on its biological activity. *Coatings* 13:400. <https://doi.org/10.3390/coatings13020400>
 50. Wang R, Cheng KJ, Advincula RC, Chen Q (2019) On the thermal processing and mechanical properties of 3D-printed polyether ether ketone. *MRS Commun* 9:1046–1052. <https://doi.org/10.1557/mrc.2019.86>
 51. Geng P, Zhao J, Wu W, Ye W, Wang Y, Wang S, Zhang S (2019) Effects of extrusion speed and printing speed on the 3D printing stability of extruded PEEK filament. *J Manuf Process* 37:266–273. <https://doi.org/10.1016/j.jmapro.2018.11.023>
 52. Petersmann S, Spoerk M, Van De Steene W, Üçal M, Wiener J, Pinter G, Arbeiter F (2020) Mechanical properties of polymeric implant materials produced by extrusion-based additive manufacturing. *J Mech Behav Biomed Mater* 104:103611. <https://doi.org/10.1016/j.jmbbm.2019.103611>
 53. Vaezi M, Yang S (2015) Extrusion-based additive manufacturing of PEEK for biomedical applications. *Virtual Phys Prototyp* 10:123–135. <https://doi.org/10.1080/17452759.2015.1097053>
 54. Oladapo BI, Zahedi SA, Chong S, Omigbodun FT, Malachi IO (2020) 3D printing of surface characterisation and finite element analysis improvement of PEEK-HAP-GO in bone implant. *Int J Adv Manuf Technol* 106:829–841. <https://doi.org/10.1007/s00170-019-04618-w>
 55. Jiang CP, Cheng YC, Lin HW, Chang YL, Pasang T, Lee SY (2022) Optimization of FDM 3D printing parameters for high strength PEEK using the Taguchi method and experimental validation. *Rapid Prototyp J* 28:1260–1271. <https://doi.org/10.1108/RPJ-07-2021-0166>
 56. Puppi D, Morelli A, Bello F, Valentini S, Chiellini F (2018) Additive manufacturing of poly(methyl methacrylate) biomedical

- implants with dual-scale porosity. *Macromol Mater Eng* 303:1–9. <https://doi.org/10.1002/mame.201800247>
57. Velu R, Singamneni S (2015) Evaluation of the influences of process parameters while selective laser sintering PMMA powders. 229:603–613. <https://doi.org/10.1177/0954406214538012>
 58. Espalin D, Arcaute K, Rodriguez D, Medina F, Posner M, Wicker R (2010) Fused deposition modeling of patient-specific polymethylmethacrylate implants. *Rapid Prototyp J* 3:164–173. <https://doi.org/10.1108/13552541011034825>
 59. Mohan N, Senthil P, Vinodh S, Jayanth N (2017) A review on composite materials and process parameters optimisation for the fused deposition modelling process. *Virtual Phys Prototyp* 12:47–59. <https://doi.org/10.1080/17452759.2016.1274490>
 60. Marin E, Boschetto F, Zanocco M, Honma T, Zhu W, Pezzotti G (2021) Explorative study on the antibacterial effects of 3D-printed PMMA/nitrides composites. *Mater Des* 206:109788. <https://doi.org/10.1016/j.matdes.2021.109788>
 61. Peltola MJ, Vallittu PK, Vuorinen V, Aho AAJ, Puntala A, Aitasalo KMJ (2012) Novel composite implant in craniofacial bone reconstruction. 623–628. <https://doi.org/10.1007/s00405-011-1607-x>
 62. Liga A, Morton JAS, Kersaudy M (2016) Safe and cost-effective rapid-prototyping of multilayer PMMA microfluidic devices. <https://doi.org/10.1007/s10404-016-1823-1>
 63. Jaiganesh V, Christopher AA, Mugilan E (2014) Manufacturing of PMMA cam shaft by rapid prototyping. *Procedia Eng* 97:2127–2135. <https://doi.org/10.1016/j.proeng.2014.12.456>
 64. Kotz F, Mader M, Dellen N, Risch P, Kick A, Helmer D, Rapp BE (2020) Fused deposition modeling of microfluidic chips in polymethylmethacrylate. *Micromachines* 11(9):873. <https://doi.org/10.3390/mi11090873>
 65. Babo S, Ferreira JL, Ramos AM, Micheluz A, Pamplona M, Casimiro MH, Ferreira M, Jo M (n.d.) Characterization and long-term stability of historical PMMA: impact of additives and acrylic sheet Industrial Production Processes
 66. Polzin C, Spath S, Seitz H (2013) Characterization and evaluation of a PMMA-based 3D printing process. *Rapid Prototyp J* 19:37–43. <https://doi.org/10.1108/13552541311292718>
 67. Bressan LP, Adamo CB, Quero RF, De Jesus DP, Da Silva JAF (2019) A simple procedure to produce FDM-based 3D-printed microfluidic devices with an integrated PMMA optical window. *Anal Methods* 11:1014–1020. <https://doi.org/10.1039/c8ay02092b>
 68. Tan WS, Chua CK, Chong TH, Fane AG, Jia A, See W, Chua CK, Chong TH, Fane AG, Jia A (2016) 3D printing by selective laser sintering of polypropylene feed channel spacers for spiral wound membrane modules for the water industry. 2759. <https://doi.org/10.1080/17452759.2016.1211925>
 69. Spoerk M, Arbeiter F, Raguž I, Weingrill G, Fischinger T, Traxler G, Schuschnigg S, Cardon L, Holzer C (2018) Polypropylene filled with glass spheres in extrusion-based additive manufacturing: effect of filler size and printing chamber temperature. 1800179. <https://doi.org/10.1002/mame.201800179>
 70. Dong M, Zhang S, Gao D, Chou B (2019) The study on polypropylene applied in fused deposition modelling. *AIP Conf Proc* 2065. <https://doi.org/10.1063/1.5088317>
 71. Silva AF, Carneiro OS, Gomes R (1896) 3D printing of polypropylene using the fused filament fabrication technique. *AIP Conf Proc* 2017:1–5. <https://doi.org/10.1063/1.5008040>
 72. Carneiro OS, Silva AF, Gomes R (2015) Fused deposition modeling with polypropylene. *Mater Des* 83:768–776. <https://doi.org/10.1016/j.matdes.2015.06.053>
 73. Jin M, Neuber C, Schmidt H (2020) Tailoring polypropylene for extrusion-based additive manufacturing. *Addit Manuf* 33:101101. <https://doi.org/10.1016/j.addma.2020.101101>
 74. Schumacher C, Schöppner V, Fels C (2019) A method to evaluate the process-specific warpage for different polymers in the FDM process. *AIP Conf Proc* 2065. <https://doi.org/10.1063/1.5088315>
 75. Sagias VD, Giannakopoulos KI, Stergiou C (2018) Mechanical properties of 3D printed polymer specimens. *Procedia Struct Integr* 10:85–90
 76. Kumar N, Jain PK, Tandon P, Mohan P (2018) ScienceDirect Experimental investigations on suitability of polypropylene (PP) and ethylene vinyl acetate (EVA) in additive manufacturing. *Mater Today Proc* 5:4118–4127. <https://doi.org/10.1016/j.matpr.2017.11.672>
 77. Swennen GRJ, Pottel L, Haers PE (2020) Custom-made 3D-printed face masks in case of pandemic crisis situations with a lack of commercially available FFP2/3 masks. *Int J Oral Maxillofac Surg* 49:673–677. <https://doi.org/10.1016/j.ijom.2020.03.015>
 78. Keller M, Guebeli A, Thieringer F, Honigmann P (2021) Overview of in-hospital 3D printing and practical applications in hand surgery. *Biomed Res Int* 2021:4650245. <https://doi.org/10.1155/2021/4650245>
 79. Kumar N (2019) Analysing the influence of raster angle, layer thickness and infill rate on the compressive behaviour of EVA through CNC-assisted fused layer modelling process. 0:1–10. <https://doi.org/10.1177/0954406219889076>
 80. Geng Y, He H, Liu H, Jing H (2020) Preparation of polycarbonate/poly(lactic acid) with improved printability and processability for fused deposition modeling. *Polym Adv Technol* 31:2848–2862. <https://doi.org/10.1002/pat.5013>
 81. Salazar-Martín AG, Pérez MA, García-Granada AA, Reyes G, Puigoriol-Forcada JM (2018) A study of creep in polycarbonate fused deposition modelling parts. *Mater Des* 141:414–425. <https://doi.org/10.1016/j.matdes.2018.01.008>
 82. Cole DP, Gardea F, Henry TC, Seppala JE, Garboczi EJ, Migler KD, Shumeyko CM, Westrich JR, Orski SV, Gair JL (2020) AMB2018 - 03: benchmark physical property measurements for material extrusion additive manufacturing of polycarbonate. *Integr Mater Manuf Innov*. <https://doi.org/10.1007/s40192-020-00188-y>
 83. Messimer SL, Patterson AE, Muna N, Deshpande AP (n.d.) Characterization and processing behavior of heated aluminum-polycarbonate composite build plates for the FDM additive manufacturing process. <https://doi.org/10.3390/jmmp2010012>
 84. Shemelya C, Cedillos F, Aguilera E, Maestas E, Ramos J, Espalin D, Muse D, Wicker R, MacDonald E (2013) 3D printed capacitive sensors. *Proc IEEE Sensors* 1–4. <https://doi.org/10.1109/ICSENS.2013.6688247>
 85. Park SJ, Lee JE, Lee HB, Park J, Lee NK, Son Y, Park SH (2020) 3D printing of bio-based polycarbonate and its potential applications in ecofriendly indoor manufacturing. *Addit Manuf* 31:100974. <https://doi.org/10.1016/j.addma.2019.100974>
 86. Masood SH, Mau K, Song WQ (2010) Tensile properties of processed FDM polycarbonate material. *Mater Sci Forum* 654–656:2556–2559. <https://doi.org/10.4028/www.scientific.net/MSF.654-656.2556>
 87. Zhou YG, Su B, Turng LS (2017) Deposition-induced effects of isotactic polypropylene and polycarbonate composites during fused deposition modeling. *Rapid Prototyp J* 23:869–880. <https://doi.org/10.1108/RPJ-12-2015-0189>
 88. Reich MJ, Woern AL, Tanikella NG, Pearce JM (2019) Mechanical properties and applications of recycled polycarbonate particle material extrusion-based additive manufacturing. *Materials (Basel)* 12:1642
 89. Pal AK, Mohanty AK, Misra M (2021) Additive manufacturing technology of polymeric materials for customized products: recent developments and future prospective. *RSC Adv* 11:36398–36438. <https://doi.org/10.1039/d1ra04060j>

90. Wang K, Xie G, Xiang J, Li T, Peng Y, Wang J, Zhang H (2022) Materials selection of 3D printed polyamide-based composites at different strain rates: a case study of automobile front bumpers. *J Manuf Process* 84:1449–1462. <https://doi.org/10.1016/j.jmapro.2022.11.024>
91. Zhang X, Fan W, Liu T (2020) Fused deposition modeling 3D printing of polyamide-based composites and its applications. *Compos Commun* 21:100413. <https://doi.org/10.1016/j.coco.2020.100413>
92. Dezaki ML, Khairol M, Mohd A (2021) An overview of fused deposition modelling (FDM): research, development and process optimisation. 3:562–582. <https://doi.org/10.1108/RPJ-08-2019-0230>
93. Zhang Y, Pursell C, Mao K, Leigh S (2020) A physical investigation of wear and thermal characteristics of 3D printed nylon spur gears. *Tribol Int* 141:105953. <https://doi.org/10.1016/j.triboint.2019.105953>
94. Peng X, He H, Jia Y, Liu H, Geng Y, Huang B, Luo C (2019) Shape memory effect of three-dimensional printed products based on polypropylene/nylon 6 alloy. *J Mater Sci* 54:9235–9246. <https://doi.org/10.1007/s10853-019-03366-2>
95. Gao X, Zhang D (2019) Fused deposition modeling with polyamide 1012. <https://doi.org/10.1108/RPJ-09-2018-0258>
96. Rahim TNAT, Abdullah AM, MdAkil H (2019) Recent developments in fused deposition modeling-based 3D printing of polymers and their composites. *Polym Rev* 59:589–624. <https://doi.org/10.1080/15583724.2019.1597883>
97. Alghamdi SS, John S, Choudhury NR, Dutta NK (2021) Additive manufacturing of polymer materials: progress, promise and challenges. *Polymers (Basel)* 13:1–39. <https://doi.org/10.3390/polym13050753>
98. Sood AK, Ohdar RK, Mahapatra SS (2009) Improving dimensional accuracy of fused deposition modelling processed part using grey Taguchi method. *Mater Des* 30:4243–4252. <https://doi.org/10.1016/j.matdes.2009.04.030>
99. Black HT, Celina MC, Mcelhanon JR (2016) Additive manufacturing of polymers: materials opportunities and emerging applications. <https://doi.org/10.2172/1561754>
100. Hsueh MH, Lai CJ, Chung CF, Wang SH, Huang WC, Pan CY, Zeng YS, Hsieh CH (2021) Effect of printing parameters on the tensile properties of 3d-printed polylactic acid (PLA) based on fused deposition modeling. *Polymers (Basel)* 13:2387. <https://doi.org/10.3390/polym13142387>
101. Corapi D, Morettini G, Pascoletti G, Zitelli C (2019) Characterization of a polylactic acid (PLA) produced by fused deposition modeling (FDM) technology. *Procedia Struct Integr* 24:289–295. <https://doi.org/10.1016/j.prostr.2020.02.026>
102. Algarni M, Ghazali S (2021) Comparative study of the sensitivity of pla, abs, peek, and petg's mechanical properties to fdm printing process parameters. *Crystals* 11(8):995. <https://doi.org/10.3390/cryst11080995>
103. Tan LJ, Zhu W, Zhou K (2020) Recent progress on polymer materials for additive manufacturing. *Adv Funct Mater* 30:1–54. <https://doi.org/10.1002/adfm.202003062>
104. Arif MF, Kumar S, Varadarajan KM, Cantwell WJ (2018) Performance of biocompatible PEEK processed by fused deposition additive manufacturing. *Mater Des* 146:249–259. <https://doi.org/10.1016/j.matdes.2018.03.015>
105. Yakout M, Elbestawi MA (2017) Additive manufacturing of composite materials: an overview, vol 29. In *Proceedings of the 6th International Conference on Virtual Machining Process Technology (VMPT)*, Montréal, QC, Canada
106. Yasa E, Ersoy K (2018) Additive manufacturing of polymer matrix composites. *Aircr Technol*. <https://doi.org/10.5772/intechopen.75628>
107. Ismail KI, Yap TC, Ahmed R (2022) 3D-printed fiber-reinforced polymer composites by fused deposition modelling (FDM): fiber length and fiber implementation techniques. *Polymers (Basel)* 14:1–36
108. Zhang H, Huang T, Jiang Q, He L, Bismarck A, Hu Q (2021) Recent progress of 3D printed continuous fiber reinforced polymer composites based on fused deposition modeling : a review. *J Mater Sci* 56:12999–13022. <https://doi.org/10.1007/s10853-021-06111-w>
109. Krajangsawadi N, Blok LG, Hamerton I, Longana ML, Woods BKS, Ivanov DS (2021) Fused deposition modelling of fibre reinforced polymer composites: a parametric review. *J Compos Sci* 5. <https://doi.org/10.3390/jcs5010029>
110. Iwai Y, Honda T, Miyajima T, Iwasaki Y, Surappa MK, Xu JF (2000) Dry sliding wear behavior of Al₂O₃ fiber reinforced aluminum composites. *Compos Sci Technol* 60:1781–1789. [https://doi.org/10.1016/S0266-3538\(00\)00068-3](https://doi.org/10.1016/S0266-3538(00)00068-3)
111. Salem Bala A, Bin Wahab S, Binti Ahmad M (2016) Elements and materials improve the FDM products: a review. *Adv Eng Forum* 16:33–51. <https://doi.org/10.4028/www.scientific.net/ae.16.33>
112. Postiglione G, Natale G, Griffini G, Levi M, Turri S (2015) Conductive 3D microstructures by direct 3D printing of polymer/carbon nanotube nanocomposites via liquid deposition modeling. *Compos Part A Appl Sci Manuf* 76:110–114. <https://doi.org/10.1016/j.compositesa.2015.05.014>
113. Velu R, Raspall F, Singamneni S (2018) 3D printing technologies and composite materials for structural applications. Elsevier Ltd. <https://doi.org/10.1016/B978-0-08-102177-4.00008-2>
114. Wang P, Zou B, Ding S, Huang C, Shi Z, Ma Y, Yao P (2020) Preparation of short CF/GF reinforced PEEK composite filaments and their comprehensive properties evaluation for FDM-3D printing. *Compos Part B Eng* 198:108175. <https://doi.org/10.1016/j.compositesb.2020.108175>
115. Azarov AV, Antonov FK, Golubev MV, Khaziev AR, Ushanov SA (2019) Composite 3D printing for the small size unmanned aerial vehicle structure. *Compos Part B Eng* 169:157–163. <https://doi.org/10.1016/j.compositesb.2019.03.073>
116. Buj-Corral I, Tejo-Otero A (2022) 3D printing of bioinert oxide ceramics for medical applications. *J Funct Biomater* 13. <https://doi.org/10.3390/jfb13030155>
117. Ahlhelm M, Günther P, Scheithauer U, Schwarzer E, Günther A, Slawik T, Moritz T, Michaelis A (2016) Innovative and novel manufacturing methods of ceramics and metal-ceramic composites for biomedical applications. *J Eur Ceram Soc* 36:2883–2888. <https://doi.org/10.1016/j.jeurceramsoc.2015.12.020>
118. Jyoti S, Bose S, Hosick HL, Bandyopadhyay A (2023) Development of controlled porosity polymer-ceramic composite scaffolds via fused deposition modelling. 23:611–620. [https://doi.org/10.1016/S0928-4931\(03\)00052-3](https://doi.org/10.1016/S0928-4931(03)00052-3)
119. Feilden E, Ferraro C, Zhang Q, García-Tuñón E, D'Elia E, Giuliani F, Vandepierre L, Saiz E (2017) 3D printing bioinspired ceramic composites. *Sci Rep* 7:1–9. <https://doi.org/10.1038/s41598-017-14236-9>
120. Goulas A, McGhee JR, Whittaker T, Ossai D, Mistry E, Whittow W, Vaidhyanathan B, Reaney IM, Vardaxoglou J(C, Engström DS (2022) Synthesis and dielectric characterisation of a low loss BaSrTiO₃/ABS ceramic/polymer composite for fused filament fabrication additive manufacturing. *Addit Manuf* 55:1–8. <https://doi.org/10.1016/j.addma.2022.102844>
121. Goulas A, Zhang S, McGhee JR, Cadman DA, Whittow WG, Vardaxoglou JC, Engström DS (2020) Fused filament fabrication of functionally graded polymer composites with variable relative permittivity for microwave devices. *Mater Des* 193:108871. <https://doi.org/10.1016/j.matdes.2020.108871>

122. ErvinaEfzan MN, Siti SN (2018) A review on effect of nanoreinforcement on mechanical properties of polymer nanocomposites. *Solid State Phenom* 280:284–293. <https://doi.org/10.4028/www.scientific.net/SSP.280.284>
123. Ryan KR, Down MP, Hurst NJ, Keefe EM, Banks CE (2022) Additive manufacturing (3D printing) of electrically conductive polymers and polymer nanocomposites and their applications. *EScience* 2:365–381. <https://doi.org/10.1016/j.esci.2022.07.003>
124. Haq RHA, Wahab MS, Jaimi NI (2014) Fabrication process of polymer nano-composite filament for fused deposition modeling. *Appl Mech Mater* 465–466:8–12. <https://doi.org/10.4028/www.scientific.net/AMM.465-466.8>
125. Tsiakatouras G, Tsellou E, Stergiou C (2014) Comparative study on nanotubes reinforced with carbon filaments for the 3D printing of mechanical parts. *World Trans Eng Technol Educ* 12:392–396
126. Dorigato A, Moretti V, Dul S, Unterberger SH, Pegoretti A (2017) Electrically conductive nanocomposites for fused deposition modelling. *Synth Met* 226:7–14. <https://doi.org/10.1016/j.synthmet.2017.01.009>
127. Díaz-García JY, Law A, Cota A, Bellido-Correa J, Ramírez-Rico R, Schäfer V (2020) Franco, Novel procedure for laboratory scale production of composite functional filaments for additive manufacturing. *Mater Today Commun* 24:101049. <https://doi.org/10.1016/j.mtcomm.2020.101049>
128. Hashemi R, Campagne C, Nierstrasz V (2017) Applied Surface Science Investigation of the adhesion properties of direct 3D printing of polymers and nanocomposites on textiles : effect of FDM printing process parameters. *Appl Surf Sci* 403:551–563. <https://doi.org/10.1016/j.apsusc.2017.01.112>
129. Tambrallimath V, Keshavamurthy R, Bavan SD, Patil AY, Khan TMY, Badruddin IA, Kamangar S (2021) Mechanical properties of PC-ABS-based graphene-reinforced polymer nanocomposites fabricated by FDM process. *Polymers (Basel)* 13:2951
130. Lei M, Wei Q, Li M, Zhang J, Yang R, Wang Y (2022) Numerical simulation and experimental study the effects of process parameters on filament morphology and mechanical properties of FDM 3D printed PLA / GNPs nanocomposite. *Polymers (Basel)* 14:3081
131. Omar NWY, Shuaib NA, Hadi MHJA, Azmi AI (2019) Mechanical properties of carbon and glass fibre reinforced composites produced by additive manufacturing: a short review. *IOP Conf Ser Mater Sci Eng* 670:012020. <https://doi.org/10.1088/1757-899X/670/1/012020>
132. Sanei SHR, Popescu D (2020) 3d-printed carbon fiber reinforced polymer composites: a systematic review. *J Compos Sci* 4:98. <https://doi.org/10.3390/jcs4030098>
133. van de Werken N, Tekinalp H, Khanbolouki P, Ozcan S, Williams A, Tehrani M (2020) Additively manufactured carbon fiber-reinforced composites: state of the art and perspective. *Addit Manuf* 31:100962. <https://doi.org/10.1016/j.addma.2019.100962>
134. Ochi S (2015) Flexural properties of long bamboo fiber/ pla composites, *Open. J Compos Mater* 05:70–78. <https://doi.org/10.4236/ojcm.2015.53010>
135. Le Duigou A, Correa D, Ueda M, Matsuzaki R, Castro M (2020) A review of 3D and 4D printing of natural fibre biocomposites. *Mater Des* 194:108911. <https://doi.org/10.1016/j.matdes.2020.108911>
136. Ahmad MN, Ishak MR, Mohammad Taha M, Mustapha F, Leman Z, Irianto (2023) Mechanical, thermal and physical characteristics of oil palm (*Elaeis Guineensis*) fiber reinforced thermoplastic composites for FDM – Type 3D printer. *Polym Test* 120:107972. <https://doi.org/10.1016/j.polymertesting.2023.107972>
137. Abramovitch H, Burgard M, Edery-Azulay L, Evans KE, Hoffmeister M, Miller W, Scarpa F, Smith CW, Tee KF (2010) Smart tetrachiral and hexachiral honeycomb: sensing and impact detection. *Compos Sci Technol* 70:1072–1079. <https://doi.org/10.1016/j.compscitech.2009.07.017>
138. Ning F, Cong W, Qiu J, Wei J, Wang S (2015) Additive manufacturing of carbon fiber reinforced thermoplastic composites using fused deposition modeling. *Compos Part B Eng* 80:369–378. <https://doi.org/10.1016/j.compositesb.2015.06.013>
139. Ueda M, Watanabe Y, Mukai Y, Katsumata N (2021) Three-dimensional printing of locally bendable short carbon fiber reinforced polymer composites. *Adv Ind Eng Polym Res* 4:264–269. <https://doi.org/10.1016/j.aiepr.2021.02.004>
140. Fernandes RR, van de Werken N, Koirala P, Yap T, Tamijani AY, Tehrani M (2021) Experimental investigation of additively manufactured continuous fiber reinforced composite parts with optimized topology and fiber paths. *Addit Manuf* 44:102056. <https://doi.org/10.1016/j.addma.2021.102056>
141. Fico D, Rizzo D, Casciaro R, Corcione CE (2022) A review of polymer-based materials for fused filament fabrication (FFF): focus on sustainability and recycled materials. *Polymers (Basel)* 14:465. <https://doi.org/10.3390/polym14030465>
142. Dul S, Fambri L, Pegoretti A (2016) Fused deposition modelling with ABS-graphene nanocomposites. *Compos Part A Appl Sci Manuf* 85:181–191. <https://doi.org/10.1016/j.compositesa.2016.03.013>
143. Weng Z, Wang J, Senthil T, Wu L (2016) Institute of research on the structure of matter, Chinese academy of sciences. *JMADE*. <https://doi.org/10.1016/j.matdes.2016.04.045>
144. Shanmugam V (2021) Fused deposition modeling based polymeric materials and their performance: a review. 1–22. <https://doi.org/10.1002/pc.26275>
145. Maqsood N, Rima M (2021) Composites Part C: Open access characterization of carbon fiber reinforced PLA composites manufactured by fused deposition modelling. 4. <https://doi.org/10.1016/j.jcocom.2021.100112>
146. Ilyas RA, Sapuan SM, Harussani MM, Hakimi MYAY, Haziq MZM, Atikah MSN, Asyraf MRM, Ishak MR, Razman MR, Nurazzi NM, Norrrahim MNF, Abrial H, Asrofi M (2021) Polylactic acid (Pla) biocomposite: processing, additive manufacturing and advanced applications. *Polymers (Basel)* 13:1326. <https://doi.org/10.3390/polym13081326>
147. Sodeifian G, Ghaseminejad S, Yousefi AA (2019) Preparation of polypropylene/short glass fiber composite as fused deposition modeling (FDM) filament. *Results Phys* 12:205–222. <https://doi.org/10.1016/j.rinp.2018.11.065>
148. Street DP, Mah AH, Patterson S, Pickel DL, Bergman JA, Stein GE, Messman JM, Kilbey SM (2018) Interfacial interactions in PMMA/silica nanocomposites enhance the performance of parts created by Fused Filament Fabrication. *Polymer (Guildf)* 157:87–94. <https://doi.org/10.1016/j.polymer.2018.10.004>
149. Zhang Z, Demir KG, Gu GX (2019) Developments in 4D-printing: a review on current smart materials, technologies, and applications. *Int J Smart Nano Mater* 10:205–224. <https://doi.org/10.1080/19475411.2019.1591541>
150. Khoo ZX, Teoh JEM, Liu Y, Chua CK, Yang S, An J, Leong KF, Yeong WY (2015) 3D printing of smart materials: a review on recent progresses in 4D printing. *Virtual Phys Prototyp* 10:103–122. <https://doi.org/10.1080/17452759.2015.1097054>
151. Kamila S (2013) Introduction, classification and applications of smart materials: an overview. *Am J Appl Sci* 10:876–880. <https://doi.org/10.3844/ajassp.2013.876.880>
152. Varadan VK, Vinoy KJ, Gopalakrishnan S (2006) Smart material systems and MEMS: design and development methodologies. Wiley
153. Le A, Correa D, Ueda M, Matsuzaki R, Castro M (2020) A review of 3D and 4D printing of natural fibre biocomposites. *Mater Des* 194:108911. <https://doi.org/10.1016/j.matdes.2020.108911>

154. Salentijn GIJ, Oomen PE, Grajewski M, Verpoorte E (2017) Fused deposition modeling 3D printing for (bio)analytical device fabrication: procedures, materials, and applications. <https://doi.org/10.1021/acs.analchem.7b00828>
155. Momeni F, Sabzpoushan S, Valizadeh R, Morad MR, Liu X, Ni J (2019) Plant leaf-mimetic smart wind turbine blades by 4D printing. *Renew Energy* 130:329–351
156. Cuan-Urquiza E, Barocio E, Tejada-Ortigoza V, Pipes RB, Rodriguez CA, Roman-Flores A (2019) Characterization of the mechanical properties of FFF structures and materials: a review on the experimental, computational and theoretical approaches. *Materials (Basel)* 16:895. <https://doi.org/10.3390/ma12060895>
157. Bakhtiari H, Aamir M, Tolouei-Rad M (2023) Effect of 3D printing parameters on the fatigue properties of parts manufactured by fused filament fabrication: a review. *Appl Sci* 13:904. <https://doi.org/10.3390/app13020904>
158. Shanmugam V, Das O, Babu K, Marimuthu U, Veerasimman A, Johnson DJ, Neisiany RE, Hedenqvist MS, Ramakrishna S, Berto F (2021) Fatigue behaviour of FDM-3D printed polymers, polymeric composites and architected cellular materials. *Int J Fatigue* 143:1–15. <https://doi.org/10.1016/j.ijfatigue.2020.106007>
159. Goh GD, Yap YL, Tan HKJ, Sing SL, Goh GL, Yeong WY (2020) Process–structure–properties in polymer additive manufacturing via material extrusion: a review. *Crit Rev Solid State Mater Sci* 45:113–133. <https://doi.org/10.1080/10408436.2018.1549977>
160. Gao G, Xu F, Xu J, Tang G, Liu Z (2022) A survey of the influence of process parameters on mechanical properties of fused deposition modeling parts. *Micromachines* 13:1–28. <https://doi.org/10.3390/mi13040553>
161. Gebisa AW, Lemu HG (2018) Investigating effects of fused-deposition modeling (FDM) processing parameters on flexural properties of ULTEM 9085 using designed experiment. *Materials (Basel)* 11:1–23. <https://doi.org/10.3390/ma11040500>
162. Khan MS, Mishra SB (2019) Minimizing surface roughness of ABS-FDM build parts: an experimental approach. *Mater Today Proc* 26:1557–1566. <https://doi.org/10.1016/j.matpr.2020.02.320>
163. Zharylkassyn B, Perveen A, Talamona D (2021) Effect of process parameters and materials on the dimensional accuracy of FDM parts. *Mater Today Proc* 44:1307–1311. <https://doi.org/10.1016/j.matpr.2020.11.332>
164. Mohamed OA, Masood SH, Bhowmik JL (2017) Experimental investigation for dynamic stiffness and dimensional accuracy of FDM manufactured part using IV-Optimal response surface design. *Rapid Prototyp J* 23:736–749. <https://doi.org/10.1108/RPJ-10-2015-0137>
165. Mohanty A, Nag KS, Bagal DK, Barua A, Jeet S, Mahapatra SS, Cherkia H (2021) Parametric optimization of parameters affecting dimension precision of FDM printed part using hybrid Taguchi-MARCOS-nature inspired heuristic optimization technique. *Mater Today Proc* 50:893–903. <https://doi.org/10.1016/j.matpr.2021.06.216>
166. Ahn SH, Montero M, Odell D, Roundy S, Wright PK (2002) Anisotropic material properties of fused deposition modeling ABS. *Rapid Prototyp J* 8:248–257. <https://doi.org/10.1108/13552540210441166>
167. Zekavat AR, Jansson A, Larsson J, Pejryd L (2019) Investigating the effect of fabrication temperature on mechanical properties of fused deposition modeling parts using X-ray computed tomography. *Int J Adv Manuf Technol* 100:287–296. <https://doi.org/10.1007/s00170-018-2664-8>
168. Gebisa AW, Lemu HG (2019) Influence of 3D printing FDM process parameters on tensile property of ultem 9085. *Procedia Manuf* 30:331–338. <https://doi.org/10.1016/j.promfg.2019.02.047>
169. Dawoud M, Taha I, Ebeid SJ (2016) Mechanical behaviour of ABS: an experimental study using FDM and injection moulding techniques. *J Manuf Process* 21:39–45. <https://doi.org/10.1016/j.jmapro.2015.11.002>
170. Rayegani F, Onwubolu GC (2014) Fused deposition modelling (fdm) process parameter prediction and optimization using group method for data handling (gmdh) and differential evolution (de). *Int J Adv Manuf Technol* 73:509–519. <https://doi.org/10.1007/s00170-014-5835-2>
171. Motaparti KP, Taylor G, Leu MC, Chandrashekhara K, Castle J, Matlack M (2016) Effects of build parameters on compression properties for ULTEM 9085 parts by fused deposition modelling. In: *Proceeding 27th Annu Int Solid Free Fabr Symp* pp 964–977
172. Too MH, Leong KF, Chua CK, Du ZH, Yang SF, Cheah CM, Ho SL (2002) Investigation of 3D non-random porous structures by fused deposition modelling. *Int J Adv Manuf Technol* 19:217–223. <https://doi.org/10.1007/s001700200016>
173. Alsoufi MS, El-Sayed A, Elsayed AE (2017) How surface roughness performance of printed parts manufactured by desktop FDM 3D printer with PLA+ is influenced by measuring direction. *Am J Mech Eng* 5:211–222. <https://doi.org/10.12691/ajme-5-5-4>
174. Nancharaiah T, Ranga Raju D, Ramachandra Raju V (2010) An experimental investigation on surface quality and dimensional accuracy of FDM components. *Int J Emerg Technol* 1:106–111
175. Kamoon SN, Masood SH, Mohamed OA (2018) Experimental investigation on flexural properties of FDM processed Nylon 12 parts using RSM. *IOP Conf Ser Mater Sci Eng* 377:012137. <https://doi.org/10.1088/1757-899X/377/1/012137>
176. Mishra SB, Malik R, Mahapatra SS (2017) Effect of external perimeter on flexural strength of FDM build parts. *Arab J Sci Eng* 42:4587–4595. <https://doi.org/10.1007/s13369-017-2598-8>
177. Hassanifard S, Behdinin K (2022) Effects of voids and raster orientations on fatigue life of notched additively manufactured PLA components. *Int J Adv Manuf Technol* 120:6241–6250. <https://doi.org/10.1007/s00170-022-09169-1>
178. Mishra SB, Mahapatra SS (2018) An experimental investigation on strain controlled fatigue behaviour of FDM build parts. *Int J Product Qual Manag* 24:323–345. <https://doi.org/10.1504/IJPMQ.2018.092980>
179. Bianchi I, Forcellese A, Mancina T, Simoncini M, Vita A (2022) Process parameters effect on environmental sustainability of composites FFF technology. *Mater Manuf Process* 37:591–601. <https://doi.org/10.1080/10426914.2022.2049300>
180. Milde J, Morović L, Blaha J (2017) Influence of the layer thickness in the fused deposition modeling process on the dimensional and shape accuracy of the upper teeth model. 02006. <https://doi.org/10.1051/mateconf/201713702006>
181. Tymrak BM, Kreiger M, Pearce JM (2014) Mechanical properties of components fabricated with open-source 3-D printers under realistic environmental conditions. *Mater Des* 58:242–246. <https://doi.org/10.1016/j.matdes.2014.02.038>
182. Uddin MS, Sidek MFR, Faizal MA, Ghomashchi R, Pramanik A (2017) Evaluating mechanical properties and failure mechanisms of fused deposition modeling acrylonitrile butadiene styrene parts. *J Manuf Sci Eng Trans ASME* 139:1–12. <https://doi.org/10.1115/1.4036713>
183. Griffiths CA, Howarth J, de Almeida Rowbotham G, Rees A (2016) Effect of build parameters on processing efficiency and material performance in fused deposition modelling. *Procedia CIRP* 49:28–32. <https://doi.org/10.1016/J.PROCIR.2015.07.024>
184. Chacón JM, Caminero MA, García-Plaza E, Núñez PJ (2017) Additive manufacturing of PLA structures using fused deposition modelling: effect of process parameters on mechanical properties and their optimal selection. *Mater Des* 124:143–157. <https://doi.org/10.1016/j.matdes.2017.03.065>
185. MengeshaMedibew T (2022) A Comprehensive review on the optimization of the fused deposition modeling process parameter

- for better tensile strength of PLA-printed parts. *Adv Mater Sci Eng* 2022;1. <https://doi.org/10.1155/2022/5490831>
186. Travieso-Rodriguez JA, Jerez-Mesa R, Llumà J, Traver-Ramos O, Gomez-Gras G, Rovira JJR (2019) Mechanical properties of 3D-printing polylactic acid parts subjected to bending stress and fatigue testing. *Materials (Basel)* 12. <https://doi.org/10.3390/ma122333859>
 187. Xu C, Cheng K, Liu Y, Wang R, Jiang X, Dong X, Xu X (2020) Effect of processing parameters on flexural properties of 3D-printed polyetherketoneketone using fused deposition modeling. *Polym Eng Sci* 61:465–476
 188. Nugroho A, Ardiansyah R, Rusita L, Larasati IL (2018) Effect of layer thickness on flexural properties of PLA (PolyLactid Acid) by 3D printing. *J Phys Conf Ser* 1130:1–10. <https://doi.org/10.1088/1742-6596/1130/1/012017>
 189. Wang P, Zou B, Ding S, Li L, Huang C (2021) Effects of FDM-3D printing parameters on mechanical properties and microstructure of CF/PEEK and GF/PEEK. *Chinese J Aeronaut* 34:236–246. <https://doi.org/10.1016/j.cja.2020.05.040>
 190. Gomez-gras G, Jerez-mesa R, Travieso-rodriguez JA, Lluma-fuentes J (2018) Fatigue performance of fused filament fabrication PLA specimens. *Mater Des* 140:278–285. <https://doi.org/10.1016/j.matdes.2017.11.072>
 191. Travieso-rodriguez JA, Jerez-mesa R, Lluma J, Traver-ramos O, Gomez-gras G, RoaRovira JJ (2019) Mechanical properties of 3D-printing polylactic acid parts subjected to bending stress and fatigue testing. *Materials (Basel)* 12:1–20
 192. Alshammari YLA, He F, Khan MA (2021) Acrylonitrile butadiene styrene (ABS) with various printing parameters and ambient temperatures. *Polymers (Basel)* 13:1–20
 193. He F, Khan M (2021) Effects of printing parameters on the fatigue behaviour of 3D-printed ABS under dynamic thermo-mechanical loads. *Polymers (Basel)* 13:1–23
 194. Domingo-Espin M, Travieso-Rodriguez J, Jerez-Mesa R, Lluma-Fuentes J (2018) Fatigue performance of ABS specimens obtained by fused filament fabrication. *Materials (Basel)* 11:1–16. <https://doi.org/10.3390/ma11122521>
 195. Travieso-rodriguez JA, Zandi MD, Jerez-mesa R, Lluma-Fuentes J (2020) Fatigue behavior of PLA-wood composite. *J Mater Res Technol* 9:8507–8516
 196. Kuznetsov VE, Solonin AN, Urzhumtsev OD, Schilling R, Tavitov AG (2018) Strength of PLA components fabricated with fused deposition technology using a desktop 3D printer as a function of geometrical parameters of the process. *Polymers (Basel)* 10:313. <https://doi.org/10.3390/polym10030313>
 197. Zaldivar RJ, Witkin DB, McLouth T, Patel DN, Schmitt K, Nokes JP (2017) Influence of processing and orientation print effects on the mechanical and thermal behavior of 3D-Printed ULTEM® 9085 Material. *Addit Manuf* 13:71–80. <https://doi.org/10.1016/j.addma.2016.11.007>
 198. Riddick JC, Haile MA, Von Wahlde R, Cole DP, Bamiduro O, Johnson TE (2016) Fractographic analysis of tensile failure of acrylonitrile-butadiene-styrene fabricated by fused deposition modeling. *Addit Manuf* 11:49–59. <https://doi.org/10.1016/j.addma.2016.03.007>
 199. Cantrell JT, Rohde S, Damiani D, Gurnani R, DiSandro L, Anton J, Young A, Jerez A, Steinbach D, Kroese C, Ifju PG (2017) Experimental characterization of the mechanical properties of 3D-printed ABS and polycarbonate parts. *Rapid Prototyp J* 23:811–824. <https://doi.org/10.1108/RPJ-03-2016-0042>
 200. Abbott AC, Tandon GP, Bradford RL, Koerner H, Baur JW (2018) Process-structure-property effects on ABS bond strength in fused filament fabrication. *Addit Manuf* 19:29–38. <https://doi.org/10.1016/j.addma.2017.11.002>
 201. Gonabadi H, Yadav A, Bull SJ (2020) The effect of processing parameters on the mechanical characteristics of PLA produced by a 3D FFF printer. *Int J Adv Manuf Technol* 111:695–709. <https://doi.org/10.1007/s00170-020-06138-4>
 202. Smith WC, Dean RW (2013) Structural characteristics of fused deposition modeling polycarbonate material. *Polym Test* 32:1306–1312. <https://doi.org/10.1016/j.polymertesting.2013.07.014>
 203. Jin Y, Wan Y, Zhang B, Liu Z (2017) Modeling of the chemical finishing process for polylactic acid parts in fused deposition modeling and investigation of its tensile properties. *J Mater Process Technol* 240:233–239. <https://doi.org/10.1016/j.jmatp.rotec.2016.10.003>
 204. Domingo-Espin M, Puigoriol-Forcada JM, Garcia-Granada AA, Llumà J, Borros S, Reyes G (2015) Mechanical property characterization and simulation of fused deposition modeling Polycarbonate parts. *Mater Des* 83:670–677. <https://doi.org/10.1016/j.matdes.2015.06.074>
 205. Yadav DK, Srivastava R, Dev S (2020) Materials Today : Proceedings Design & fabrication of ABS part by FDM for automobile application. *Mater Today Proc* 26:2089–2093. <https://doi.org/10.1016/j.matpr.2020.02.451>
 206. Thiery G, Wang X, Mason L, Leu MC, Chandrashekhara K, Schniepp T, Jones R (2018) Flexural behavior of additively manufactured Ultem 1010: experiment and simulation. *Rapid Prototyp J* 24:1003–1011. <https://doi.org/10.1108/RPJ-02-2018-0037>
 207. Raut S, Jatti VS, Khedkar NK, Singh TP (2014) Investigation of the effect of built orientation on mechanical properties and total cost of FDM parts. *Procedia. Mater Sci* 6:1625–1630. <https://doi.org/10.1016/j.mspro.2014.07.146>
 208. Beattie N, Bock N, Anderson T, Edgeworth T, Kloss T, Swanson J (2021) Effects of build orientation on mechanical properties of fused deposition modeling parts. *J Mater Eng Perform* 30:5059–5065. <https://doi.org/10.1007/s11665-021-05624-4>
 209. Afrose MF, Masood SH, Iovenitti P, Nikzad M, Sbarski I (2016) Effects of part build orientations on fatigue behaviour of FDM-processed PLA material. *Prog Addit Manuf* 1:21–28. <https://doi.org/10.1007/s40964-015-0002-3>
 210. Puigoriol-Forcada JM, Alsina A, Salazar-Martín AG, Gomez-Gras G, Pérez MA (2018) Flexural fatigue properties of polycarbonate fused-deposition modelling specimens. *Mater Des* 155:414–421. <https://doi.org/10.1016/j.matdes.2018.06.018>
 211. Terekhina S, Tarasova T, Egorov S, Skorniyakov I, Guillaumat L, Hattali ML (2020) The effect of build orientation on both flexural quasi-static and fatigue behaviours of filament deposited PA6 polymer. *Int J Fatigue* 140:105825. <https://doi.org/10.1016/j.ijfatigue.2020.105825>
 212. Fischer M, Schöppner V (2017) Fatigue behavior of FDM parts manufactured with Ultem 9085. *Jom* 69:563–568. <https://doi.org/10.1007/s11837-016-2197-2>
 213. Azadi M, Dadashi A, Dezhianian S, Kianifar M, Torkaman S, Chiyani M (2021) High-cycle bending fatigue properties of additive-manufactured ABS and PLA polymers fabricated by fused deposition modeling 3D-printing. *Forces Mech* 3:100016. <https://doi.org/10.1016/j.finmec.2021.100016>
 214. Hassanifard S, Hashemi SM (2020) On the strain-life fatigue parameters of additive manufactured plastic materials through fused filament fabrication process. *Addit Manuf* 32:1–8. <https://doi.org/10.1016/j.addma.2019.100973>
 215. Rajan K, Samykano M, Kadirgama K, Harun WSW, Rahman MM (2022) Fused deposition modeling: process, materials, parameters, properties, and applications. *Int J Adv Manuf Technol*. <https://doi.org/10.1007/s00170-022-08860-7>
 216. Çakan BG (2021) Effects of raster angle on tensile and surface roughness properties of various FDM filaments. *J Mech Sci Technol* 35:3347–3353. <https://doi.org/10.1007/s12206-021-0708-8>
 217. Es-Said OS, Foyos J, Noorani R, Mendelson M, Marloth R, Pregarer BA (2000) Effect of layer orientation on mechanical

- properties of rapid prototyped samples. *Mater Manuf Process* 15:107–122. <https://doi.org/10.1080/10426910008912976>
218. Melenka GW, Schofield JS, Dawson MR, Carey JP (2015) Evaluation of dimensional accuracy and material properties of the MakerBot 3D desktop printer. *Rapid Prototyp J* 21:618–627. <https://doi.org/10.1108/RPJ-09-2013-0093>
 219. Rajpurohit SR, Dave HK (2018) Flexural strength of fused filament fabricated (FFF) PLA parts on an open-source 3D printer. *Adv Manuf* 6:430–441. <https://doi.org/10.1007/s40436-018-0237-6>
 220. Christiyan KGJ, Chandrasekhar U, Venkateswarlu K (2016) Flexural properties of PLA Components under various test condition manufactured by 3D printer. *J Inst Eng.* <https://doi.org/10.1007/s40032-016-0344-8>
 221. Styrene AB, Qayyum H, Hussain G, Sulaiman M, Hassan M, Ali A, Muhammad R, Wei H, Shehbaz T, Aamir M, Altaf K (2022) Applied sciences effect of raster angle and infill pattern on the in-plane and edgewise flexural properties of fused filament fabricated acrylonitrile-butadiene-styrene. *Appl Sci* 12:1–15
 222. Srinivasan S, Iyer G, Keles O (2022) Effect of raster angle on mechanical properties of 3D printed short carbon fiber reinforced acrylonitrile butadiene styrene. *Compos Commun* 32:101163. <https://doi.org/10.1016/j.coco.2022.101163>
 223. Srinivasan Ganesh Iyer S, Keles O (2022) Effect of raster angle on mechanical properties of 3D printed short carbon fiber reinforced acrylonitrile butadiene styrene. *Compos Commun* 32:101163. <https://doi.org/10.1016/j.coco.2022.101163>
 224. Ziemian S, Okwara M, Ziemian CW (2015) Tensile and fatigue behavior of layered acrylonitrile butadiene styrene. *Rapid Prototyp J* 3:270–278. <https://doi.org/10.1108/RPJ-09-2013-0086>
 225. Mayén J, Del Carmen Gallegos-Melgar A, Pereyra I, Poblano-Salas CA, Hernández-Hernández M, Betancourt-Cantera JA, Mercado-Lemus VH, Del Angel Monroy M (2022) Descriptive and inferential study of hardness, fatigue life, and crack propagation on PLA 3D-printed parts. *Mater Today Commun* 32:103948. <https://doi.org/10.1016/j.mtcomm.2022.103948>
 226. Jap NSF, Pearce GM, Hellier AK, Russell N, Parr WC, Walsh WR (2019) The effect of raster orientation on the static and fatigue properties of filament deposited ABS polymer. *Int J Fatigue* 124:328–337. <https://doi.org/10.1016/j.ijfatigue.2019.02.042>
 227. Alshammari YLA, He F, Khan MA (2021) Modelling and investigation of crack growth for 3d-printed acrylonitrile butadiene styrene (ABS) with various printing parameters and ambient temperatures. *Polymers (Basel)* 13:3737. <https://doi.org/10.3390/polym13213737>
 228. Ezeh OH, Susmel L (2019) Fatigue strength of additively manufactured polylactide (PLA): effect of raster angle and non-zero mean stresses. *Int J Fatigue* 126:319–326. <https://doi.org/10.1016/j.ijfatigue.2019.05.014>
 229. Ezeh OH, Susmel L (2018) On the fatigue strength of 3D-printed polylactide (PLA). *Procedia Struct Integr* 9:29–36. <https://doi.org/10.1016/j.prostr.2018.06.007>
 230. Hassanifard S, Hashemi SM (2020) On the strain-life fatigue parameters of additive manufactured plastic materials through fused filament fabrication process. *Addit Manuf* 32:100973. <https://doi.org/10.1016/j.addma.2019.100973>
 231. Letcher T, Waytashek M (2016) Material property testing of 3D-printed specimen in PLA on an entry-level 3D printer. *Proc ASME 2014 Int Mech Eng Congr Expo* 1–8. <http://www.asme.org/about-asme/terms-of-use>
 232. Dialami N, Chiumenti M, Cervera M, Rossi R, Chasco U, Domingo M (2021) Numerical and experimental analysis of the structural performance of AM components built by fused filament fabrication. *Int J Mech Mater Des* 17:225–244. <https://doi.org/10.1007/s10999-020-09524-8>
 233. Mahmood S, Qureshi AJ, Goh KL, Talamona D (2017) Tensile strength of partially filled FFF printed parts: experimental results. *Rapid Prototyp J* 23:122–128. <https://doi.org/10.1108/RPJ-08-2015-0115>
 234. Rashed K, Kafi A, Simons R, Bateman S (2022) Effects of fused filament fabrication process parameters on tensile properties of polyether ketone ketone (PEKK). *Int J Adv Manuf Technol* 122:3607–3621. <https://doi.org/10.1007/s00170-022-10134-1>
 235. Giri J, Shahane P, Jachak S, Chadge R, Giri P (2021) Optimization of fdm process parameters for dual extruder 3d printer using artificial neural network. *Mater Today Proc* 43:3242–3249. <https://doi.org/10.1016/j.matpr.2021.01.899>
 236. Crococolo D, De Agostinis M, Olmi G (2013) Experimental characterization and analytical modelling of the mechanical behaviour of fused deposition processed parts made of ABS-M30. *Comput Mater Sci* 79:506–518. <https://doi.org/10.1016/j.commatsci.2013.06.041>
 237. Hikmat M, Rostam S, Ahmed YM (2021) Investigation of tensile property-based Taguchi method of PLA parts fabricated by FDM 3D printing technology. *Results Eng* 11:100264. <https://doi.org/10.1016/j.rineng.2021.100264>
 238. Kumar N, Jain PK, Tandon P, Pandey PM (2018) The effect of process parameters on tensile behavior of 3D printed flexible parts of ethylene vinyl acetate (EVA). *J Manuf Process* 35:317–326. <https://doi.org/10.1016/j.jmapro.2018.08.013>
 239. Bruère VM, Lion A, Holtmannspötter J, Jehlitz M (2023) The influence of printing parameters on the mechanical properties of 3D printed TPU-based elastomers. *Prog Addit Manuf.* <https://doi.org/10.1007/s40964-023-00418-7>
 240. Mohamed OA, Masood SH, Bhowmik JL (2016) Mathematical modeling and FDM process parameters optimization using response surface methodology based on Q-optimal design. *Appl Math Model* 40:10052–10073. <https://doi.org/10.1016/j.apm.2016.06.055>
 241. Choudhary N, Sharma V, Kumar P (2023) Polylactic acid-based composite using fused filament fabrication: process optimization and biomedical application. *Polym Compos* 44:69–88. <https://doi.org/10.1002/pc.27027>
 242. Rashed K, Kafi A, Simons R, Bateman S (2023) Optimization of material extrusion additive manufacturing process parameters for polyether ketone ketone (PEKK). *Int J Adv Manuf Technol.* <https://doi.org/10.1007/s00170-023-11167-w>
 243. Chowdary BV, Bob AA (2021) Impact of processing parameters on fatigue life of fused filament fabricated parts: application of central composite design and genetic algorithm tools. *Int J Rapid Manuf* 10:80–104
 244. Gordelier TJ, Thies PR, Turner L, Johanning L (2019) Optimising the FDM additive manufacturing process to achieve maximum tensile strength: a state-of-the-art review. *Rapid Prototyp J* 25:953–971. <https://doi.org/10.1108/RPJ-07-2018-0183>
 245. Khan I, Kumar N (2020) Fused deposition modelling process parameters influence on the mechanical properties of ABS: A review. *Mater Today Proc* 44:4004–4008. <https://doi.org/10.1016/j.matpr.2020.10.202>
 246. Sandanamsamy L, Harun WSW, Ishak I, Romlay FRM, Kadirgama K, Ramasamy D, Idris SRA, Tsumori F (2022) A comprehensive review on fused deposition modelling of polylactic acid. *Prog Addit Manuf.* <https://doi.org/10.1007/s40964-022-00356-w>
 247. Vishwas M, Basavaraj CK (2017) Studies on optimizing process parameters of fused deposition modelling technology for ABS. *Mater Today Proc* 4:10994–11003. <https://doi.org/10.1016/j.matpr.2017.08.057>
 248. Syrlybayev D, Zharylkassyn B, Seisekulova A, Akhmetov M, Perveen A, Talamona D (2021) Optimisation of strength properties of FDM printed parts — a. *Polymers (Basel)* 13:1–35
 249. Bakır AA, Atik R, Özerinç S (2021) Mechanical properties of thermoplastic parts produced by fused deposition modeling:a

- review. *Rapid Prototyp J* 27:537–561. <https://doi.org/10.1108/RPJ-03-2020-0061>
250. Chohan JS, Singh R (2017) Pre and post processing techniques to improve surface characteristics of FDM parts: a state of art review and future applications. *Rapid Prototyp J* 23:495
 251. Kaur G, Singari RM, Kumar H (2021) A review of fused filament fabrication (FFF): process parameters and their impact on the tribological behavior of polymers (ABS). *Mater Today Proc* 51:854–860. <https://doi.org/10.1016/j.matpr.2021.06.274>
 252. Vicente CMS, Martins TS, Leite M, Ribeiro A, Reis L (2020) Influence of fused deposition modeling parameters on the mechanical properties of ABS parts. *Polym Adv Technol* 31:501–507. <https://doi.org/10.1002/pat.4787>
 253. Zhang X, Chen L, Mulholland T, Osswald TA (2019) Effects of raster angle on the mechanical properties of PLA and Al / PLA composite part produced by fused deposition modelling. 2122–2135. <https://doi.org/10.1002/pat.4645>
 254. Krajangsawadi N, Blok LG, Hamerton I, Longana ML, Woods BKS, Ivanov DS (2021) Fused deposition modelling of fibre reinforced polymer composites : a parametric review. *J Compos Sci* 5:1–38
 255. Ramesh M, Rajeshkumar L, Balaji D (2021) Influence of process parameters on the properties of additively manufactured fiber-reinforced polymer composite materials : a review. *J Mater Eng Perform* 30:4792–4807
 256. Jiang D, Smith DE (2017) Anisotropic mechanical properties of oriented carbon fiber filled polymer composites produced with fused filament fabrication. *Addit Manuf* 18:84–94. <https://doi.org/10.1016/j.addma.2017.08.006>
 257. Peng X, Zhang M, Guo Z, Sang L, Hou W (2020) Investigation of processing parameters on tensile performance for FDM-printed carbon fiber reinforced polyamide 6 composites. *Compos Commun* 22:1–7. <https://doi.org/10.1016/j.coco.2020.100478>
 258. Tekinalp HL, Kunc V, Velez-Garcia GM, Duty CE, Love LJ, Naskar AK, Blue CA, Ozcan S (2014) Highly oriented carbon fiber–polymer composites via additive manufacturing. *Compos Sci Technol* 105:144–150
 259. Chacón JM, Caminero MA, Núñez PJ, García-Plaza E, García-Moreno I, Reverte JM (2019) Additive manufacturing of continuous fibre reinforced thermoplastic composites using fused deposition modelling: effect of process parameters on mechanical properties. *Compos Sci Technol* 181:107688. <https://doi.org/10.1016/j.compscitech.2019.107688>
 260. Ramalingam PS, Mayandi K, Balasubramanian V, Chandrasekar K, Stalany VM, Munaf AA (2020) Effect of 3D printing process parameters on the impact strength of onyx – glass fiber reinforced composites. *Mater Today Proc* 45:6154–6159. <https://doi.org/10.1016/j.matpr.2020.10.467>
 261. Mohan KHR, Benal MGM, Pradeep KGS, Tambrallimath V, Geetha HR, Khan TMY, Rajhi AA, Baig MAA (2022) Influence of short glass fibre reinforcement on mechanical properties of 3D printed ABS-based polymer composites. *Polymers (Basel)* 14:1182. <https://doi.org/10.3390/polym14061182>
 262. Rigon D, Ricotta M, Ardengo G, Meneghetti G (2021) Static mechanical properties of virgin and recycled short glass fiber-reinforced polypropylene produced by pellet additive manufacturing. *Fatigue Fract Eng Mater Struct* 44:2554–2569. <https://doi.org/10.1111/ffe.13517>
 263. Goh GD, Dikshit V, Nagalingam AP, Goh GL, Agarwala S, Sing SL, Wei J, Yeong WY (2018) Characterization of mechanical properties and fracture mode of additively manufactured carbon fiber and glass fiber reinforced thermoplastics. *Mater Des* 137:79–89. <https://doi.org/10.1016/j.matdes.2017.10.021>
 264. Alarifi IM (2022) A performance evaluation study of 3d printed nylon/glass fiber and nylon/carbon fiber composite materials. *J Mater Res Technol* 21:884–892. <https://doi.org/10.1016/j.jmrt.2022.09.085>
 265. Wang Y, Kong D, Zhang Q, Li W, Liu J (2021) Process parameters and mechanical properties of continuous glass fiber reinforced composites-poly(lactic acid) by fused deposition modeling. *J Reinf Plast Compos* 40:686–698. <https://doi.org/10.1177/0731684421998017>
 266. Penumakala PK, Santo J, Thomas A (2020) A critical review on the fused deposition modeling of thermoplastic polymer composites. *Compos Part B Eng* 201:108336. <https://doi.org/10.1016/j.compositesb.2020.108336>
 267. Zhong W, Li F, Zhang Z, Song L, Li Z (2001) Short fiber reinforced composites for fused deposition modeling. *Mater Sci Eng A* 301:125–130. [https://doi.org/10.1016/S0921-5093\(00\)01810-4](https://doi.org/10.1016/S0921-5093(00)01810-4)
 268. Yang D, Zhang H, Wu J, McCarthy ED (2021) Fibre flow and void formation in 3D printing of short-fibre reinforced thermoplastic composites: an experimental benchmark exercise. *Addit Manuf* 37:101686. <https://doi.org/10.1016/j.addma.2020.101686>
 269. Justo J, Távora L, García-Guzmán L, París F (2018) Characterization of 3D printed long fibre reinforced composites. *Compos Struct* 185:537–548. <https://doi.org/10.1016/j.compstruct.2017.11.052>
 270. Ahmad MN, Ishak MR, Taha MM, Mustapha F, Leman Z (2022) Rheological properties of natural fiber reinforced thermoplastic composite for fused deposition modeling (FDM): a short review. *J Adv Res Fluid Mech Therm Sci* 98:157–164. <https://doi.org/10.37934/arfm.98.2.157164>
 271. RajendranRoyan NR, Leong JS, Chan WN, Tan JR, Shamsuddin ZSB (2021) Current state and challenges of natural fibre-reinforced polymer composites as feeder in fdm-based 3d printing. *Polymers (Basel)* 13:2289. <https://doi.org/10.3390/polym13142289>
 272. Lee CH, Padzil FNBM, Lee SH, Ainun ZMA, Abdullah LC (2021) Potential for natural fiber reinforcement in pla polymer filaments for fused deposition modeling (Fdm) additive manufacturing: a review. *Polymers (Basel)* 13:1407. <https://doi.org/10.3390/polym13091407>
 273. Aida HJ, Nadlene R, Mastura MT, Yusriah L, Sivakumar D, Ilyas RA (2021) Natural fibre filament for fused deposition modelling (FDM): a review. *Int J Sustain Eng* 14:1988–2008. <https://doi.org/10.1080/19397038.2021.1962426>
 274. Fidan I, Imeri A, Gupta A, Hasanov S, Nasirov A, Elliott A, Alifui-Segbaya F, Nanami N (2019) The trends and challenges of fiber reinforced additive manufacturing. *Int J Adv Manuf Technol* 102:1801–1818. <https://doi.org/10.1007/s00170-018-03269-7>
 275. Mazzanti V, Malagutti L, Mollica F (2019) FDM 3D printing of polymers containing natural fillers: a review of their mechanical properties. *Polymers (Basel)* 11:1–22. <https://doi.org/10.3390/polym11071094>
 276. Scaffaro R, Citarrella MC, Gulino EF, Morreale M (2022) Hedysarum coronarium-based green composites prepared by compression molding and fused deposition modeling. *Materials (Basel)* 15:465. <https://doi.org/10.3390/ma15020465>
 277. Pereira DF, Branco AC, Cláudio R, Marques AC, Figueiredo-Pina CG (2023) Development of composites of PLA filled with different amounts of rice husk fibers for fused deposition modelling. *J Nat Fibers* 20. <https://doi.org/10.1080/15440478.2022.2162183>
 278. Deb D, Jafferson JM (2021) Natural fibers reinforced FDM 3D printing filaments. *Mater Today Proc* 46:1308–1318. <https://doi.org/10.1016/j.matpr.2021.02.397>
 279. Zhang Q, Cai H, Zhang A, Lin X, Yi W, Zhang J (2018) Effects of lubricant and toughening agent on the fluidity and toughness of poplar powder-reinforced poly(lactic acid) 3D printing materials. *Polymers (Basel)* 10:932. <https://doi.org/10.3390/polym10090932>

280. Balla VK, Kate KH, Satyavolu J, Singh P, Tadimeti JGD (2019) Additive manufacturing of natural fiber reinforced polymer composites: processing and prospects. *Compos Part B Eng* 174:106956. <https://doi.org/10.1016/j.compositesb.2019.106956>
281. Badouard C, Traon F, Denoual C, Mayer-Laigle C, Paës G, Bourmaud A (2019) Exploring mechanical properties of fully compostable flax reinforced composite filaments for 3D printing applications. *Ind Crops Prod* 135:246–250. <https://doi.org/10.1016/j.indcrop.2019.04.049>
282. Han SNMF, Taha MM, Mansor MR, Rahman MAA (2022) Investigation of tensile and flexural properties of kenaf fiber-reinforced acrylonitrile butadiene styrene composites fabricated by fused deposition modeling. *J Eng Appl Sci* 69:1–18. <https://doi.org/10.1186/s44147-022-00109-0>
283. Liu Z, Lei Q, Xing S (2019) Mechanical characteristics of wood, ceramic, metal and carbon fiber-based PLA composites fabricated by FDM. *J Mater Res Technol* 8:3743–3753. <https://doi.org/10.1016/j.jmrt.2019.06.034>
284. Shanmugam V, Rajendran DJJ, Babu K, Rajendran S, Veerasimman A, Marimuthu U, Singh S, Das O, Neisiany RE, Hedenqvist MS, Berto F, Ramakrishna S (2021) The mechanical testing and performance analysis of polymer-fibre composites prepared through the additive manufacturing. *Polym Test* 93:106925. <https://doi.org/10.1016/j.polymertesting.2020.106925>
285. Rafiee M, Abidnejad R, Ranta A, Ojha K, Karakoç A, Paltakari J (2021) Exploring the possibilities of FDM filaments comprising natural fiber-reinforced biocomposites for additive manufacturing. *AIMS Mater Sci* 8:524–537. <https://doi.org/10.3934/mater-sci.2021032>
286. Mazur KE, Borucka A, Kaczor P, Gądek S, Bogucki R, Mirzawiński D, Kuciel S (2022) Mechanical, thermal and microstructural characteristic of 3D printed polylactide composites with natural fibers: wood, bamboo and cork. *J Polym Environ* 30:2341–2354. <https://doi.org/10.1007/s10924-021-02356-3>
287. Cheng CY, Xie H, Xu Z, Li L, Jiang MN, Tang L, Yang KK, Wang YZ (2020) 4D printing of shape memory aliphatic copolyester via UV-assisted FDM strategy for medical protective devices. *Chem Eng J* 396:125242. <https://doi.org/10.1016/j.cej.2020.125242>
288. Fischer NA, Robinson AL, Lee TJ, Calascione TM, Koerner L, Nelson-Cheeseman BB (2022) Magnetic annealing of extruded thermoplastic magnetic elastomers for 3D-Printing via FDM. *J Magn Magn Mater* 553:169266. <https://doi.org/10.1016/j.jmmm.2022.169266>
289. Kačergis L, Mitkus R, Sinapius M (2019) Influence of fused deposition modeling process parameters on the transformation of 4D printed morphing structures. *Smart Mater Struct* 28:105042. <https://doi.org/10.1088/1361-665X/ab3d18>
290. Ly ST, Kim JY (2017) 4D printing – fused deposition modeling printing with thermal-responsive shape memory polymers. *Int J Precis Eng Manuf - Green Technol* 4:267–272. <https://doi.org/10.1007/s40684-017-0032-z>
291. Arif ZU, Khalid MY, Zolfagharian A, Bodaghi M (2022) 4D bioprinting of smart polymers for biomedical applications: recent progress, challenges, and future perspectives. *React Funct Polym* 179:105374. <https://doi.org/10.1016/j.reactfunctpolym.2022.105374>
292. dos Santos J, de Oliveira RS, de Oliveira TV, Velho MC, Konrad MV, da Silva GS, Deon M, Beck RCR (2021) 3D printing and nanotechnology: a multiscale alliance in personalized medicine. *Adv Funct Mater* 31. <https://doi.org/10.1002/adfm.202009691>
293. Cano-Vicent A, Tambuwala MM, Hassan SS, Barh D, Aljabali AAA, Birkett M, Arjunan A, Serrano-Aroca Á (2021) Fused deposition modelling: current status, methodology, applications and future prospects. *Addit Manuf* 47:102378. <https://doi.org/10.1016/j.addma.2021.102378>
294. Dabbagh SR, Sarabi MR, Birtek MT, Seyfi S, Sitti M, Tasoglu S (2022) 3D-printed microrobots from design to translation. *Nat Commun* 13. <https://doi.org/10.1038/s41467-022-33409-3>
295. Palmara G, Frascella F, Roppolo I, Chiappone A, Chiadò A (2021) Functional 3D printing: approaches and bioapplications. *Biosens Bioelectron* 175:112849. <https://doi.org/10.1016/j.bios.2020.112849>
296. González-Henríquez CM, Sarabia-Vallejos MA, Rodríguez-Hernández J (2019) Polymers for additive manufacturing and 4D-printing: materials, methodologies, and biomedical applications. *Prog Polym Sci* 94:57–116. <https://doi.org/10.1016/j.progpolymsci.2019.03.001>
297. Tiwary VK, Arunkumar P, Deshpande AS, Rangaswamy N (2019) Surface enhancement of FDM patterns to be used in rapid investment casting for making medical implants. *Rapid Prototyp J* 25:904–914. <https://doi.org/10.1108/RPJ-07-2018-0176>
298. Melocchi A, Briatico-vangosa F, Uboldi M, Parietti F, Turchi M, Von Zeppelin D, Maroni A, Zema L, Gazzaniga A, Zidan A (2021) Quality considerations on the pharmaceutical applications of fused deposition modeling 3D printing. *Int J Pharm* 592:119901. <https://doi.org/10.1016/j.ijpharm.2020.119901>
299. Jeon S, Hoshiar AK, Kim K, Lee S, Kim E, Lee S, Kim JY, Nelson BJ, Cha HJ, Yi BJ, Choi H (2019) A magnetically controlled soft microrobot steering a guidewire in a three-dimensional phantom vascular network. *Soft Robot* 6:54–68. <https://doi.org/10.1089/soro.2018.0019>
300. Fischer P, Ghosh A (2011) Magnetically actuated propulsion at low Reynolds numbers: towards nanoscale control. *Nanoscale* 3:557–563. <https://doi.org/10.1039/c0nr00566e>
301. Bastola AK, Hossain M (2021) The shape – morphing performance of magnetoactive soft materials. *Mater Des* 211:1–25. <https://doi.org/10.1016/j.matdes.2021.110172>
302. Kumar S, Singh R, Singh TP, Batish A (2021) Investigations for magnetic properties of PLA-PVC-Fe₃O₄-wood dust blend for self-assembly applications. *J Thermoplast Compos Mater* 34:929–951. <https://doi.org/10.1177/0892705719857778>
303. Kumar S, Singh R, Singh TP, Batish A (2019) On mechanical characterization of 3-D printed PLA-PVC-wood dust-Fe₃O₄ composite. *J Thermoplast Compos Mater* 35:1–18. <https://doi.org/10.1177/0892705719879195>
304. Calascione TM, Fischer NA, Lee TJ, Thatcher HG (2021) Controlling magnetic properties of 3D-printed magnetic elastomer structures via fused deposition modeling. *AIP Adv* 11:1–7. <https://doi.org/10.1063/9.0000220>
305. Migliorini L, Villa SM, Santaniello T, Milani P (2022) Nanomaterials and printing techniques for 2D and 3D soft electronics. *Nano Futur* 6:1–16
306. Sarobol P, Cook A, Clem PG, Keicher D, Hirschfeld D, Hall AC, Bell NS (2016) Additive manufacturing of hybrid circuits. *Annu Rev* 1–22. <https://doi.org/10.1146/annurev-matsci-070115-031632>
307. Zhou L, Fu J, He Y (2020) A review of 3D printing technologies for soft polymer materials. *Adv Funct Mater* 2000187:1–38. <https://doi.org/10.1002/adfm.202000187>
308. Zhang P, Lei IM, Chen G, Lin J, Chen X, Zhang J, Cai C, Liang X, Liu J (2022) Integrated 3D printing of flexible electroluminescent devices and soft robots. *Nat Commun* 13:1–8. <https://doi.org/10.1038/s41467-022-32126-1>
309. Yang H, Leow WR, Chen X (2018) 3D printing of flexible electronic devices. *Small. Methods* 2:1–7. <https://doi.org/10.1002/smt.201700259>
310. Yan X, Tong Y, Wang X, Hou F, Liang J (2022) Extrusion-based 3D-printed supercapacitors: recent progress and challenges. *Energy Environ Mater* 5:800–822
311. Wu W, Ye W, Wu Z, Geng P, Wang Y, Zhao J (2017) Influence of layer thickness, raster angle, deformation temperature and

- recovery temperature on the shape-memory effect of 3D-printed polylactic acid samples. *Materials (Basel)* 10:970. <https://doi.org/10.3390/ma10080970>
312. Lee YC, Alshehly YS, Nafea M (2022) Joule heating activation of 4D printed conductive PLA actuators. 2022 IEEE Int Conf Autom Control Intell Syst I2CACIS 2022 – Proc 221–225. <https://doi.org/10.1109/I2CACIS54679.2022.9815495>
313. Yang H, Leow WR, Wang T, Wang J, Yu J, He K, Qi D, Wan C, Chen X (2017) 3D printed photoresponsive devices based on shape memory composites. *Adv Mater* 29:1–7. <https://doi.org/10.1002/adma.201701627>
314. Ahmed W, Alnajjar F, Zanelidin E, Al-Marzouqi AH, Gochoo M, Khalid S (2020) Implementing FDM 3D printing strategies using natural fibers to produce biomass composite. *Materials (Basel)* 13:4065. <https://doi.org/10.3390/ma13184065>
315. KrapežTomec D, Kariž M (2022) Use of wood in additive manufacturing: review and future prospects. *Polymers (Basel)* 14:1174. <https://doi.org/10.3390/polym14061174>
316. Le Duigou A, Castro M, Bevan R, Martin N (2016) 3D printing of wood fibre biocomposites: from mechanical to actuation functionality. *Mater Des* 96:106–114. <https://doi.org/10.1016/j.matdes.2016.02.018>
317. Correa D, Papadopoulou A, Guberan C, Jhaveri N, Reichert S, Menges A, Tibbits S (2015) 3D-printed wood: programming hygroscopic material transformations, *3D Print. Addit Manuf* 2:106–116. <https://doi.org/10.1089/3dp.2015.0022>
318. de Kergariou C, Le Duigou A, Perriman A, Scarpa F (2023) Design space and manufacturing of programmable 4D printed continuous flax fibre polylactic acid composite hygromorphs. *Mater Des* 225:111472. <https://doi.org/10.1016/j.matdes.2022.111472>
319. Le Duigou A, Barbé A, Guillou E, Castro M (2019) 3D printing of continuous flax fibre reinforced biocomposites for structural applications. *Mater Des* 180:107884. <https://doi.org/10.1016/j.matdes.2019.107884>
320. Nguyen PD, Nguyen TQ, Tao QB, Vogel F, Nguyen-Xuan H (2022) A data-driven machine learning approach for the 3D printing process optimisation. *Virtual Phys Prototyp.* <https://doi.org/10.1080/17452759.2022.2068446>

Publisher's Note Springer Nature remains neutral with regard to jurisdictional claims in published maps and institutional affiliations.

Springer Nature or its licensor (e.g. a society or other partner) holds exclusive rights to this article under a publishing agreement with the author(s) or other rightsholder(s); author self-archiving of the accepted manuscript version of this article is solely governed by the terms of such publishing agreement and applicable law.